An-Najah National University
Faculty of Graduate Studies

GIS-Based Hydrological Modeling of Semiarid Catchments

(The Case of Faria Catchment)

By

Sameer 'Mohammad Khairi' Shhadi Abedel-Kareem

Supervisors

Dr. Hafez Q. Shaheen
Dr. Anan F. Jayyousi

Submitted in Partial Fulfillment of the Requirements for the Degree of Master of Science in Water and Environmental Engineering, Faculty of Graduate Studies, at An-Najah National University, Nablus, Palestine

2005

GIS-Based Hydrological Modeling of Semiarid Catchments
(The Case of Faria Catchment)

By

Sameer 'Mohammad Khairi' Shhadi Abedel-Kareem

This Thesis was defended successfully on 25/12/2005 and approved by:

Committee Members	**Signature**
1. Dr. Hafez Shaheen (Supervisor)	....
2. Dr. Anan Jayyousi (Supervisor)	....
3. Dr. Marwan Ghanem (External Examiner)	....
4. Dr. Mohammad Almasri (Internal Examiner)	....

بسم الله الرحمن الرحيم

أَنْزَلَ مِنَ السَّمَاءِ مَاءً فَسَالَتْ أَوْدِيَةٌ بِقَدَرِهَا فَاحْتَمَلَ السَّيْلُ زَبَدًا رَابِيًا.........ألرعد (16)

صدق الله العظيم

… Dedicated to
My parents, wife and my daughter (Muna)

Acknowledgments

First of all, praise is to Allah for making this thesis possible. I would like to express my sincere gratitude to Dr. Hafez Shaheen and Dr. Anan Jayyousi for their supervision, guidance and constructive advice. Special thanks go also to the defense committee members.

Thanks also go to those who helped in providing the data used in this study. Water and Environmental Studies Institute or giving me the chance to work on GLOWA project, Palestinian Water Authority (PWA) for producing of water data used in this study.

My parents, brothers and sisters, thank you for being a great source of support and encouragement. All my friends and fellow graduate students, thank you.

Special thanks to my friend Eng. Rami Qashou' who's support will never be forgotten.

Finally, thanks to my dear wife Heba for her love, moral support and patience.

Table of Contents

List of Abbreviations

Symbol	The meaning
KW-GIUH	Kinematic Wave based Geomorphological Instantaneous Unit Hydrograph
GIS	Geographical Information System
DEM	Digital Elevation Model
EAB	Eastern Aquifer Basin
PHG	Palestinian Hydrology Group
PWA	Palestinian Water Authority
IDF	Intensity Duration Frequency Curves
MOT	Meteorological Office of Transport
WESI	Water and Environmental Studies Institute
N	Optimal number of stations
E_p	Allowable percentage of error
C_v	Coefficient of variation
P_{av}	Mean of rainfall
σ_{n-1}	Standard deviation
P(x)	Probability of exceedance
$T_{x_{oi}}$	Time for the flow to reach equilibrium
q_{o_i}	ith-order overland flow discharge per unit width
q_L	Lateral flow rate
h_{os_i}	ith-order water depth at equilibrium
Q_{cs_i}	ith-order channel discharge at equilibrium
$T_{x_{rk}}$	Travel time for the channel storage component
$T_{x_{ck}}$	Travel time for the channel translation component
P_{OA_i}	Ratio of the ith-order overland area to the catchment area
A	Total area of the catchment
N_i	ith-order stream number
$\overline{L}_{c_i}$	ith-order stream length
n_o	Overland flow roughness
n_c	Channel flow roughness
$\overline{A_i}$	ith-order sub catchment contributing area
$\overline{S_{o\,i}}$	ith-order overland slope
$\overline{S_{c\,i}}$	ith-order channel slope
$P_{x_i x_j}$	Stream network transitional probability
B_Ω	Channel width at catchment outlet
Ω	Stream network order

List of Tables

List of Figures

GIS-Based Hydrological Modeling
of Semiarid Catchments
(The Case of Faria Catchment)

By
Sameer 'Mohammad Khairi' Shhadi Abedel-Kareem
Supervisors
Dr. Hafez Q. Shaheen
Dr. Anan F. Jayyousi

Abstract

Extreme events, such as severe storms, floods, and droughts are the main features characterizing the hydrological system of a region. In the West Bank, which is characterized as semiarid; little work has been carried out about hydrological modeling. This thesis is an attempt to model the rainfall-runoff process in Faria catchment, which is considered as one of the most important catchments of the West Bank. Faria catchment dominating the north eastern slopes of the West Bank is a catchment of about 334 km^2 and has the semiarid characteristics of the region. The catchment is gauged by six rainfall stations and two runoff flumes.

Statistical analysis including annual average, standard deviation, maximum and minimum rainfall was carried out for the rainfall stations. The internal consistency of rainfall measurements of the six stations was examined by using the double mass curve technique. The results show that all station measurements are internally consistent.

Gumbel distribution fits well the annual rainfall and can be used for future estimations. It provides means to understand and evaluate the distribution characteristics of the rainfall in the Faria catchment. Trend analysis of the rainfall has shows an increasing trend for the stations with high elevations and a decreasing trend for low elevated ones. The multiple regression analysis applied to the six rainfall stations proved to be strongly correlated.

GIS-based KW-GIUH hydrological model was used to simulate the rainfall-runoff process in the Faria catchment. GIUH unit hydrographs were derived for the three sub-catchments of Faria namely Al-Badan, Al-Faria and Al-Malaqi. The KW-GIUH model is tested by comparing the simulated and observed hydrographs of Al-Badan sub-catchment for two rainstorms with good results. Sensitivity of the KW-GIUH model parameters was also investigated. The simulated runoff hydrographs proved that the GIS-based KW-GIUH model is applicable to semiarid regions and can be used to estimate the unit hydrographs in the West Bank catchments.

CHAPTER ONE

INTRODUCTION

1.1 Background

Water is the chief ingredient of life and all ancient civilizations flourished only near the water sources and then probably collapsed when the water supply failed. Water is a finite resource, essential for agriculture, industry and human existence. Without water of adequate quantity and quality, sustainable development is impossible. Water resources management is essential to ensure the availability of water, when and where it is needed, and to safeguard its quality.

Hydrologists and water engineers are always concerned with discharge rates resulting from rainfall. Not only measuring rainfall and the resulting runoff are of interest, but also the process of transforming the rainfall hyetograph into runoff hydrograph. Peak flow rate and time to peak are the two important hydrograph characteristics that need to be estimated for any catchment. Unfortunately, the classic problem of predicting these parameters is usually difficult to resolve because many rivers and streams are ungauged, especially those in developing regions or isolated areas. Even in cases where catchments are gauged, the period of record is often too short to allow accurate estimates of the different hydraulic parameters.

Flood frequency analysis enables the user to predict flow rates with certain return periods. Historical flow data is necessary to conduct such analysis. Hydrological models that incorporate catchment characteristics to predict flow rates at a given location in the catchment is another tool to be utilized in cases where historical flow records are not available.

Hydrological simulation models can take the form of theoretical linkage between the geomorphology and hydrology. The geomorphological instantaneous unit hydrograph (GIUH) is one approach of this kind of model. The GIUH focuses on finding the catchment response given its geomorphological features. The GIUH model is applied in this study to Faria catchment in the northern West Bank. The model uses catchment characteristics to predict flow rates.

West Bank is a semiarid region. In arid and semiarid regions storm water drainage and hydrological modeling is important as in humid regions because it is not only a drainage problem but also a water resources management and planning problem. Hydrological modeling in the West Bank has not been given enough care and no intensive studies have been done.

In characterizing the catchment, GIS has been applied. Using GIS in hydrology has become an important issue since the beginning of 1980 and up to the present. It enables the user to handle and analyze the hydrological data more efficiently.

This thesis concentrates on modeling the rainfall-runoff process in the upper part of the Faria catchment in the northern West Bank. GIS-based KW-GIUH hydrological model was applied as it is available and can model ungauged catchments. The KW-GIUH model can be applied to any excess rainfall through convolution to produce the direct runoff hydrograph.

1.2 Objectives

Modeling the runoff in the Faria catchment will provide basic information for the managers to understand runoff generation within the catchment and thus support the decision-making process about future development of the water resources in the area. This will enhance the development of the agricultural sector. It will also support the studies of the Jordan River Basin as Wadi Faria catchment is a major contribution to the Jordan River.

The main objective of this research is to model the rainfall runoff process of the Faria catchment and to derive the unit hydrograph for the catchment. The KW-GIUH model that was developed for ungauged catchments is to be used in this research. The geomorphological and topographic characteristics were provided using the GIS system.

The other objectives of this study are:

1. Analysis of rainfall data of the Faria catchment.
2. Investigate the rainfall runoff process in semiarid regions.

1.3 Research Needs and Motivations

Faria catchment is predominantly arid and semiarid characterized by its natural water resources scarcity, low per capita water allocation and conflicting demands as well as shared water resources. This scarcity leads to the limited availability of water resources and the dire need to manage these resources.

Faria catchment, located in the northeastern part of the West Bank, Palestine, is one of the most important agricultural areas in the West Bank. The predominantly rural population in the catchment is growing rapidly, which results in increasing demand for natural water resources.

The prolonged drought periods in the catchment and the high population growth rate in addition to other artificial constraints have negatively affected the existing obtainable surface water and groundwater resources.

Due to the fact that the available water resources in the Faria catchment are limited and are not sufficient to fulfill the agricultural and residential water demand, reliability assessment of water availability in the Faria catchment is of great importance in order to optimally manage the local water resources.

Rural population in the Faria catchment faces a series of problems. These problems are related to different causes including inefficient management, water shortages, environmental pollution, and Israeli occupation. The key problems of the Faria catchment relevant to the water resources can be summarized as follows:

1. Lack of proper management of water resources causes over utilization of the scarce water resources.

2. The water is not properly allocated between upstream and downstream communities and thus water use rights need to be well established and institutionalized.

3. More than 40% of the people in the catchment lacks water supply for drinking purposes.

4. The estimated annual water gap between water needs and obtainable water supply is about 20 millions cubic meters. This gap is increasing rapidly with time.

5. Lack of storage capacity and non existence of small dams to capture the rain floods during the rainy season in order to be used later (As to peace agreements, permits for such projects are required from Israeli occupation authorities, which are almost impossible to obtain).

6. Unbalanced utilization of groundwater causes increasing salinity especially in the south eastern part of the catchment in the proximity of the Jordan River.

7. Water losses through evaporation and infiltration from the agricultural canals are high and thus large quantities of water are not fully utilized.

8. Soil erosion in the lower part of the catchment is of great concern.

9. Water pollution is an ongoing problem. For instances surface water originating from the springs mixes with wastewater coming from Nablus City and Faria refugee camp.

10. There is no treatment plant in the catchment.

11. Cesspools are major threats to pollute the groundwater aquifers and springs.

12. The unbalanced use of fertilizers and pesticides has led to the pollution of the scarce water resources.

13. Unmanaged solid waste dumping in some areas adds additional complexity to the pollution problems.

14. Lack of permits to rehabilitate and remediate the deteriorated wells.

15. In contrast to the shallow Palestinian wells, Israeli wells are pumping largely from deep aquifers and thus lowering the water table.

From the above it can be inferred that Faria catchment is under a severe problematic conditions that need to be investigated in order to set up proper strategies and management alternatives to address these problems efficiently indemnify.

For the aforementioned discussion, this study is of great importance. Due to the fact that the available water resources in the Faria catchment are limited and cannot suffice for increasing water demand to fulfill the agricultural and residential requirements, reliability assessment of water availability in the Faria catchment is of great importance in order to optimally manage the local water resources. This situation has compelled the motivation for conducting a hydrological modeling to better understand and to evaluate the water resources availability in the Faria catchment. This modeling is essential to provide input data for a management system and to enable the development of optimal water allocation policies and management alternatives to bridge the gap between water needs and obtainable water supply under drought conditions.

1.4 Methodology

To achieve the above objectives, the available topographic maps of the region were scanned and the catchment was subdivided into sub-catchments. Drainage lines and divides were digitized. The stream paths, possible flow directions and slopes have been determined using the available Digital Elevation Model (DEM) and the base map of the Faria catchment has been prepared. All the information including topography, land use, drainage lines, water divides, soil and geology have been processed using the GIS ArcView 3.2 software.

The rainfall data recorded by the different stations of the Faria catchment were analyzed for typical and maximum rainfall intensities and amounts.

These were used as a tool to describe the spatial structure of the rain events and to regionalize point station data to catchment rainfall. Rainfall and runoff were measured continuously during the rainstorms of the last two rainy seasons of the hydrological years 2003-2004 and 2004-2005. Accordingly the input parameters to the KW-GIUH model have been estimated.

The following summarizes the main steps that were followed:

1. Collect all data and information from national and local institutions.
2. Hydrological measurements and sampling of rainfall-runoff events completed for the two rainy seasons.
3. Analysis of rainfall and runoff data.
4. Set up GIS-based data as input for the model.
5. Model application to the available different rainfall events.
6. Model verification and sensitivity analysis.
7. The final results of the modeling have been formulated.

The overall methodology followed in this study is illustrated in **Figure 1**.

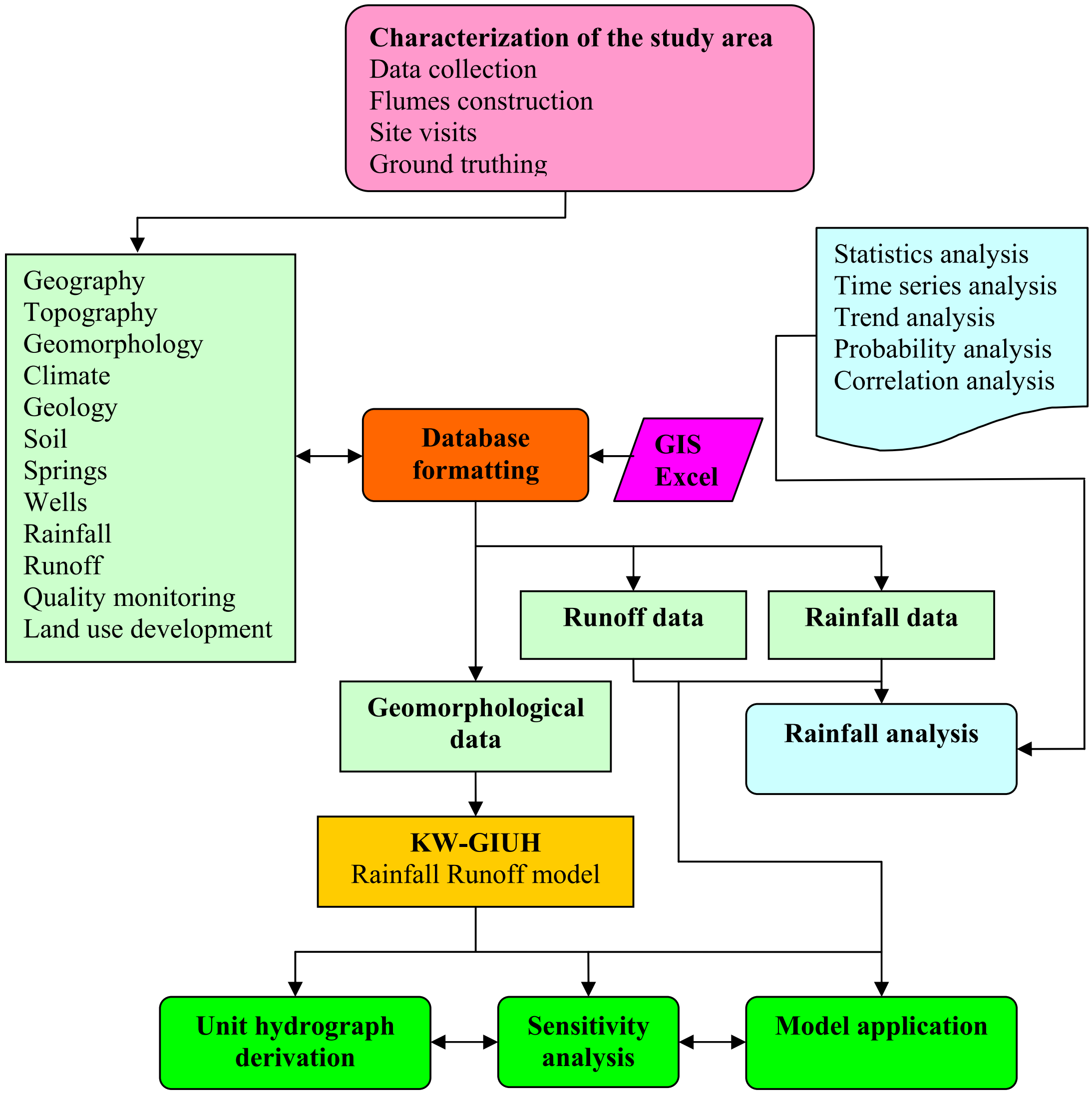

Figure 1: A flow Chart Depicting the General Methodology Followed in this Study

1.5 Data Collection

Hydrological data in the West Bank is very limited. Difficulties have been faced in collecting the necessary data for this study due to continuous closure of the West Bank cities. Nevertheless the catchment was visited several times to collect further data. Most of the data have been collected from the following sources:

1. Contour Map. The available 1:50000 scale topographic maps have been used to collect elevation data. The maps have been scanned and used within the GIS environment to delineate the catchment and sub-catchments boundaries and divides. The stream paths, possible flow directions and slopes have been determined using the available Digital Elevation Model (DEM).

2. Water resources (springs and wells) data were obtained from the Palestinian Water Authority (PWA) databank. The data included monthly and annual measurements of the abstraction of the wells and yield of springs in addition to the name and coordinates of these resources. The information obtained was in MS Excel format.

3. Rainfall data necessary for the analysis of the rainfall-runoff process have been collected from the PWA and from Nablus Meteorological Station for five different stations (Taluza, Tammun, Tubas, Beit Dajan and Al-Faria).

4. The climatic data for this study was obtained from the Palestine Climate Data Handbook published by the Metrological Office of the Ministry of Transport (MOT), 1998. Climatic data included average monthly values for maximum and minimum temperature, hourly mean wind speed, daily mean sunshine duration, mean relative humidity, pan evaporation and mean monthly rainfall for Nablus and Al-Faria stations.

CHAPTER TWO

LITERATURE REVIEW

2.1 Hydrology of Semiarid Regions

One way to define aridity is the moisture deficit, or the aridity index, which is the ratio of mean annual precipitation (P) to mean annual potential evapotranspiration (PET). This index is then reclassified into four main aridity zones and one humid zone and one cold tundra mountains zone, according to the ranges defined by UNESCO (1984). These zones are: hyper-arid (P/PET < 0.05), arid (0.05 <= P/ PET < 0.20), semiarid (0.20 <= P/ PET < 0.50), dry sub-humid (0.50 <= P/ PET < 0.65), humid (P/ PET >=0.65) and cold, which area that have more than six months of an average temperature below 0 degrees and not more than three months where the temperatures reach above 6 degree centigrade. The six arid regions around the world are shown in **Figure 2**.

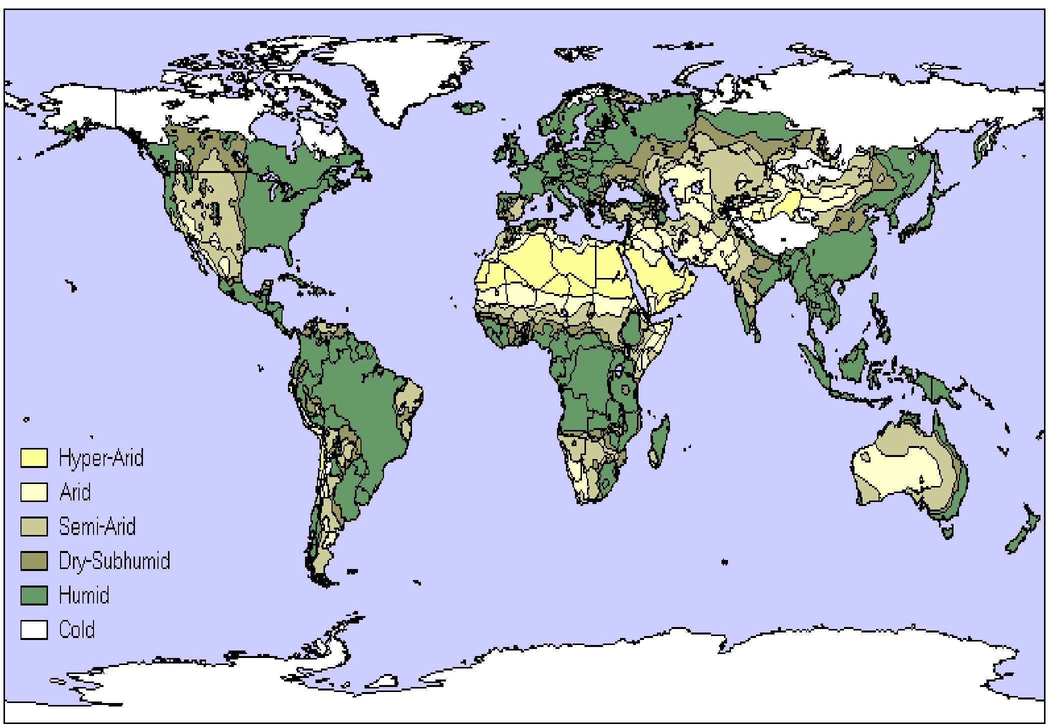

Figure 2: Arid Regions around the World (UNESCO, 1984)

The main hydrological difference between humid areas and arid zones is a high variability in both space and time of all hydrologic parameters (e.g. rainfall intensity, infiltration rates, runoff rates). Floods, although infrequent and rare, appear in arid areas and often cause loss of life and property (Schick et al, 1997, cited by Thormählen, 2003). Many semiarid regions are particularly affected by flash floods, caused mainly by convective storm systems. The main processes that dominate during flashy floods are the generation of Hortonian overland flow on dryland terrain and transmission losses into the dry alluvial beds of ephemeral channels. In dry environments, the hydrological regime is governed by missing baseflow and single episodic flood events traveling on dry river beds, induced by localized, high intensity rainfall (Thormählen, 2003).

2.1.1 Climate and Rainfall

The main climatological feature of arid regions is the ephemeral and often localized nature of precipitation usually associated with immense variations in space and time (Thormählen, 2003). The arid zone is characterized by excessive heat and inadequate variable precipitation; however, contrasts in climate occur. In general, these climatic contrasts result from differences in temperature, the season in which rain falls, and in the degree of aridity. Three major types of climate are distinguished when describing the arid zone: the Mediterranean climate, the tropical climate and the continental climate (FAO, 1989).

In the Mediterranean climate, the rainy season is during autumn and winter. Summers are hot with no rains; winter temperatures are mild, with a wet season starting in October and ending in April or May, followed by 5 to 6 months of dry season.

In the tropical climate, rainfall occurs during the summer. Winters are long and dry. In Sennar, Sudan, an area that is typical of the tropical climate, the wet season extends from the middle of June until the end of September, followed by a dry season of almost 9 months.

In the continental climate, the rainfall is distributed evenly throughout the year, although there is a tendency toward greater summer precipitation. In Alice Springs, Australia, each monthly precipitation is less than twice corresponding mean monthly temperature; hence, the dry season extends over the whole year.

The rainfall that falls is either intercepted by trees, shrubs, and other vegetation, or it strikes the ground surface and becomes overland flow, subsurface flow, and groundwater flow. Regardless of its deposition, much of the rainfall eventually is returned to the atmosphere by evapotranspiration processes from the vegetation and soil or by evaporation from streams and other bodies of water into which overland, subsurface, and groundwater flow move. These processes are as illustrated by the hydrologic cycle in **Figure 3**, in which global annual average water balances are given in units relative to a value of 100 for the rate of precipitation on land.

Rainfall intensity is another parameter which must be considered when evaluating the rainfall runoff process. Because the soil may not be able to absorb all the water during a heavy rainfall, water may be lost by runoff. Likewise, the water from a rain of low intensity can be lost due to evaporation, particularly if it falls on a dry surface.

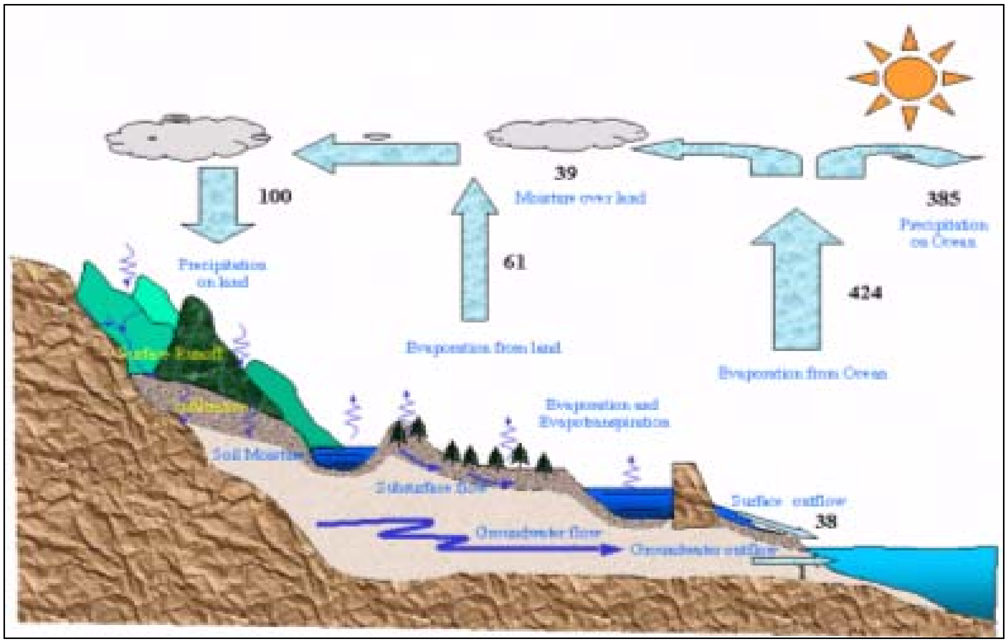

Figure 3: Hydrologic Cycle with Global Annual Average Water Balance (Chow et al., 1988)

A semiarid region is subject to seasonal precipitation, with little or no precipitation in other parts of the years. Rainfall patterns vary widely from region to region and, within a certain region. Temperature is high and annual precipitation amounts are moderate (Ponce, 1989).

Evaporation is affected by several climatic elements (e.g. air temperature, relative humidity, net radiation). It is necessary to distinguish between actual rates of evaporation and potential rates. The concept of the potential evaporation assumes that water is not limited and is at all times sufficient to supply the requirements of the dry air and the transpiring cover. Clearly, in semiarid regions, the value for actual evaporation seldom equals the potential evaporation, but is much lower. Generally in semiarid farm lands there is large gap between potential Evapotranspiration and rain depth.

2.1.2 Runoff Generation and Channel Flow

The high variability of rainfall both in time and space, leads to very high variability of runoff. In humid regions different runoff generation processes (e.g. runoff from saturated areas and slow outflow of large groundwater bodies) deliver more or less permanently water to perennial rivers. In contrast, in arid regions Hortonian overland flow, generated as infiltration excess runoff, is generally assumed to be the dominant mechanism of runoff generation (Abrahams et. al, 1994). The overland flow is described as water that flows over the ground surface heading for the next stream channel and as the initial phase of surface runoff in arid environments (Lange et al., 2003). On plane surfaces a quasi laminar sheet flow may develop, but, more usually, flow is concentrated by topographic irregularities and water flows anatomizing in small gullies and minor rivulets downhill. The main cause of overland flow is the inability of water to infiltrate the surface as a result of high intensity of rainfall or a low value of infiltration capacity or both phenomena (Thormählen, 2003). The difference between rainfall rate and infiltration rate is the concept of calculation the runoff of Hortonian overland flow. Water accumulates on the top of the ground surface, if the infiltration capacity of the soil is exceeded. Surface depressions have to be filled with water, after that runoff generation start to runs down slope. Arid areas with moderate to steep slopes and sparse vegetation cover form the ideal conditions for Hortonian runoff.

Streams in the arid and semiarid areas are usually ephemeral, since rainfall events are seldom occurred. Arid and semiarid ephemeral streams flowing only occasionally as a direct response to runoff generating rainstorms and remaining dry for most of the year. Flow in the large streams with their origin outside the arid zone (e.g. Nile River, Indus River or Colorado River) and small spring fed streams are the only exceptions (Thormählen, 2003). Floods in small dryland basins are usually of the flash flood type, either single peak floods or multiple peak events. Flash floods are almost produced by convective rain storm cells and are typical for small scale catchments (<100km²), because most thunderstorm cells are relatively small in diameter. Flash floods are defined as stream flows that increase from zero to a maximum within a few minutes or at most few hours (Graf, 1988).

Surface runoff in the eastern slopes of the West Bank where the Faria catchment is located is mostly intermittent and occurs when rainfall exceeds 50 mm in one day or 70 mm in two consecutive days (Forward, 1998, cited by Takruri, 2003). Rofe and Raffety (1965) studied runoff in the West Bank through monitoring and studying runoff data from seventeen flow gauging stations within the boundaries of the West Bank. They concluded that surface runoff constitute nearly 2.2% of its total equivalent rainfall.

2.1.3 Storages

Two types of surface flow losses occur in the arid lands, which fill temporal storages (Lange, 1999):

1. Infiltration is a direct loss with Hortonian runoff that governs the volume of storm runoff. Further direct losses occur when water is temporarily stored on route or in the stream system as detention loss or when depression storages retain water in depressions on the surface.

2. Linear transmission losses into the riverbed alluvium of the stream channels reduce flood volume as indirect losses, after surface flow has been generated and flows spatially concentrated.

The main water storage in dry environments is formed by coarse river bed alluvium. With rainfall events broadly separated in time, the alluvial fill has a large available volume for flood water infiltration practically at all times. The alluvial storages form an infiltration trap for water that flows into them either through the orderly tributary system or directly from adjoining slopes. The alluvial bodies, filled by indirect losses may be relatively permanent and quite deep, serving as important water storage for vegetation or local population. Compared to alluvial fills, the second type of storage is shallower. It is recharged by direct losses and is quickly emptied by evaporation within a few days after the rainfall event. Percolation from rainfall to deep aquifers is generally very small.

2.2 Rainfall-Runoff Modeling

The selection, analysis and use of recorded hydrographs for direct simulation purposes are reflected in variation of the unit hydrograph technique. This technique, which assumes a linearity of the transfer function, is computationally attractive and often sufficiently accurate. Unit hydrograph techniques may be applied to synthesize hydrographs either from recorded rainfall events or from specific return period storms extracted from intensity-duration-return period curves and hypothetical time duration patterns (Chow et al., 1988). Hydrological modeling is concerned with the accurate prediction of the partitioning of water among the various pathways of the hydrological cycle (Dooge, 1992 cited by Lange, 1999). Hydrological systems are generally analyzed by using mathematical models. These models may be empirical or statistical, or founded on known physical laws. They may be used for such simple purposes as determining the rate of flow that roadway grate must be designed to handle, or they may be used to guide decisions about the best way to develop a river basin for a multiplicity of objectives. The choice of the model should be tailored to the purpose for which it is to be used. In general, the simplest model capable of producing information adequate to deal with the issue should be chosen (Viessman et al., 2003).

Hydrological models are used for several practical purposes. Imagine a flood disaster; during the flood event a model may help to predict when and where there is a risk of flooding (e.g., which areas should be evacuated). After the flood, models may be used to quantify the risk that a flood of similar or larger magnitude will occur during the coming years and to decide what measures of flood protection may be needed for the future. Furthermore, models may help to understand the reasons for the magnitude of flood (e.g., if the flood was enlarged by human activities in the catchment) (Lundin et al., 1998).

2.2.1 Historical Overview

The development and application of hydrological models have gone through a long time period. The origins of rainfall-runoff modeling in the broad sense can be found in the middle of the 19th century, when Mulvaney, an Irish engineer who used in the first time the rational equation to give the peak flow from rainfall intensity data and catchment characteristics. A major step forward in hydrological analysis was the concept of the unit hydrograph introduced by Sherman in 1932 on the basis of superposition principle. The use of unit hydrograph made it possible to calculate not only the flood peak discharge (as the rational method does) but also the whole hydrograph (the volume of surface runoff produced by the rainfall event). The real breakthrough came in the 1950s when hydrologists became aware of system engineering approaches used for the analysis of complex dynamic systems (Todini, 1988). This was the period when conceptual linear models originated (Nash, 1958). Many other approaches to rainfall-runoff modeling were considered in the 1960s. A large number of conceptual, lumped, rainfall-runoff models appeared thereafter including the famous Stanford Watershed Model (SWM-IV) (Crawford and Linsley, 1966) and the HBV model (Bergström and Forsman, 1973). A great variety of these conceptual hydrological models has appeared up to the present date. TOPMODEL is one remarkable model developed in the late 1970s (Beven and Kirkby, 1979) that is based on the idea that topography exerts a dominant control on flow routing through upland catchments.

To meet the need of forecasting (1) the effects of land use changes, (2) the effects of spatially variable inputs and outputs, (3) the movements of pollutants and sediments, and (4) the hydrological response of ungauged catchments where no data are available for calibration of a lumped model, the physically based distributed parameter models were developed. SHE model is an excellent example of such models (Lange, 1999).

Geomorphological Instantaneous Unit Hydrograph (GIUH) (Rodriguez-Iturbe and Valdes 1979) is a recently developed physically based rainfall-runoff approach for the simulation of runoff hydrograph, especially appropriate for ungauged catchments. Lange 1999 mentioned that GIUH model has been used by Allam (1990), Nouh (1990) and Al-Turbak (1996) to develop unit hydrograph for several catchments in the Kingdom of Saudi

Arabia. In the semiarid experimental catchment of Walnut Gulch, Arizona, USA, the long history of research provides good runoff records, which facilitated the successful application of calibrated models (Goodrich et al. 1997 and Renard et al.1993 cited by Thormählen, 2003). The long history of research also allowed a non-calibrated model run of KINEROS, a complex distributed model developed for semiarid catchments (Thormählen, 2003). Lange et al. (1999) develop a model not depending on calibration but accounting for the dominant processes of arid zone flood generation. This has been done for the 1400 km² Zin catchment in the Nagab Desert. The ZIN-Model has been developed especially for large arid catchments and has been tested successfully for 250 km² in the semiarid Wadi Natuf (Lange et al. 2001).

2.2.2 Classification of Models and Basic Definitions

Two types of mathematical models can be used in hydrology; stochastic and deterministic models. In the stochastic models, the chance of occurrence of the variable is considered thus introducing the concept of probability. In the deterministic models, the chance of occurrence of the variables involved is ignored and the model is considered to follow a definite law of certainty but not any law of probability (Raghunath, 1985). Different classification schemes have been proposed (e.g. Chow et al., 1988, Todini 1988). **Figure 4** provide a general overview of the hydrological model using the classification criteria randomness, spatial discretization and model structure. To find the desired hydrological model one should ask the following questions (Lange, 1999):

1- Is there a need to consider randomness?

2- Is there a need to consider spatial variations of model input or parameter?

3- To what extent the governing physical laws have to be considered?

Randomness is not considered in a deterministic model; a given input rainfall always produces the same output runoff. The outputs of a stochastic model are at least partially random. A deterministic distributed model considers the hydrological process taking place at various points in space. It may either be physically based, i.e. reproducing the rainfall-runoff process only by physical principals on the conservation of mass and momentum, or conceptual reflecting these principals in a simplified approximate manner. In deterministic lumped models hydrological systems are spatially averaged or regarded as a single point in scale without dimensions. Since hydrological processes generally are space dependent, spatial lumping always includes crude conceptualization. Empirical models do not explicitly consider the governing physical laws of the processes involved. They only relate input through some empirical transformed function. Stochastic models are termed space-independent or space-correlated according to whether or not random variables at different points in space influence each other.

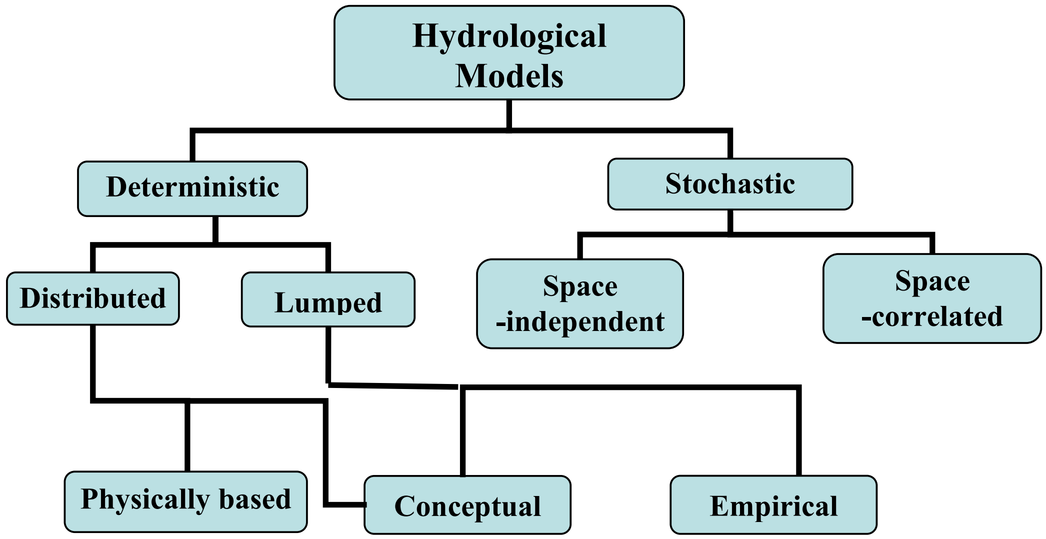

Figure 4: Classification of Hydrological Models (Lange, 1999)

2.3 Use of GIS in Hydrology

Geographic Information Systems (GIS) can be defined as computer based tools that display, store, analyze, retrieve, and process spatial data. GIS is being more and more involved in hydrology and water resources and showing promising results. GIS provides representations of the spatial features of the earth, while hydrological models are concerned with the flow of water and its constituents over the land surface and in the subsurface environment.

GIS with its upcoming advanced technology has been a great advantage to hydrological modeling. Hydrological modeling using GIS has been great developed during the last decade when people realized the utility of incorporating GIS with hydrologic modeling. The use of digital terrain models have showed there potential to a number of analysis in hydrology. Lee (1985) cited by Al-Smadi (1998) concluded that GIS is an efficient tool for compiling input data for use in hydrological investigations and best suited distributed hydrologic models. Al-Smadi (1998) mentioned that;

Berry and Sailor (1987) noted some of the advantages of GIS in hydrology and water resources. According to them, GIS provides a powerful tool for expressing complex spatial relationships. It provides an opportunity to fully incorporate spatial conditions into hydrologic inquiries. Different proposed levels of development can be made rapidly and the resulting hydrologic effects easily communicated to decision makers.

GIS are highly specialized database management systems for spatially distributed data. GIS provides a digital representation of the catchment characterization used in hydrological modeling. Maidment (1996) summarized the different levels of hydrological modeling in association with GIS as follows: hydrologic assessment; hydrologic parameter determinations; hydrologic modeling inside GIS; and linking GIS and hydrologic models. GIS integrates different elements like automated mapping, facilities management, remote sensing, land information systems and spatial statistics. GIS serves as an input to the management information systems in the corporate domain and modeling. Maidment (1996) tries to focus on the data model which is the key to the GIS modeling in hydrology concluding that "It is probably true that the factor most limiting hydrological modeling is not the ability to characterize hydrological processes mathematically, or to solve the resulting equations, but rather the ability to specify values of the model parameters representing the flow environment accurately". GIS will help overcome that limitation. Bhaskar et al. (1992) simulated watershed runoff using the Geomorphological Instantaneous Unit Hydrograph (GIUH) with the Arc-Info GIS to compile the required data.

In this study GIS has been employed as a tool to determine the hydrologic parameter for the Faria catchment needed to compile the KW-GIUH model.

Digital Elevation Model (DEM) is used in number of sub-domains in hydrology. Varied hydrological applications can be driven by different users accessing the same pool of information. As a result, the structure of the database that supports the GIS, quality of the data and the way in which the database is managed lie at the heart of development of many GIS applications. The DEM have proved to be very efficient in extracting the hydrological data from the DEM by analyzing different topographical attributes (elevation, slope, aspect, relief, curvatures) for modeling purposes. DEM has potentially proved to be a valuable tool for the topographic parameterization of hydrological models especially for drainage analysis, hill slope hydrology, watersheds, groundwater flow and contaminant transport etc. The reason of adopting GIS technology in hydrological models is because it allows the spatial information to be displaced in integrative ways that are readily comprehensible and visual. The spatial information collected is further subjected to continuous GIS analysis. The GIS techniques have the potential for widespread application to resource evaluation, planning and management (Grover, 2003). Several of the most popular computer models such as HEC-RAS, HEC-HMS, and Mike SWMM have GIS capabilities that are seldom used. GIS technology has not been used more widely because:

- Lack of suitable data.
- The technology is too expensive.
- The engineering community lack training and education in GIS.

2.4 Previous Work in the Study Area

Few reports appear in the literature concerning the runoff estimatation and analysis of rainfall data in the West Bank. Rofe and Raffety (1965) have installed special gauging networks which was designed and illustrated for ten wadis. The data were recorded for the year 1962/63 only. The results of this study show that the overall percentage of the rainfall-runoff was 2.2%. Rofe and Raffety (1965) also concluded that runoff was negligible in North West Bank. After the occupation of the West Bank in 1967, the runoff has cautioned to be measured by Israelis from many gauging stations located outside the boundaries of the West Bank. There are some stations located near the Green line (the 1967 cease fire agreement between the Palestinians and Israelis) which may provide reliable historic records on surface runoff.

Husary et al., (1995) analyze the rainfall data for the northern west bank. They presented the relationship between rainfall and runoff in Hadera catchment. They found that the ratio of runoff to rainfall ranges from 0.1% to 16.2% with an average of 4.5% for the period of 1982/83-1991/92.

Ghanem (1999) conducted a hydrological and hydrochemical investigation of the Faria drainage basin using GIS. According to Ghanem runoff is 2% of rainfall for the upper Faria and about 1% for the lower Faria. Al-Nubani (2000) studied the temporal characteristics of the rainfall data of Nablus meteorological station. By correlating the occurrences of runoff in Rujeeb watershed east of Nablus to the total rainfall values, he concluded that runoff occurs when total rainfall exceeds 48 mm distributed over less that 15 hours duration. As a result of Al-Nubani the runoff is 13.5% of rainfall. Barakat (2000) studied the rainfall runoff process of the upper Soreq catchment in Jerusalem district and developed the unit hydrograph related to four recorded events. Shaheen (2002) has studied the storm water drainage in arid and semiarid regions. He evaluated several rainfall-runoff processes of Soreq watershed. He has also evaluated the application of KW-GIUH model on semiarid watershed. Shadeed and Wahsh (2002) studied the runoff generation in the upper part of the Faria catchment using synthetic models, KW-GIUH model was also used in their study. The annual rainfall recorded at Nablus station for the period 1946-2002 was analyzed including frequency and trend analysis. Intensity-duration-frequency relationships were constructed. Takruri (2003) studied rainfall data in Faria catchment and developed approximate IDF curves for Beit Dajan station. She developed the unit hydrograph for the Faria catchment using traditional methods.

From the above it is clear that the ratio of rainfall to runoff in West Bank catchments has a wide range indicating that individual events of different characteristics dominate the rainfall-runoff process. Therefore there is a need for further investigations including detailed and accurate data acquisition of single events and proper modeling in the West Bank catchments. However, the outcomes of the previous studies indicate that the Faria catchment has not been modeled using appropriate rainfall-runoff models. Therefore the obtained results are weak and doubtful. This motivates the study of surface runoff in Faria catchment. This study is an attempt to hydrologically investigate and analyze the Faria catchment as one of the most important catchments of the West Bank, since the catchment has not been modeled using appropriate rainfall runoff models so far.

CHAPTER THREE

DESCRIPTION OF THE STUDY AREA

3.1 Location and Topography

The area under consideration is the Faria catchment which is located in the northeastern part of the West Bank and extends from the ridges of Nablus Mountains down the eastern slopes to the Jordan River and the Dead Sea as shown in **Figure 5.** Faria catchment overlies three districts of the West Bank. Those are: Nablus, Tubas and Jericho district and has a catchment area of about 334 km^2 which accounts for about 6% of the total area of the West Bank (5650 km^2) (see **Figure 5**). The Faria catchment lies within the Eastern Aquifer Basin (EAB), which is one of the three major groundwater aquifers forming the West Bank groundwater resources.

The Faria catchment borders are: North Jordan and Fassayel-Auja drainage basins from the north and south respectively, Alexander, Yarkon and Al-Khidera drainage basins from the west and Jordan River from the east. The western boundary of the study area lies at the main catchment between the Mediterranean Sea and the Jordan River.

The Faria wadi extends from the upper part of the catchment to the Jordan River. Al-Faria and Al-Badan wadis are the two main streams contributing to the Faria catchment. These wadis meet at Al-Malaqi Bridge located 25 km east of Nablus city. The Faria wadi is the major water supply system in the catchment. Springs are located around the stream and discharge water to the stream, through which water is conveyed to irrigation ditches and pipelines that distribute irrigation water to the farms along both sides of the stream.

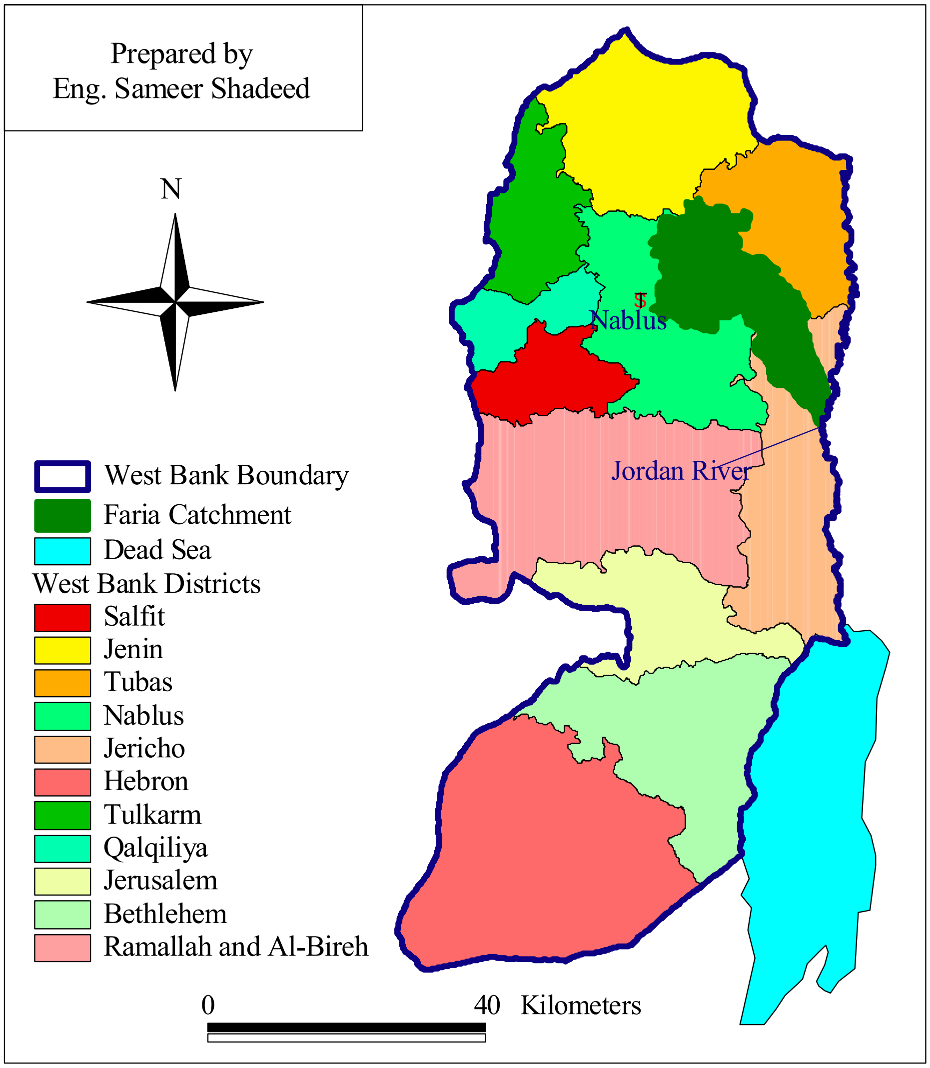

Figure 5: Location of the Faria Catchment within the West Bank

Irrigation wells are available in the Faria catchment to supply additional water. Within the Faria catchment there exist 13 fresh water springs and 70 groundwater wells as presented in **Figure 6**. The fertile alluvial soils, the availability of water through a number of springs and the meteorological conditions of the catchment made the catchment one of the most important irrigated agricultural areas in the West Bank.

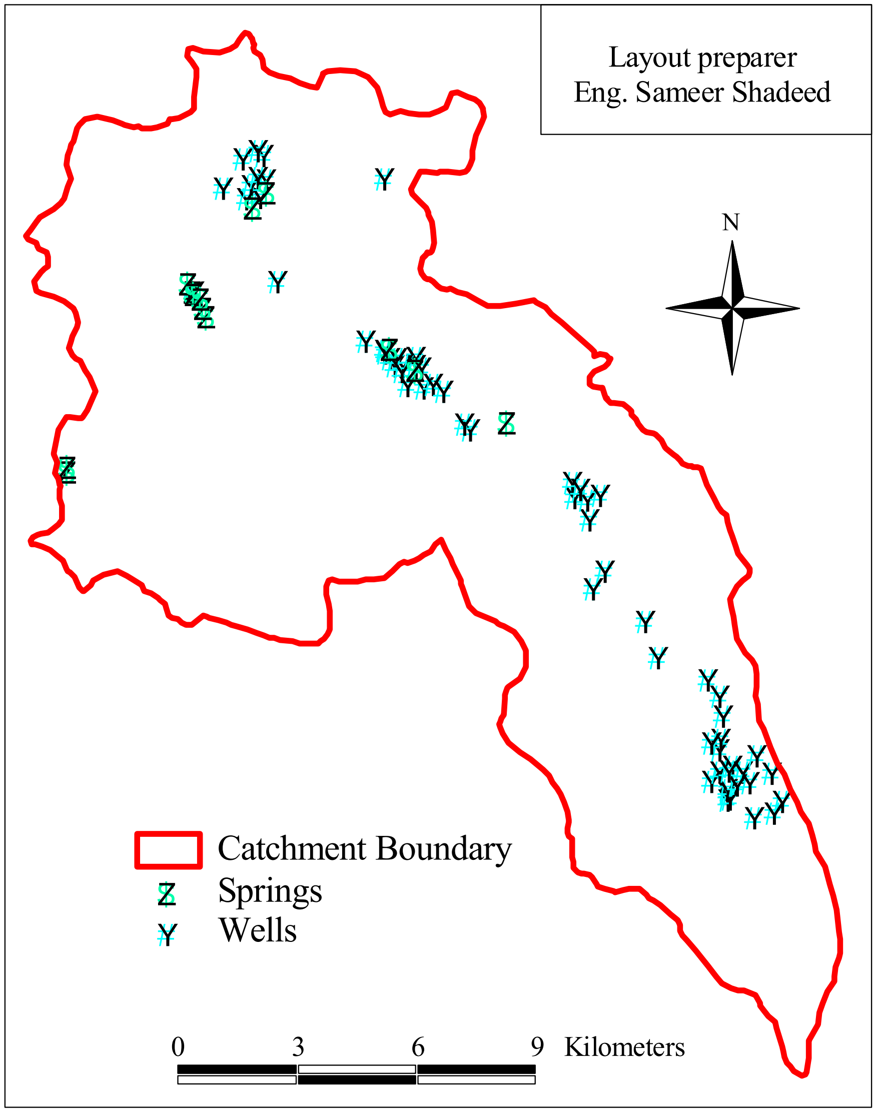

Figure 6: Springs and Wells within the Faria Catchment

Topography is a unique factor in the Faria catchment which starts at an elevation of about 900 meters above mean sea level in Nablus Mountains and descends drastically to about 350 meters below mean sea level at the point where the Faria wadi meets the Jordan River. This means that topographic relief changes significantly throughout the catchment. In less than 30 km there is a 1.25 km change in elevation. Such an elevation decline in a relatively short distance has considerable effects on the prevailing meteorological conditions in the area as a whole and, in fact, adds to its importance and uniqueness.

Topographic map of the Faria catchment (**Figure 7**), uploaded into the GIS ArcView system and used in the delineation of flow paths and divides as discussed in section 5.6 of this study.

Faria catchment includes about twenty communities within its borders. Most of these communities are rural communities except the eastern part of the city of Nablus, the refugee camps and parts of the town of Tubas and other villages in the upper part of the catchment.

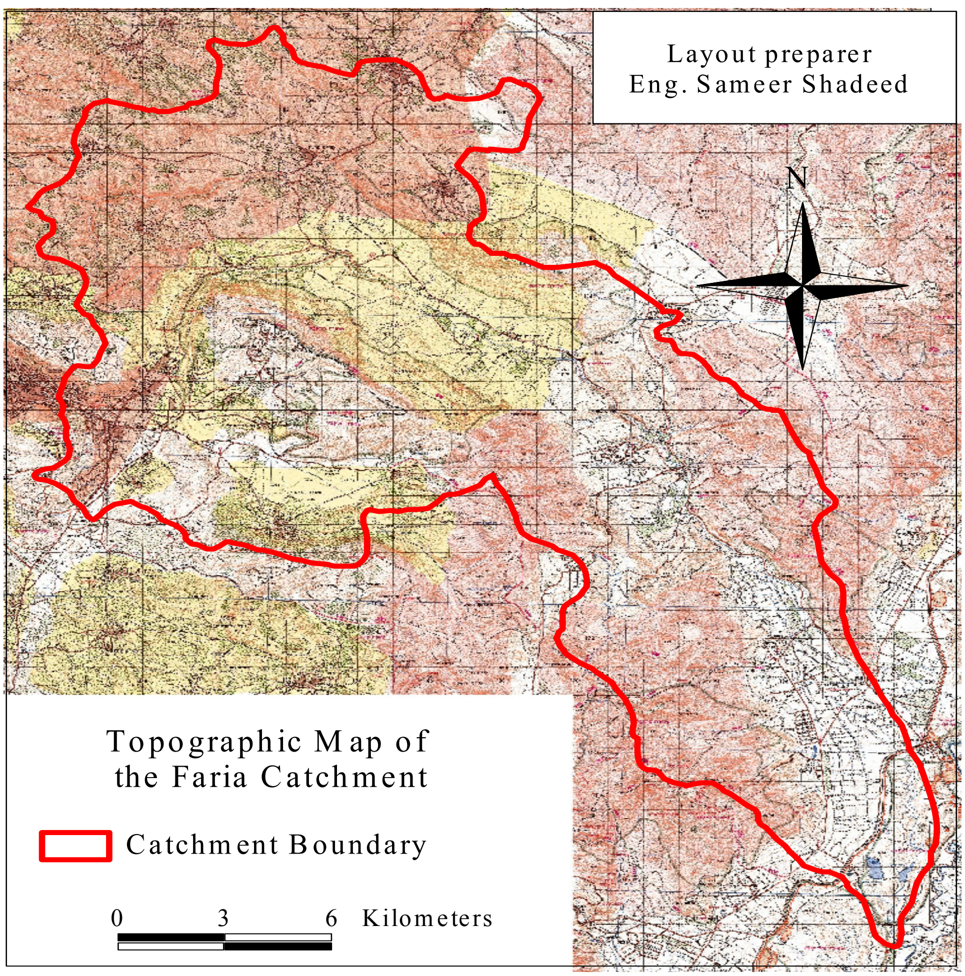

Figure 7: Topographic Map of the Faria Catchment

3.2 Climate

In the West Bank, climatic stations are mainly concentrated in the principal towns and villages. Since the Faria catchment does not contain significantly large built up areas, therefore only two climatic stations are located within the Faria catchment. One of the stations is located in Nablus (570 m elevation) and the other is located in Al-Jiftlik (-237 m elevation).

Climatic data for these stations were obtained from the Palestine Climate Data Handbook published by the Meteorological Office of the Ministry of Transport (MOT) (1998). Climatic data included average monthly values for maximum and minimum temperature, mean wind speed, mean sunshine duration, mean relative humidity and pan evaporation. The average values for the climatic conditions prevailing in the catchment area are presented in **Appendix A1**. The information has been spatially delineated using the GIS ArcView 3.2 software based on data input of temperature and evapotranspiration.

3.2.1 Wind

The main wind direction is from west, southwest and northwest. Variation during winter is associated with the pattern of depressions passing from west to east over the Mediterranean (Ghanem, 1999). The prevailing winds in the area are the southwest and northwest winds with an annual average wind speed of 237 km per day in Nablus at a height of 10 meters from ground surface. When this value is adjusted for 2 meters height (the 2 meters height value is used in most of the potential evapotranspiration estimates), average wind velocity drops to 185 km per day. During summer, wind moves with relatively cooler air from the Mediterranean towards the north, with an average wind speed of 288 km per day in June in

Nablus at a height of 10 meters. At night the land areas become cooler, causing diurnal fluctuations in wind speed, due to the reduction of the pressure gradient. In winter, the wind moves from west to east over the Mediterranean, bringing westerly rain bearing winds of average wind speed 209 km per day in January. The Khamaseen, desert storm, may occur during the period from April to June. During the Khamaseen, the temperature increases, the humidity decreases and the atmosphere becomes hazy with dust of desert origin. Wind velocities decrease with elevation, thus wind velocities in Al-Jiftlik in the lower part of the catchment are significantly lower than those in Nablus located in the upper part of the catchment. Existing wind data showed that measurements of wind velocities were recorded at a height of 10 meters in Nablus and at a height of 2 meters in Al-Jiftlik. Due to the elevation of Al-Jiftlik which is 237 meters below sea level and the existing mountains surrounding Al-Jiftlik, wind velocities are much lower than those at Nablus. Annual average wind velocity in Al-Jiftlik was estimated at 106 km/day at a height of 2 meters which is much less than the 185 Km/day estimated in Nablus at the same height from ground surface.

3.2.2 Temperature

Faria catchment is characterized by high temperature variations over space and over time. Temperatures reduce with increasing elevation in the catchment. The average temperature variation between Nablus and Al-Jiftlik is about 5 ^{o}C. The mean annual temperature changes from 18 ^{o}C in the western side of the catchment in Nablus to 24 ^{o}C in the eastern side of the catchment at Al-Jiftlik. **Figure 8** shows the variation in average monthly temperatures in Nablus and Al-Faria stations. Spatial representation of the mean annual temperature in the catchment is presented in **Figure 9**.

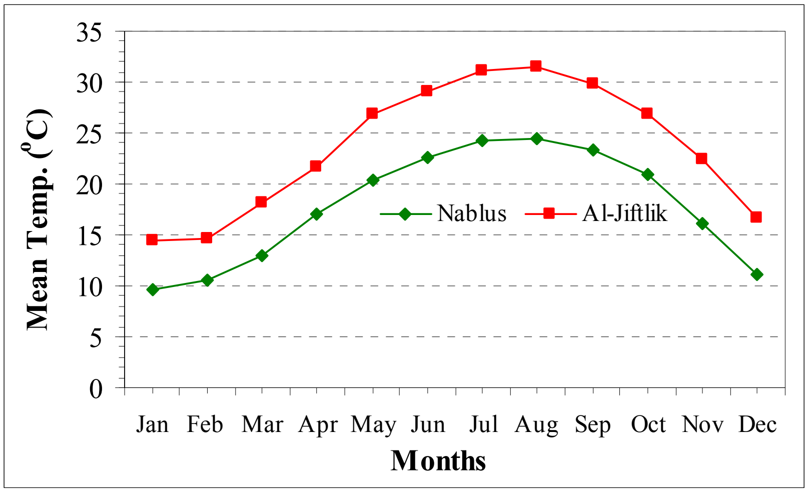

Figure 8: Mean Monthly Temperatures in Nablus and Al-Jiftlik

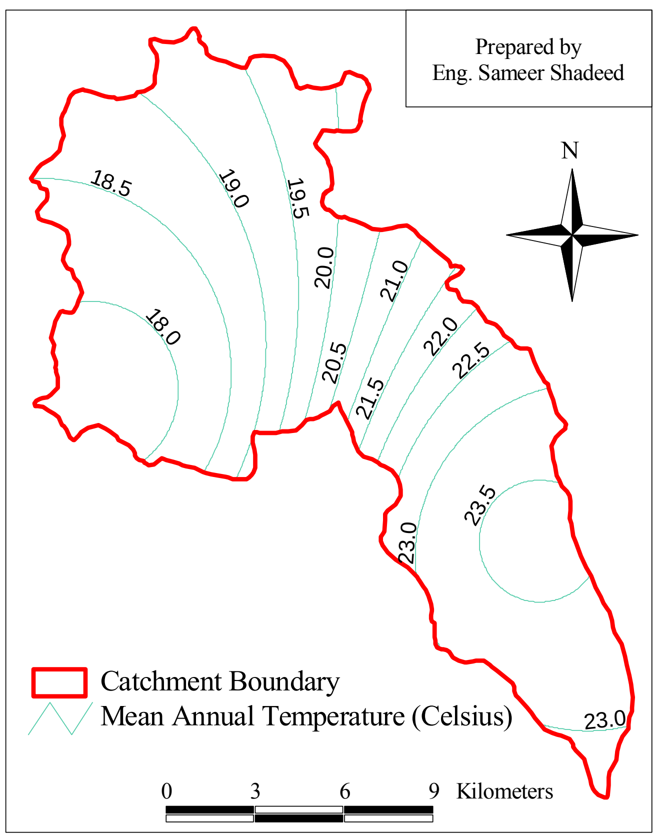

Figure 9: Spatial Distribution of the Mean Annual Temperature in the Faria Catchment

3.2.3 Relative Humidity

The mean annual relative humidity of Nablus area is 61%. The minimum value of relative humidity is 51% which occurs in May during the Khamaseen weather, while the maximum relative humidity of 67% is usually registered in December, January and February. Relative humidity is in general low in the entire catchment especially in summer months because the catchment is located on the eastern side of the West Bank Mountains. The source of humidity in the region is the Mediterranean Sea, where the western winds bring humidity to the catchment. Eastern winds coming from the desert are usually dry.

3.2.4 Rainfall

The West Bank is considered semiarid and has the Mediterranean type climate. Regionally, the winter rainy season is from October to April in the catchment. Rainfall events predominantly occur in autumn and winter and account for 90% of the total annual precipitation events. Although the summer months are dry, some rain events occur occasionally and a high-pressure area governs the weather over the Mediterranean. The continental low-pressure area to the east and south creates a strong pressure gradient across the country, which results in eastward moving sea breezes of relatively cooler air. In winter, the predominately low-pressure area of the Mediterranean centered between two air masses, the north Atlantic high on North Africa and the Euro-Asian winter high located over Russia, is the primary cause of winter weather in the area. The presence of hills in the west of Palestine affects the behavior of the low-pressure area, resulting in westernlies, which force moist air upwards, causing precipitation on the hill ridges. The steep gradient of Jordan Valley produces a lee effect, which greatly reduces the quantity of the rainfall in the Jordan Valley rift area (Husary et al., 1995). The rainfall distribution within the Faria catchment ranges from 640 mm at the headwater to 150 mm at the outlet to the Jordan River. **Figure 10** presents the spatial presentation of the rainfall data within the Faria catchment.

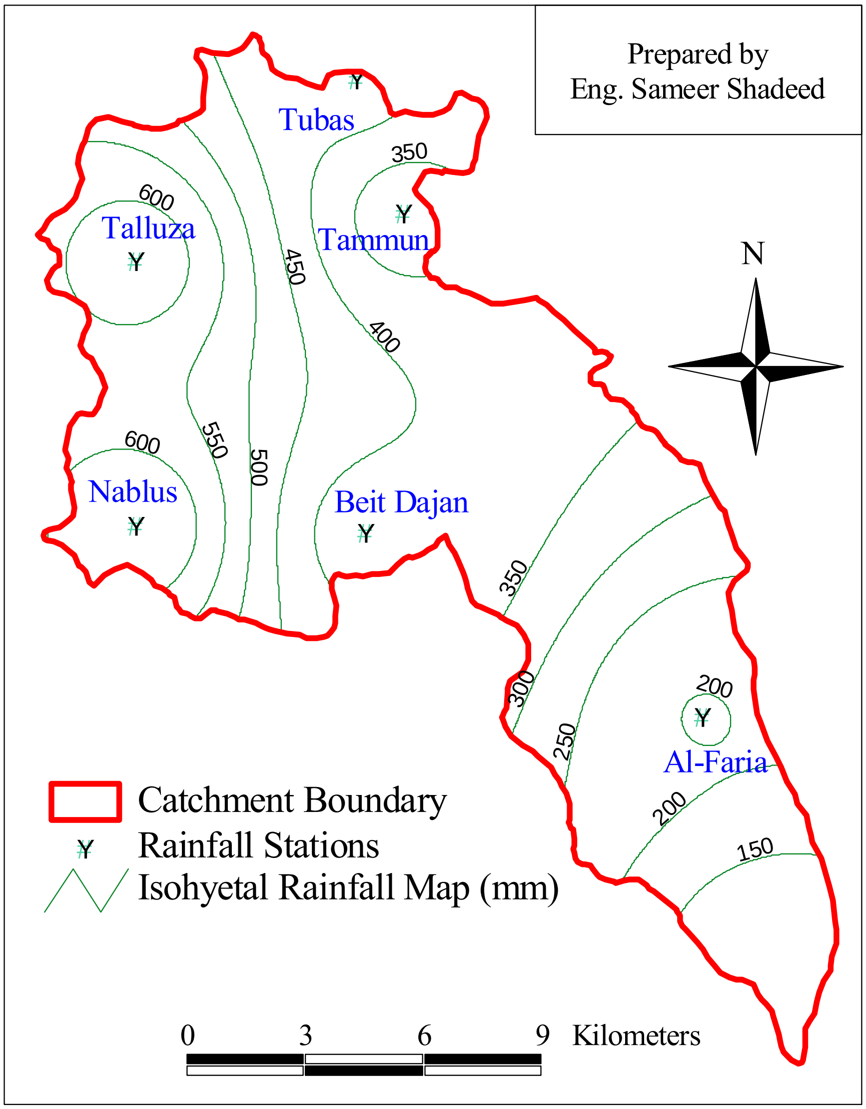

Figure 10: Rainfall Stations and Rainfall Distribution within the Faria Catchment

3.2.5 Evaporation

The Mediterranean climate (hot and dry in the summer, mild and wet in the winter) has six to seven months of dryness in the year. Winter months where moisture is available from rain have low evapotranspiration rates. Summer months with high potential evapotranspiration rates have no rain and thus actual evapotranspiration is limited by the availability of moisture.

Evaporation rates in Faria regions are measured from a US Class A pan at Nablus station as shown in the table of **Appendix A1**. From the table it is noticed that the average annual evaporation measured at Nablus station is about 1682 mm. Evapotranspiration is usually smaller than pan evaporation. Evaporation rates should be multiplied by a pan coefficient (less than 1) to estimate evapotranspiration rates. A more accurate way to estimate evapotranspiration is from climatic data.

Monthly potential evapotranspiration rates were estimated according to Penman-Monteith method as modified by FAO using CROPWAT 4 Windows version 4.2 model (FAO, 1998). The maximum potential rate of Evapotranspiration was estimated at 1540 mm/year at Al-Jiftlik and 1408 mm/year in Nablus. Although the temperature variability between Nablus and Al-Jiftlik might indicate a larger difference in evapotranspiration, this difference was reduced as a result of higher wind velocities in dry summer months in Nablus.

In the upper part of the Faria catchment, at Nablus, precipitation exceeds potential evapotranspiration in five months of the year (November through March). However, in the lower part of the catchment, at Al-Jiftlik, precipitation exceeds potential evapotranspiration in two months of the year only (December and January). Therefore, irrigation is required during most months of the year in the lower part of the catchment in comparison to the upper part. **Figure 11** shows the relation between potential evapotranspiration and rainfall for Nablus and Al-Jiftlik stations. The spatiality of the potential annual evapotranspiration rates in the Faria catchment is presented in **Figure 12** as computed using CROPWAT 4 model. From the figure it is noticed that the spatiality of the potential annual evapotranspiration rates is roughly coincide to the spatiality of the mean annual temperature (**Figure 9**). CROPWAT 4 output results for Nablus and Al-Faria stations are presented in **Appendix A2**.

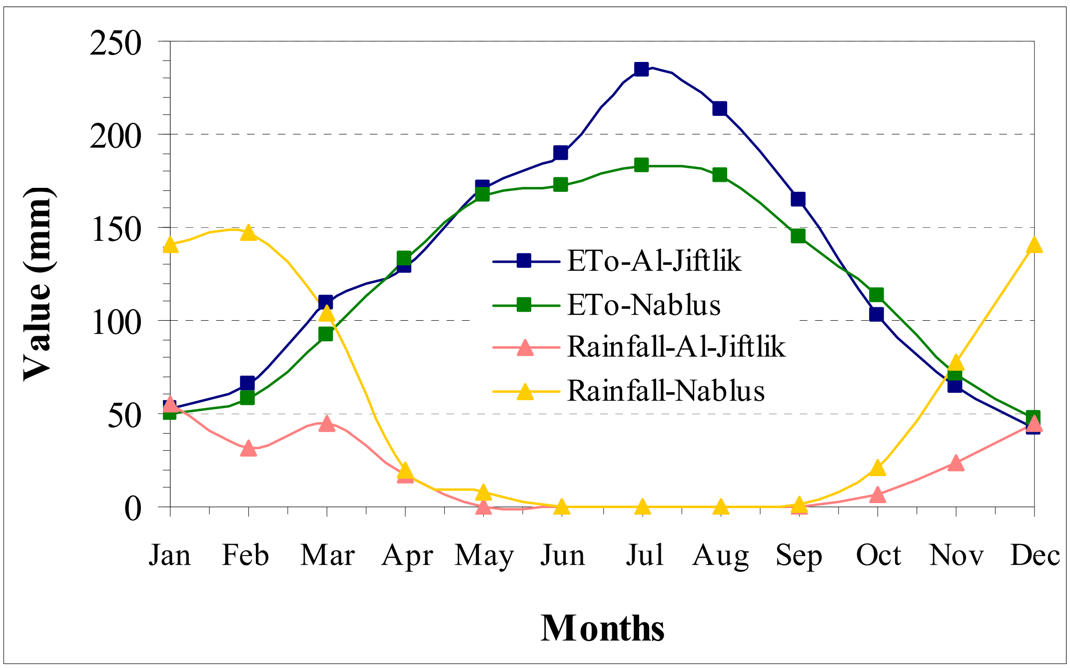

Figure 11: Monthly Rainfall and Potential Evapotranspiration Rates (ET_o) in Nablus and Al-Jiftlik

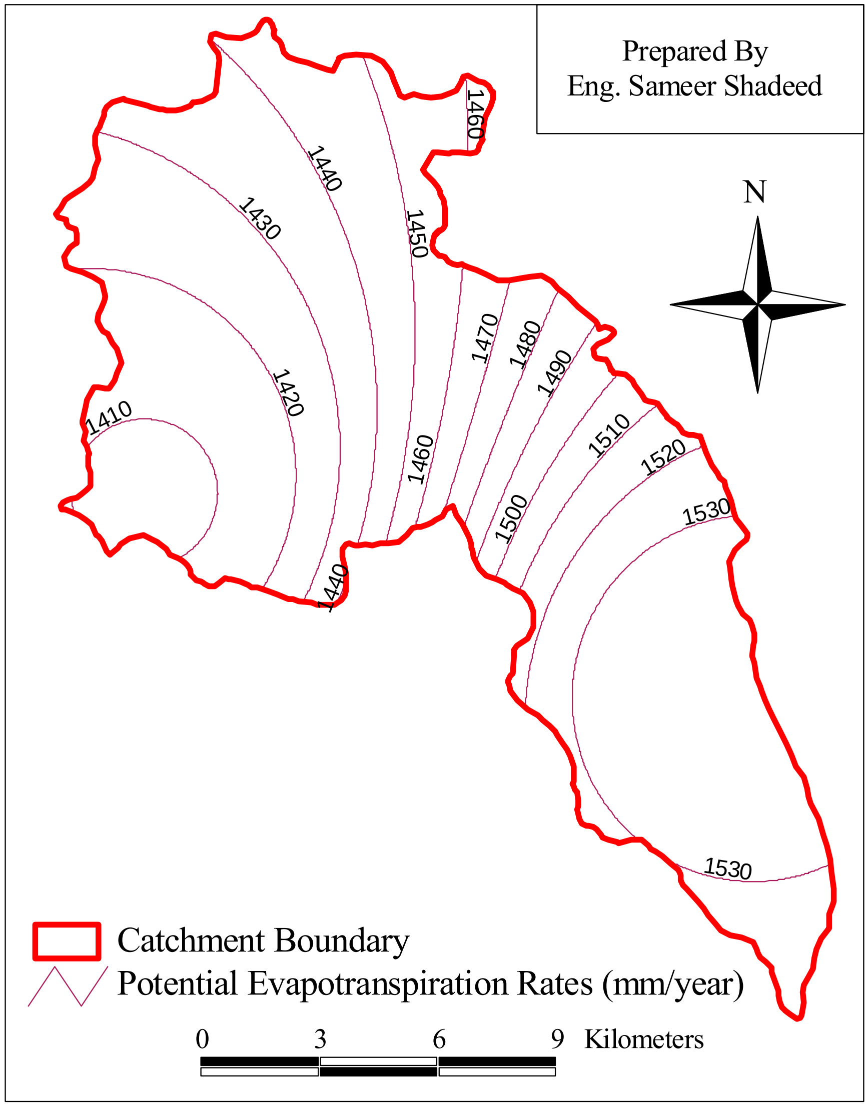

Figure 12: Potential Annual Evapotranspiration Rates in the Faria Catchment

3.2.6 Aridity of the Catchment

As to UNESCO (1984), aridity can be defined in several different ways and most simply it is a moisture deficit. The moisture deficit, or an aridity index, is determined by the ratio of mean annual precipitation (P) to mean annual potential evapotranspiration (PET). The index ranges for defining arid and semiarid regions are: arid (0.05 <= P/PET < 0.20), semiarid (0.20 <= P/PET < 0.50).

Monthly potential evapotranspiration rates were estimated according to Penman-Monteith method as modified by FAO (1998) using CROPWAT 4 Windows version 4.2 model. The results of applying CROPWAT 4 model are presented in the previous section and **Appendix A2**. It was estimated that the annual potential rate of Evapotranspiration is 1540 mm and 1408 mm at Al-Jiftlik and Nablus stations respectively. For these stations, the long term average annual rainfall is 198 mm and 642 mm respectively. Therefore, the aridity index is 0.13 for Al-Jiftlik and 0.46 for Nablus. This means that arid conditions prevail in Al-Jiftlik, whereas semiarid conditions prevail in Nablus.

3.3 Water Resources

3.3.1 Groundwater Wells

There are 69 wells in the Faria catchment; of which 61 are agricultural wells, 3 are domestic and 5 are Israeli wells. These wells are drilled in four sub-aquifers. These sub-aquifers are Eocene, Cenomanian, Neogene and Pleistocene sub-aquifers. All these wells are located in the study area mainly in the areas of Ras Al-Faria, Al-Aqrabanieh, Al-Nasaria, Froush Beit Dajan and Jiftlik along the flexure of wadi Faria.

Based on the available data (**Table 1**), the total utilization of the Palestinian wells ranges from 4.4 to 11.5 MCM/year. Data on the pumping rates from the Israeli wells is available for four wells for only four years from 1997-2000. The average total abstraction from these four wells was found to be about 8 MCM/year. Average well abstraction from Israeli wells is about 2 MCM/year. Thus, considering the fifth Israeli well without data available, the total abstraction from the five Israeli wells in the Faria catchment is estimated at 10 MCM/year, which is more than the 61 Palestinian agricultural wells combined. **Table 1** presents the total annual abstraction from wells in the Faria catchment from 1984 -2003.

Wells basic data includes coordinates, well name, location, district, usage, basin, and well depth were obtained from the Palestinian Water Authority (PWA). **Appendix A3** gives a summary of these basic data for all wells within the Faria catchment.

Table 1: Abstraction from Wells in the Faria Catchment

Year	Abstraction MCM			
	Agricultural	Domestic	Total	Israeli
1984	4.7	*	4.7	*
1985	5.7	*	5.7	*
1986	5.7	2.2	7.9	*
1987	7.0	2.3	9.2	*
1988	6.8	2.9	9.7	*
1989	6.6	3.3	9.9	*
1990	6.7	3.3	10.0	*
1991	6.3	3.0	9.3	*
1992	4.1	*	4.1	*
1993	5.0	*	5.0	*
1994	5.9	3.0	8.9	*
1995	6.4	3.1	9.5	*
1996	6.6	2.6	9.2	*
1997	5.8	2.8	8.6	6.7
1998	7.6	2.5	10.2	8.3
1999	8.2	3.3	11.5	8.4
2000	7.4	3.9	11.3	8.2
2001	6.1	2.5	8.6	*
2002	6.6	2.7	9.3	*
2003	5.1	2.8	7.9	*

* Missing Data

3.3.2 Springs

Within the Faria catchment there exists 13 fresh water springs that are divided into four groups. These groups are Faria, Badan, Miska and Nablus.

The basic data available on these springs include group name, spring name, coordinates, average annual discharge, minimum annual discharge and maximum annual discharge. **Table 2** presents a summary of these basic data. Monthly spring discharge measurements for more than 30 years are available for these springs as presented in **Appendix A4**. Discharge data of the springs show high spring discharge variability. Annual discharge from these springs varies from 3.8 to 38.3 MCM/year with an average amount of 14.4 MCM/year.

The location of the springs and wells within the Faria catchment are shown in **Figure 6**.

Table 2: Spring Groups and Spring Information within Faria catchment

Group	**Spring Name**	**Coordinates**			**Ave. Annual Discharge MCM**	**Min. Annual Discharge MCM**	**Max. Annual Discharge MCM**
		X (km)	**Y (km)**	**Elevation (m)**			
Faria	El Faria	182.40	188.40	160	5.23	1.71	10.53
	El Duleb	182.00	187.95	155	1.27	0.06	8.60
Badan	Asubian	180.52	184.56	130	0.19	0.14	0.23
	Beida & Hammad	180.12	185.32	215	0.81	0.10	1.75
	Sidreh	179.95	185.58	240	1.34	0.00	8.12
	Tabban	180.42	184.82	160	1.38	0.98	1.63
	Qudeira	180.13	185.28	215	1.33	0.00	2.33
	Jiser	180.37	185.10	170	0.14	0.03	0.23
Miska	Miska	187.03	182.90	-38	1.32	0.02	2.21
	Shibli	189.90	181.28	-80	0.95	0.71	1.15
	Abu Saleh	186.26	183.57	-19	0.19	0.00	0.50
Nablus	Balata	176.20	179.77	510	0.17	0.05	0.55
	Dafna	176.20	179.90	560	0.13	0.02	0.49
Total					**14.44**	**3.81**	**38.31**

3.3.3 Analysis of Springs Discharge

There are sex springs within Al-Badan sub-catchment, in addition to other two springs that are entirely utilized by the city of Nablus, whereas Al

Faria sub-catchment contained two springs in its area. Preliminary analysis on the available monthly discharge measurements including minimum, maximum and average discharge was performed. From the analysis it is concluded that the average annual volume of Al-Badan springs for the 30 years monthly data is about 4 MCM, while the minimum and maximum volumes are about 1.1 MCM and 16 MCM respectively. On the other hand, the average annual volume of Al-Faria springs is about 7 MCM, while the minimum and maximum volumes are 1.4 MCM and 24 MCM. **Figures 13** and **14** illustrate the sum of the minimum, maximum and average values of Al-Badan and Al-Faria springs respectively. From figures it is clear that high variability in the spring discharge exists. Results also suggest that the data do not follow a normal distribution and the average value is much closer to the minimum rather than the maximum.

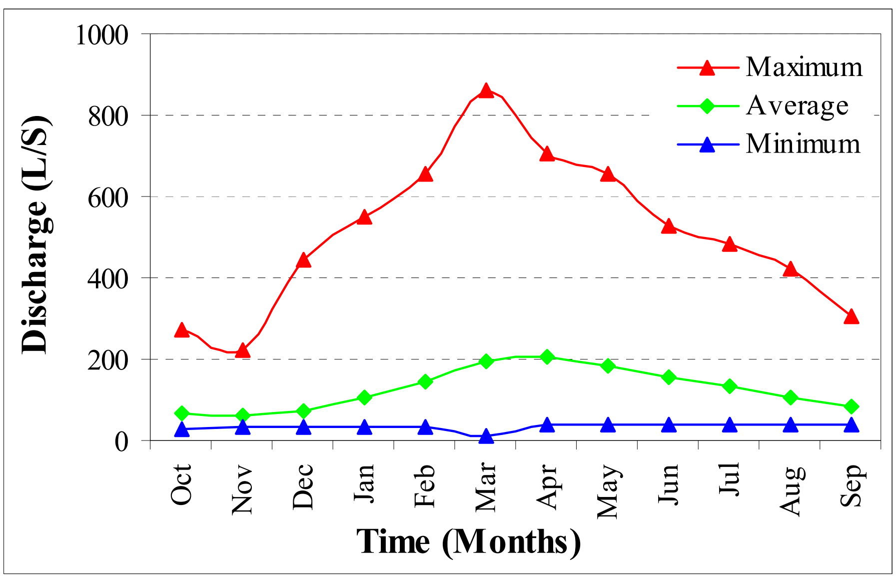

Figure 13: Average, Maximum and Minimum Monthly Discharge of Total Springs within Al-Badan Sub-catchment

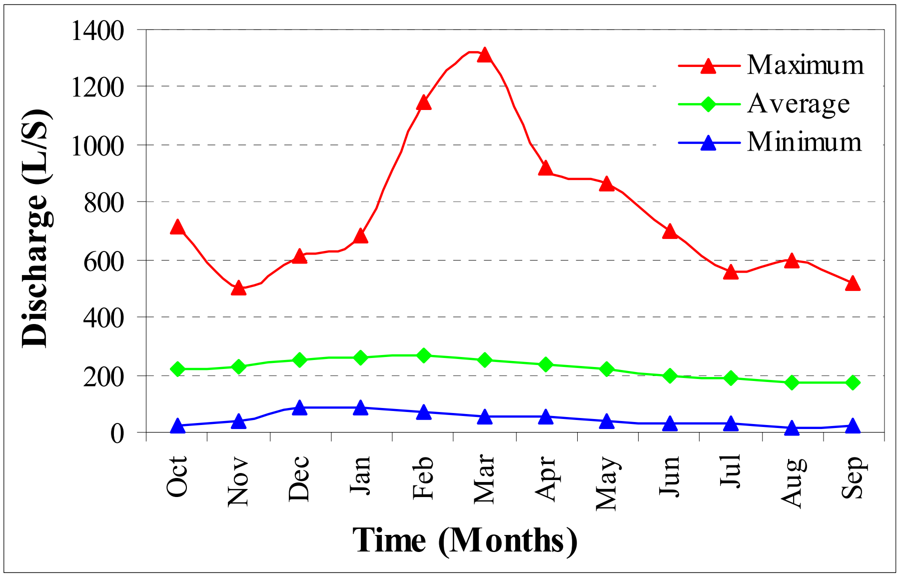

Figure 14: Average, Maximum and Minimum Monthly Discharge of Total Springs within Al-Faria Sub-catchment

3.4 Surface Water

3.4.1 Flow Measurements

No detailed runoff data were available for Faria catchment. The only hydraulic structure which was constructed in the early 70's for measuring surface runoff in the Faria catchment is located next to Ein Shibli in the lower central part of the catchment. This hydraulic structure is a wide crested weir which is used as a diversion structure to Al-Faria Irrigation Project. The structure has an upstream stage gage which could be monitored to estimate runoff flows. However, the structure does not have an automatic recorder to register water stage continuously. Therefore, only few sporadic measurements are available for runoff rates from structure. These measurements are not sufficient to estimate the volume of annual runoff through the structure. In August 2003, An-Najah National University in coordination with GLOWA JR project established two

Venturi Flumes at Jiser Al-Malaqi to measure runoff rates from both Al-Faria and Al-Badan wadis. GLOWA JR project is an interdisciplinary project that studies the "Impacts of Global Changes on Water Resources in Wadis Contributing to the Lower Jordan Basin". GLOWA project is a German funded project by the German Ministry of Education and Research and is managed by German, Jordanian and Palestinian institutes. Water and Environmental Studies Institute (WESI) of An-Najah University is a counterpartner for Package 2 of GLOWA project researching the water resources in Jordan River.

The Flume of Al-Badan wadi was designed to measure 25 m^3/s and 0.23 m^3/s of maximum and minimum flows respectively. Maximum and minimum flows that can be measured by Al-Faria wadi Flume are 15 m^3/s and 0.19 m^3/s respectively. In case of low flows the Parshall Flumes are not significantly accurate.

There are two reading gauges at each Flume to measure the flow depths at the critical sections, which are converted into flow rates using the designed empirical formulas. The constructed Flumes are still working and the records are available for the two years (2003-2005) since their construction. The Flumes did not have automatic recorders during the first year. The automatic recorders were constructed later and are available since the second year. Photos of the two Flumes are presented in **Appendix D1**. The recorded runoff data are tabulated as in **Appendix A5**.

Surface runoff of the Faria catchment is considered high compared to other catchments in the West Bank. Within the catchment the runoff decreases from west to east as the slope becomes relatively gentile eastwards down the main stream where rainfall rates reduce also.

The city of Nablus discharges untreated industrial and domestic wastewater effluents to Al-Badan wadi while Al-Faria camp discharges untreated domestic wastewater to Al-Faria wadi. Therefore, the stream flow of the Faria catchment is a mix of:

1. Runoff generated from winter storms. This includes urban runoff from the eastern side of the city of Nablus and other built up areas in the catchment.

2. Untreated wastewater of the eastern part of Nablus and of Al-Faria camp.

3. Fresh water from springs which provides the baseflow for the wadi preventing it from drying up during hot summers.

Farmers use part of the flowing water for irrigation while the rest discharge into the lower Jordan valley or lost through evaporation.

3.4.2 Quality Considerations

No considerable measurements for surface water quality are available for the Faria streams. All the quality measurements conducted in the area are performed for the springs and wells. Since the source of water for the Faria wadi are mostly from springs, then the water quality is dependent on the water quality of these springs. Measurements for spring water quality showed that these springs are generally of good water quality especially chemical quality. The chemical quality data of water from all the springs of the Faria catchment show low concentrations of salts. Therefore, the chemical quality of the Faria streams is good and water is suitable for irrigation (EQA, 2004). A major source of pollution comes from the Nablus municipality. Nablus dumps untreated effluent from its sewage network directly into the Al-Badan wadi, a tributary of the mean wadi of the Faria catchment. The Faria refugee camp disposes of some of its solid waste in pits and the rest by trucking it to a site 1.5 km from the camp to be burned. The effluent is drained into the wadi a few hundred meters away from the camp and wastewater from homes is often dumped directly into the streams or into open ditches.

Another source of water contamination is the livestock that use wadis and springs as a drinking water source, and pollute the water with fecal matter. Moreover, local herders bring their sheep and goats to the streams to wash them and to shear the sheep, thereby polluting the surface waters. Finally, an extremely significant pollution factor is the waste disposal and use of agricultural chemicals by the Israeli colonies. However, no information or data are currently available to be considered in this study.

However, due to the discharge of untreated wastewater into the wadi its quality has deteriorated significantly. An eye inspection of the wadi and the wastewater entering into it gives an indication of the high deterioration in its quality. Historical data and measurements are not available to quantify such deterioration. Accordingly, samples from the outlet streams (Flumes) of the upper two sub-catchments were collected and analyzed in the context of GLOWA JR project. Samples were taken during different times to study the seasonal variation of the surface water quality. **Table 3** shows a summary of the results for the samples collected during the years 2004 and 2005.

Table 3: Surface Water Quality Parameters for Badan and Faria Streams

Date		Parameters						
		EC *µs/cm*	PO_4 Ppm	NO_3 ppm	COD Ppm	Turbidity Unit	Total.C /100ml	Fecal.C /100ml
May, 2004	Badan	844	0.30	39.1	32	1.1	1200	700
	Faria	571	0.00	15.9	0	5.7	900	600
Aug, 2004	Badan	790	0.40	16.3	120	3.1	3500	2500
	Faria	494	0.00	13.6	0.0	3.5	2600	1500
Dec, 2004	Badan	806	0.03	19.8	46.5	5.5	3000	2100
	Faria	610	6.00	17.1	0.0	4.1	500	300
Jan, 2005	Badan	732	3.00	16.7	0.0	3.5	2300	1900
	Faria	630	0.27	14.0	0.0	18.7	1400	1000
Feb, 2005	Badan	616	0.30	19.8	0.0	3.1	10000	8000
	Faria	636	0.22	19.4	0.0	10.5	1000	800
Mar, 2005	Badan	695	0.20	22.4	0.0	1.2	9000	7000
	Faria	697	0.01	25.0	0.0	5.4	8000	6500

Results of the wadi water quality analysis show that runoff during winter as well as peak discharge periods improve the quality of the water in the stream. This is mainly due to the mixing factor. In addition, the microbiological analysis shows that contamination of the water is caused by the untreated wastewater that is flowing from Nablus city and Faria Village and Camp. In general, it is concluded that effluent of untreated wastewater is the main threat to surface water quality of the catchment. This wastewater disposal is causing a major threat not only to the quality of surface water but also to land and soil resources within the catchment.

3.5 Soil

The major soil types found in the Faria catchment are as follows (Orthor et al., 2001):

1. Grumusols

2. Loessial Seozems

3. Calcareous Serozems

4. Terra Rossas Brown Rendzinas

Characteristics of these types are adopted from the document entitled, Environmental Profile for The West Bank, Volume 5, Nablus Profile, ARIJ, 1996. **Table 4** shows the characteristics and the areas of the major soil types in Faria catchment. These soil types are spatially distributed over the catchment as illustrated in **Figure 15**.

From the table and the figure it is noticed that Terra Rossas Brown Rendzinas soil and Loessial Seozems cover most of the catchment. These two types; taking up not more less than 70% of the total area. In addition, Loessial Seozems is concentrated in the middle part of the catchment, where Grumusols is distributed over the catchment.

Table 4: Major Soil Types and Characteristics in Faria Catchment

Soil Type	General Characteristics	Area (%)
Grumusols	Parent materials are fine textural alluvial or Aeolian sediments	13
Loessial Seozems	Parent rocks are conglomerate and chalk	25
Calcareous Serozems	The soil is highly calcareous with grayish-brown color. The texture is medium to fine. Parent rocks are limestone, chalk and marl	19
Terra Rossas Brown Rendzinas	The parent materials for this type of soil are originated from mainly dolomite and hard limestone. Soil depth varies from shallow to deep (0.5 to 2 m)	44
Total		**100**

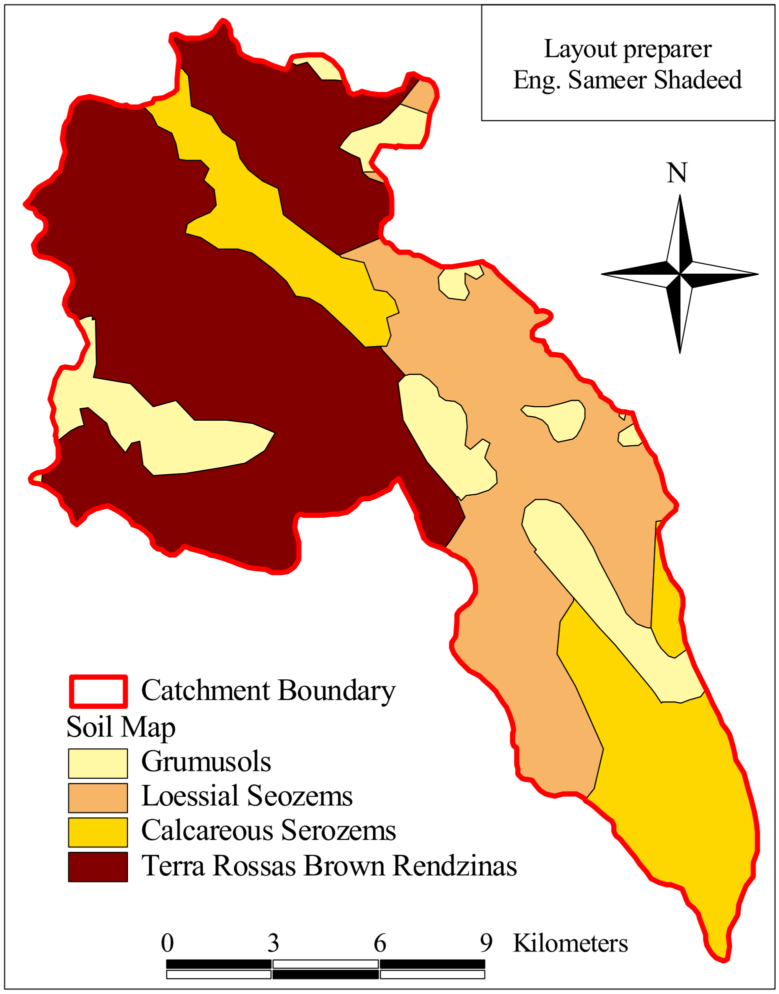

Figure 15: Soil Types of the Faria Catchment

3.6 Geology

Faria catchment is a structurally complex system with Al-Faria Anticline that trends northeast to southwest acting as the primary controlling feature. Additionally, a series of smaller faults and joints perpendicular to this anticline have a significant effect on the surface water drainage area. The geological structure of the Faria catchment is composed form limestone, dolomite and marl. The rocks vary in its thickness, some of them are more than two meters and some of them are intermediate thickness of about 40-100cm. The rock formations were deposited at the second time Mezosy and mostly refer to the geological Era of Mezosy. The rocks have much intensity of fissures, because of the geological history that the area had faced. The faults and fissures reflect the geological conditions of the area passed and affected the hydrology by a huge infiltration quantity and the appearance of many springs as Badan, Faria, and Miska (Ghanem, 1999).

Figure 16 illustrates the geology map of the Faria catchment. **Figures 16** and **15** were taken and modified from the data base of the study entitled, A Harmonized Water Data Base for the Lower Jordan Valley (Orthor et al., 2001).

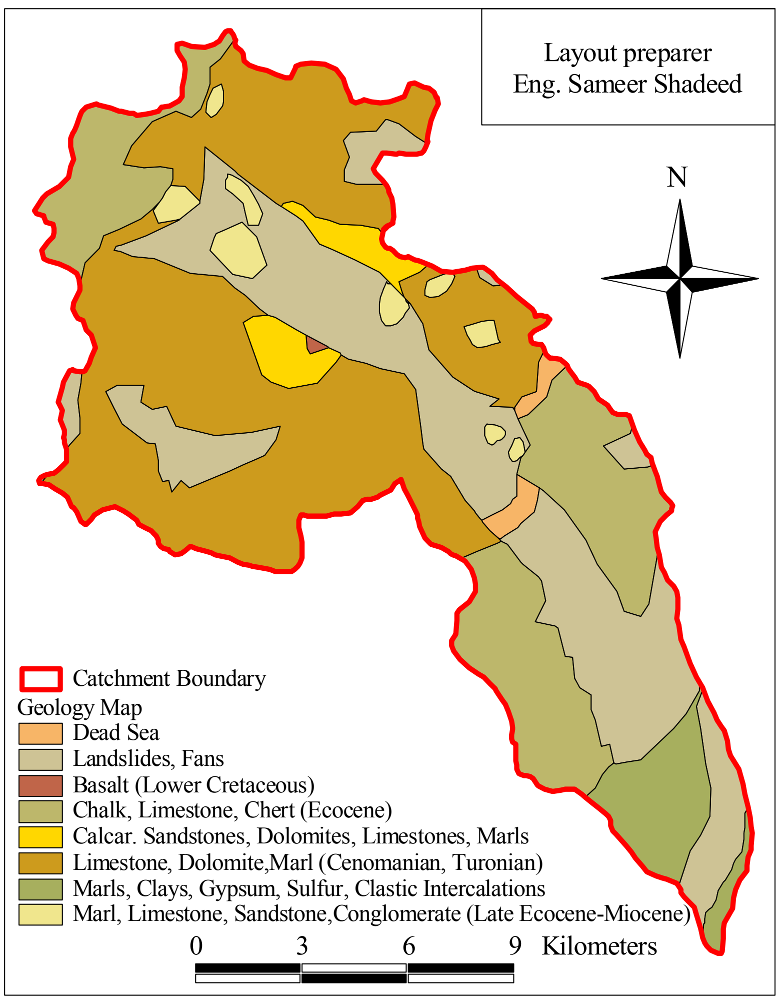

Figure 16: Geology Map of the Faria Catchment

3.7 Land Use

The catchment area which has an area of about 334 km^2 includes Al-Faria Valley which is one of the most important agricultural areas in the West Bank. A new land use map of the Faria catchment has been developed in the context of GLOWA JR project. The land use images, which are available by Environmental Quality Authority, PHG and Birzeit University, were used in addition to the topographic map and airphotos to shape the new land use map. Part of the airphotos that were used is illustrated in **Figure 17**.

Figure 17: Part of the airphotos of Faria Catchment

Ground truthing has been conducted to investigate the actual ground cover. For that purpose, the catchment was visited several times and several photos were snapped that cover the natures of the catchment as presented in **Appendix D2**.

The land use map of the Faria catchment was classified into four classes. These classes are artificial surfaces, agricultural areas, forests and semi natural areas and water bodies. **Table 5** presents these classes, the area of each class, its categories and its percent from the whole catchment. The following is a description of these land use classes.

1. Artificial Surfaces

The artificial surfaces in the catchment are composed of refugee camps, urban fabrics, Israeli colonies and military camps. The military camps and colonies are used by the Israeli occupation authorities and settlers. The total area of the artificial surfaces is 18047 dunum presenting about 5.5 % of the total area of the catchment. The actual figure is higher due to the fact that most of the roads and associated land were kept out of the scope of the study because of the unit limitations. This percentage is less than that of artificial surfaces in the West Bank (8%) which indicates that the area is not densely populated due to the harsh topography of the nonagricultural area in addition to the political restrictions (EQA, 2004).

2. Agricultural Areas

The agricultural land in the catchment is composed of an arable land and heterogeneous agricultural areas. Arable land involves non-irrigated arable land, drip-irrigated arable land, olive groves, palm groves and citrus plantations. The heterogeneous agricultural areas involve irrigated and non-irrigated complex cultivated pattern and land principally occupied by agriculture with significant areas of natural vegetation. The area of the agricultural part of Faria catchment is 115447 dunum which represents about 34.4%. This percentage is lower than that of the West Bank of about 39% (EQA, 2004).

3. Forests and Semi Natural Bodies

This group of land use cover is composed of coniferous forests, natural grassland, bare rocks, sparsely vegetated area and halophytes. The forests and semi natural bodies in the Faria catchment occupy an area of about 201087 dunum representing 60% from the total area. It is worth mentioning that most of the Israeli colonies were built at the expense of forests and semi natural areas under the cover of many military laws that consider the forests and vast natural areas as state owned land.

4. Water Bodies

No perennial rivers are available in West Bank other than the Jordan River that represents the eastern border of West Bank and Faria wadi. Most of the water courses are seasonal and could be added to the land use maps as linear features of a width less than the threshold of the smallest unit mapped.

There are no water bodies controlled by the Palestinians that are large enough to be drawn on the maps of this study. On the other hand there are few water bodies on the Jordan Valley and Faria stream near the Jordan River that are controlled by the Israeli occupation and are utilized for irrigation and fishing (EQA, 2004). One of the artificial water surfaces constructed by the Israeli Authorities is the Tirza reservoir, which has an area of about 250 dunum.

Table 5 displays the total land use cover of the Faria catchment. From the table, it is clear that the nonagricultural area is dominant and above the average of the nonagricultural area in the West Bank. The modified land use map is shown in **Figure 18**.

Table 5: Total Land use Cover of the Faria Catchment

Land use Cover	**Area (Dunum)**	**(%)**
Artificial Surfaces		
Urban fabrics	13300	4
Refugee camps	972	0.3
Israeli colonies	3107	0.9
Military camps	668	0.2
Sub Total	**18047**	**5.5**
Agricultural Areas		
Olive groves	26506	7.9
Palm groves	394	0.1
Citrus plantations	4650	1.4
Non-irrigated arable land	37289	11.1
Drip-irrigated arable land	6978	2.1
Land principally occupied by agriculture	20458	6.1
Irrigated and non-irrigated complex cultivated patterns	19172	5.7
Sub Total	**115447**	**34.4**
Forests and Semi Natural Vegetation		
Bare rocks	12523	3.7
Halophytes	8757	2.6
Natural grassland	111205	33.2
Coniferous forests	4716	1.4
Sparsely vegetated area	63886	19.1
Sub Total	**201087**	**60**
Water bodies/ Artificial surfaces	250	0.1
Total	**334831**	

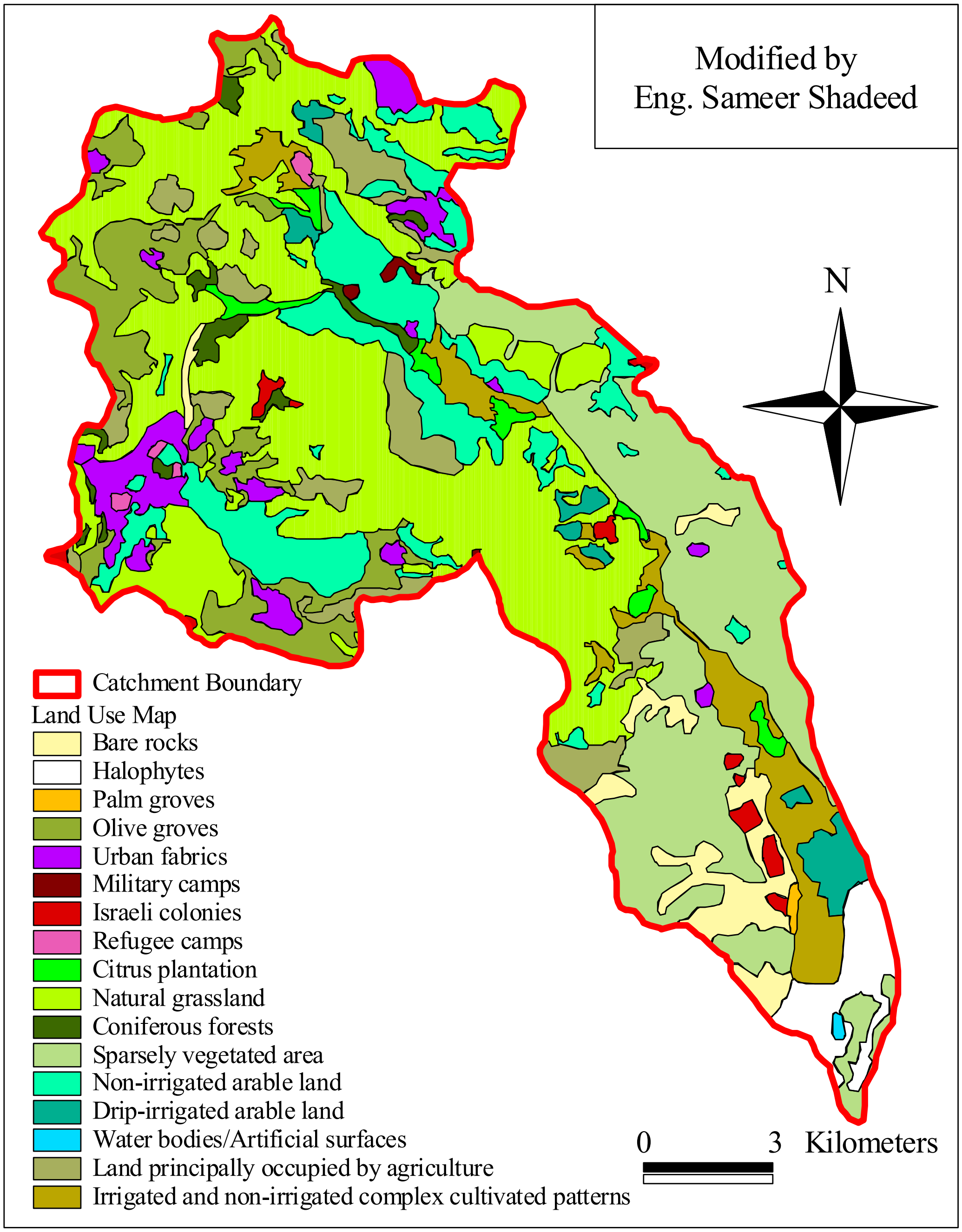

Figure 18: The New Land use Map of the Faria Catchment

CHAPTER FOUR

RAINFALL ANALYSIS

4.1 Rainfall Stations

The Faria catchment is gauged by six rainfall stations that record rainfall. These stations are: Nablus, Taluza, Tammon, Tubas, Beit Dajan and Al-Faria stations. Before 1994, these stations were controlled by the Israeli Authorities. After the establishment of the Palestinian Authority, the stations except one became under the control of the Palestinians. The Nablus station is a regular weather station in which most climatic data are measured. Monthly and annual precipitation for this station is available for more than 55 years.

Al-Faria station is located in Al-Jiftlik village in the lower part of the catchment and is still under Israeli control. This station was established by the Jordanian government as an agricultural experimental station similar to the Deir Alla station on the eastern side of the Jordan River. The station was taken over by the Israeli Occupation Authorities in 1967. The Israeli Authorities neglected the station and therefore its role in serving the Palestinian farmers became insignificant. In 1994, when the Palestinian Authority was established, the Israeli Authorities refused to hand it over to the Palestinians. Therefore, data available from this station is limited to only few years.

The other four rainfall stations are located in the schools of Taluza, Tubas, Tammon and Beit Dajan (see **Figure 10**). These stations are simple rain gages which measure daily precipitation. Data from these stations cover also monthly and annual precipitation for 30 to 40 years. No rainfall intensity charts are available in the catchment except from Nablus station where few years are covered and are available. This is due to lack of continuous measuring instruments for precipitation or other weather data.

Recently, in the context of EXACT project, four Tipping Bucket Rain Gauges were installed in the schools of Taluza, Tubas, Tammon and Beit Dajan. EXACT project is a multilateral project implemented by PWA for the purpose of water resources development including water recharge in the Faria catchment. Data are available for the last rainy season and for three stations only, since Taluza gauge is not functioning.

Selected rainstorm events were chosen from these data and used to test the developed KW-GIUH model as discussed in chapter six. Summary data of the six stations, their elevations and range of data are presented in the **Table 6**.

Table 6: Available Rainfall Stations within the Faria Catchment

Rainfall Station	**Elev. (m)**	**Type of Data**		
		Annual	**Monthly**	**Daily**
		Period		
Nablus Meteorological Station	570	1946-2004	1975-2004	1975-2004
Taluza Primary School Station	500	1963-2004	1963-2004	1967-2004
Tubas Secondary School Station	375	1967-2004	1979-2004	1979-2004
Beit Dajan Station	520	1952-2004	1963-2004	1967-2004
Tammon Primary School Station	340	1966-2004	1958-2004	1967-2004
Al Faria Meteorological Station	-237	1952-1989	1967-1989	1967-1989

4.2 Catchment Rainfall

4.2.1 Density of Rain Gauges

The following statistical analysis helps to obtain the number of gauges for a catchment optimally on the basis of an assigned percentage of error in estimating the mean areal rainfall.

$$N = \left\{ \frac{C_v}{E_p} \right\}^2 \qquad 1$$

Where N is the optimal number of stations, E_p the allowable percentage of error in the estimation of mean aerial rainfall, C_v is the coefficient of variation of the rainfall from the existing stations in percentage. Coefficient of variation can be calculated applying the following steps on the data of existing n stations.

1. Calculate the mean of rainfall from the equation $P_{av} = (1/n)\sum P_i$ **2**

2. Calculate the standard deviation as $\sigma_{n-1} = \left\{ \frac{1}{(n-1)} \sum (P_i - P_{av})^2 \right\}^{\frac{1}{2}}$ **3**

3. Compute the coefficient of variation as $C_v = \frac{\sigma_{n-1} \times 100}{P_{av}}$ **4**

If the allowable percent of error in estimating the mean rainfall is taken higher, then the catchment will require fewer numbers of gauges and vice-versa. The allowable percentage of error E_p is normally taken as 10%. While computing the value of C_v and if its value comes less than 10%, it can be assumed that the existing stations are sufficient for the catchment. The additional station required for the catchment can be found as (N-n). Annual rainfall values are normally used in the above analysis. Additional stations are to be established at the appropriate locations giving an even distribution over the catchment (Patra, 2001).

Based on information from the six stations in Faria catchment, the above statistical parameters have been calculated:

$P_{av} = 431.4$

$\sigma_{n-1} = 175.1$

$C_v = 40.6$

$N = 11$

Based on a 12% permissible error and rainfall data of available stations, the minimum required number of stations is 11.

Existing stations (n) = 6

Additional stations required = (N-n) = 5

4.2.2 Consistency of Rainfall Data

When analyzing rainfall data; it is essential to check the consistency of the records of the rainfall stations. For Faria catchment, the missing data were first estimated, and then consistency analysis was applied.

Double mass curve technique was used to check the consistency of the stations of the Faria catchment. The cumulative rainfall data of a specific station is plotted against the accumulative average rainfall of the remaining stations. The results of the consistency analysis are plotted in **Figure 19**. From the figure, it is clear that all the stations are internally consistent, and the data can be further analyzed. The data plotted in **Figure 19** are for the periods 1946-2003 for all the stations except for Al-Faria station, which are for 1951-1989.

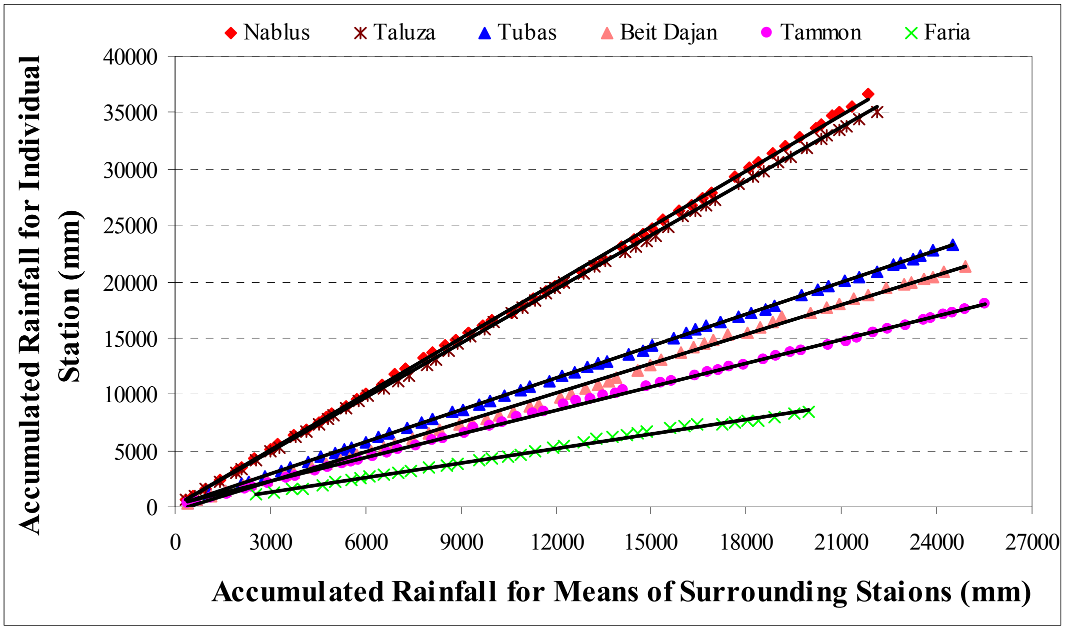

Figure 19: Double Mass Curve for the Stations of Faria Catchment

4.2.3 Monthly Rainfall

The average monthly rainfall of the six stations of the catchment is plotted in **Figure 20**. The plots indicate the wet period from November until April and that there is a relatively dry period from May to October. This is associated with the climatic conditions of the catchment.

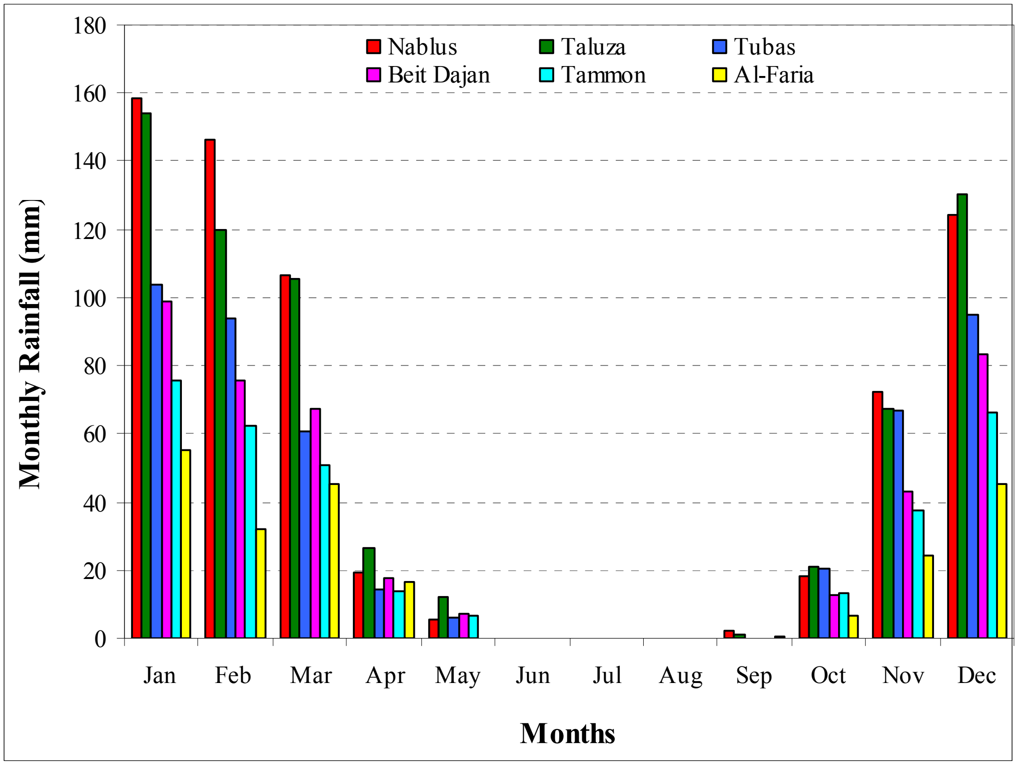

Figure 20: Mean Monthly Rainfall of the Six Stations of the Faria Catchment

Monthly rainfall data from the meteorological station in Nablus are analyzed for the years from 1970 to 2000. The average monthly rainfall, standard deviation, maximum and minimum were estimated, the results are presented in **Table 7**. The available data for the 30 years were divided into six intervals. The intervals include the rainfall of the years of 1970-75, 1975-80, 1980-85, 1985-90, 1990-95 and 1995-00 respectively. The % monthly average of the rainy months of each group was found. The cumulative percent was estimated and plotted in **Figure 21**. It can be concluded that there is no significant difference between the monthly distributions of the rainfall during the years. All plots have nearly the same slopes and shapes. This means that the monthly distribution of the rainfall during the months has nearly the same style.

Table 7: Monthly Rainfall Totals of Nablus Station (mm)

Year	Sept.	Oct.	Nov.	Dec.	Jan.	Feb.	Mar.	Apr.	May.
70-71	8.5	7.1	9.5	124.6	104.6	110.9	49.3	224.6	0.0
71-72	0.0	0.0	57.3	184.3	140.7	167.2	94.3	27.3	0.0
72-73	0.1	14.0	39.6	63.6	163.9	23.2	104.3	12.5	21.8
73-74	0.0	16.3	105.5	66.5	389.3	115.6	41.3	39.5	0.0
74-75	0.0	0.0	55.4	137.1	55.4	194.6	82.0	4.2	0.0
75-76	23.1	3.8	47.2	108.3	93.1	152.0	150.1	27.0	0.0
76-77	0.2	32.7	90.1	46.6	158.5	73.1	128.2	85.7	1.5
77-78	0.0	82.6	2.9	192.6	79.2	60.0	82.8	8.2	0.0
78-79	0.0	20.1	6.7	104.2	116.7	20.4	75.7	5.0	0.3
79-80	0.0	39.7	158.9	226.5	113.8	165.4	155.5	21.8	1.7
80-81	0.4	15.0	8.9	192.7	211.3	142.5	67.3	23.1	0.0
81-82	0.0	0.0	135.1	19.9	92.6	171.2	129.6	7.0	2.3
82-83	0.0	10.3	0.0	115.8	267.0	322.9	219.9	14.8	3.6
83-84	0.9	0.0	70.4	24.2	155.2	85.2	0.0	0.0	0.0
84-85	0.0	21.5	29.6	58.5	65.5	245.3	20.1	23.2	1.4
85-86	0.0	19.9	47.1	42.9	93.0	163.2	48.7	46.8	65.1
86-87	0.5	52.4	249.6	141.4	130.0	62.3	120.0	1.9	0.0
87-88	0.0	52.9	23.2	224.0	126.9	310.9	94.9	0.0	0.0
88-89	0.0	16.0	55.8	236.7	96.3	46.6	115.2	0.0	0.0
89-90	0.0	5.9	94.9	128.3	131.6	98.9	53.3	53.0	0.0
90-91	0.0	3.5	24.3	9.5	251.4	74.3	103.8	30.1	8.0
91-92	0.0	12.7	153.5	472.2	266.8	444.7	69.7	4.7	28.5
92-93	0.0	0.0	84.9	360.9	142.3	117.7	68.5	5.8	18.5
93-94	0.0	14.7	20.8	28.7	192.5	114.0	129.1	9.0	0.0
94-95	0.0	20.6	263.5	186.0	57.9	95.4	43.1	35.3	0.2
95-96	0.0	1.8	118.8	59.2	229.8	35.9	228.7	33.4	0.0
96-97	0.0	34.1	16.4	85.44	166.0	268.6	233.1	22.7	40.2
97-98	17.6	16.3	59.9	167.9	148.2	91.9	244.5	5.0	7.8
98-99	1.6	1.6	4.9	40.3	169.1	64.4	41.5	21.6	0.0
99-00	0.0	5.8	16.3	39.9	471.2	84.7	80.1	0.4	0.0
AVG	1.8	17.5	68.4	129.6	162.7	137.4	102.5	26.5	6.7
STD	5.3	19.5	68.3	104.4	93.6	97.9	63.4	42.0	14.7
MAX	23.1	82.6	263.5	472.2	471.2	444.7	244.5	224.6	65.1
MIN	0.0	0.0	0.0	9.5	55.4	20.4	0.0	0.0	0.0

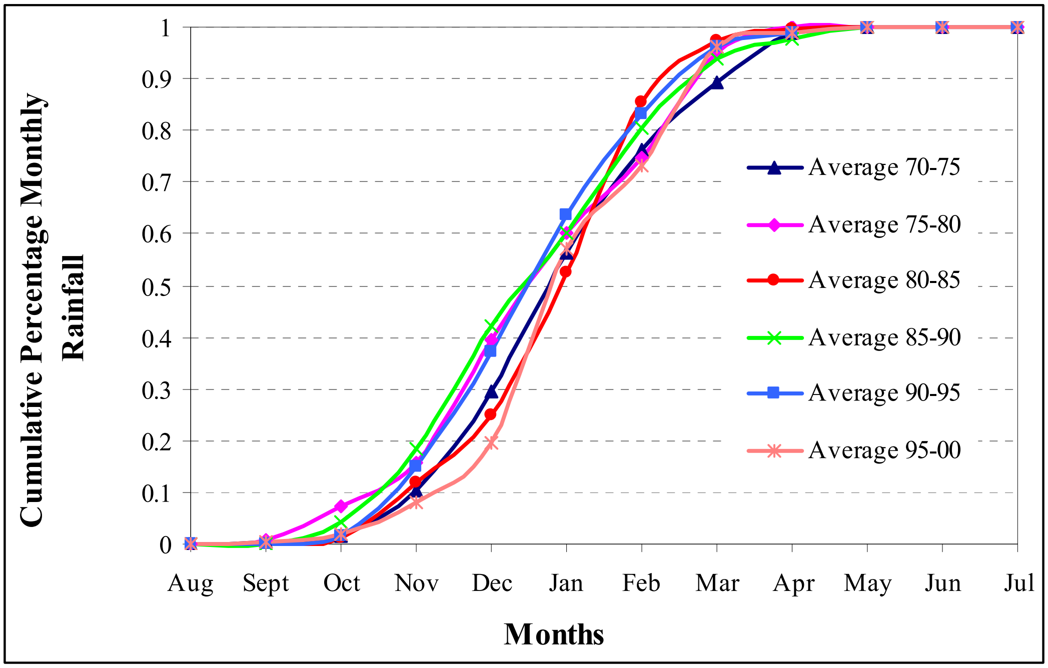

Figure 21: Monthly Average Rainfall of Nablus Station Plotted As Averages of Five Years Intervals

4.2.4 Annual Rainfall

Rainfall data for five stations were obtained from PWA and from Nablus meteorological station for Nablus station. The rainfall data for the stations for the 50 last years are presented in **Appendix A6**.

Statistical analysis has been utilized for the rainfall data of the six stations of the Faria catchment. This includes the annual average (AVG), the standard deviation (STD), the maximum (MAX) and the minimum (MIN) rainfalls recorded by these stations as tabulated in **Table 8**.

Table 8: Statistical Measurements of the Annual Rainfall of the Six Stations of Faria Catchment

Rainfall Station	AVG (mm)	STD	MAX (mm)	MIN (mm)
Nablus Meteorological Station	642.6	203.3	1387.6	315.5
Taluza Primary School	630.5	196	1303.1	292.2
Tubas Secondary School	415.2	143.9	899.5	201.5
Beit Dajan Station	379.1	134.8	777	141
Tammon Primary School	322.3	106.4	616.1	124.2
Al-Faria Meteorological Station	198.6	83	424	30

From the table it is noticed that Nablus and Taluza stations have the largest average annual rainfalls, whereas Al-Faria station has the lowest average annual rainfall. Tubas station has an average annual rainfall of 415 mm, which nearly equals the arithmetic average of the annual average rainfalls of the six stations of the Faria catchment at about 430 mm. In general, rainfall decreases from north to south and west to east. All stations are functioning except Al-Faria meteorological station which was put in still in the year 1989.

The annual rainfall for Nablus station is as shown in **Figure 22**. The full time series for all six stations are enclosed in **Appendix B1**.

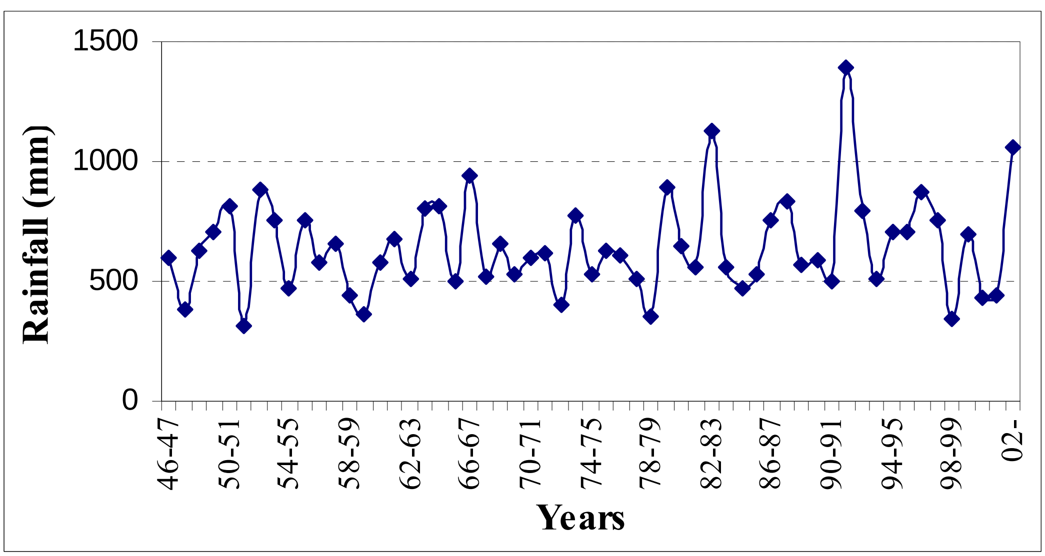

Figure 22: Yearly Rainfall of Nablus Station

From the figure it is noticed the highest total annual rainfall occurred in the year of 1992 and reached about 1350 mm. In other words, the exceedance probability for such extreme value is equal zero.

4.2.5 Trend Analysis

Simple trend analysis of the 5-years moving average is applied to the available annual rainfall data of the six stations. The average of the first 5-years rainfalls is calculated, and then the average of the next 5 records excluding the first and including the sixth is computed. The procedure continues by finding the average of the following 5 years and so on. **Figures 23** and **24** show the trends for the six stations, whereas **Table 9** tabulates the results of the linear regression applied to the moving average values of the stations.

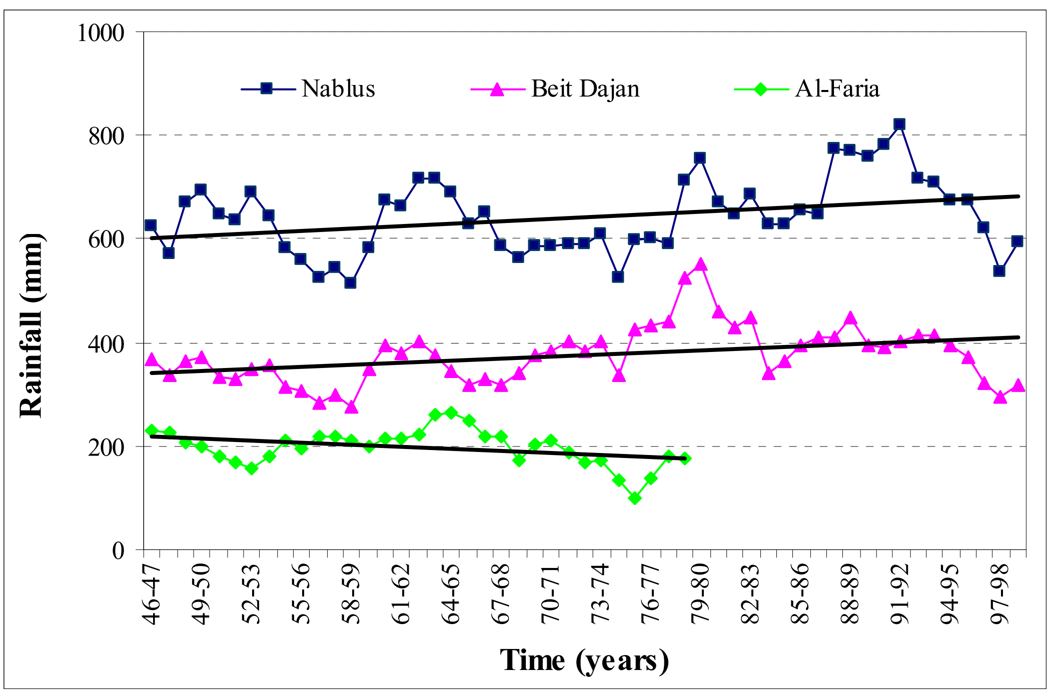

Figure 23: The 5-year Moving Average of Nablus, Beit Dajan and Al-Faria Stations

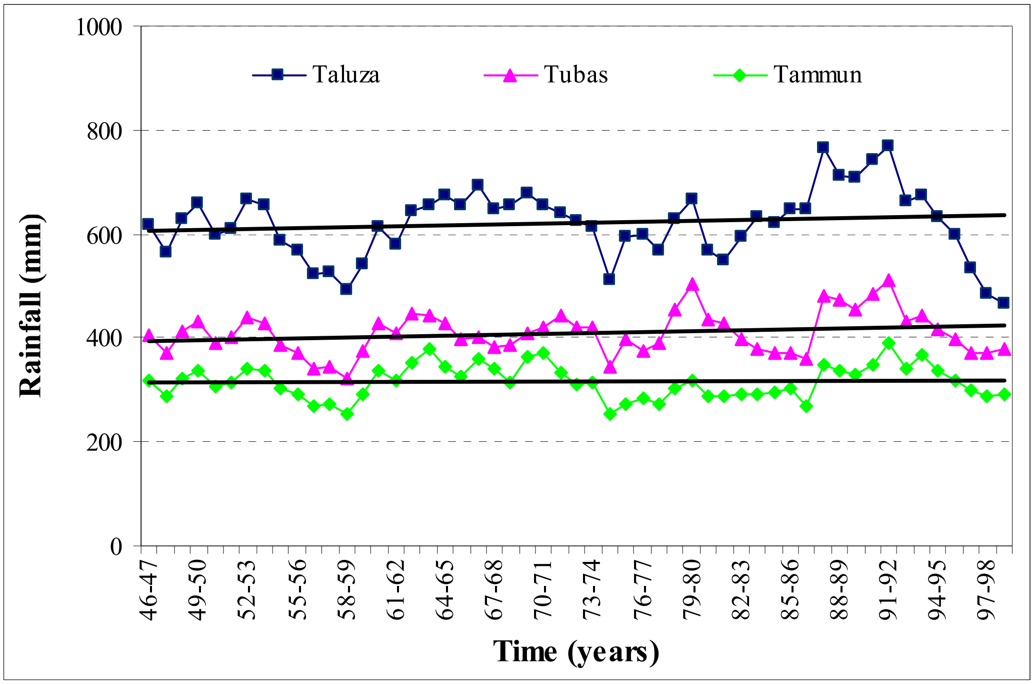

Figure 24: The 5-year Moving Average of Tubas, Taluza and Tammun Stations

Table 9: Trend Equations for the 5-years Moving Average of the Six Stations

Rainfall Station	**Trend Equation Y = (bX+a)**	r^2
Nablus Meteorological Station	1.550 X + 601.5	0.1107
Taluza Primary School	0.565 X + 604.9	0.0172
Tubas Secondary School	0.594 X + 393.0	0.0514
Beit Dajan Station	1.327 X + 340.0	0.1352
Tammon Primary School	0.087 X + 313.5	0.0017
Al Faria Meteorological Station	-1.363 X + 220.2	0.138

The table and the figures indicate that there is an increasing trend for all stations except for Al-Faria station where the trend is decreasing. The degree of trend which is reflected by the independent variable coefficient (b) of the regression equation varies from 1.55 to 0.087 for the stations of increasing trend.

The significance of the regression equations of the trends can be evaluated by testing the hypothesis H_o: b=0. If this hypothesis is accepted, then estimated Y equals mean Y, i.e.: $\hat{Y} = \bar{Y}$, where $\hat{Y}$ is estimated Y and $\bar{Y}$ is mean Y, or the regression line does not explain a significant amount of the variation in Y, where Y = bX + a.

In this situation one would use mean Y as an estimator for Y regardless of the value of X. The hypothesis H_o: $b=B_o=0$ is equivalent to the hypothesis H_o: r = 0, where r is the correlation coefficient. Test of hypothesis concerning (b) can be done noting that

$$\left(\frac{b - B_o}{s_b}\right) \qquad \mathbf{5}$$

has t-distribution with (n-2) degrees of freedom. Thus the hypothesis H_o: $b=B_o=0$ versus H_o: $b \neq B_o$ is tested by computing

$$t = \left(\frac{b - B_o}{s_b}\right) \qquad \mathbf{6}$$

H_o is rejected if

$$|t| > t_{1-\frac{\alpha}{2}, n-2}$$

The t-test has been conducted for 90% and 95% confidence intervals. The above testing procedure is described in (Hann ,1977). The results of testing are presented in **Table 10**. From the table it is noticed that the hypothesis H_o: $B_o=0$ versus H_o: $B_o \neq 0$ is accepted for all stations except for Nablus and Beit Dajan stations where the hypothesis is rejected. This means that there is no significant trend of the 5-years moving average rainfall within the Faria catchment except for Nablus and Beit Dajan stations.

Table 10: $|t|$ and $t_{1-\frac{\alpha}{2},n-2}$ with 90% and 95% Confidence Intervals

Rainfall Station	$\lvert t \rvert$	$t_{1-\frac{\alpha}{2},n-2}$	
		95%	**90%**
Nablus Meteorological Station	2.5	2	1.67
Taluza Primary School	0.95	2	1.67
Tubas Secondary School	1.66	2	1.67
Beit Dajan Station	2.8	2	1.67
Tammon Primary School	0.29	2	1.67
Al Faria Meteorological Station	1.57	2.04	1.69

4.3 Extreme Value Distribution

The study of extreme hydrologic events involves the selection of a sequence of the largest or smallest observations from the sets of data. For example, the study of peak flows considers only the largest flow recorded each year at a gauging station. Since these observations are located in the extreme tail of the probability distribution of all observations from which they are drawn (the parent population), it is not surprising that their probability distribution is different from that of the parent population. There are three asymptotic forms of the distributions of extreme values, named Type I, Type II and Type III respectively. Type I which is known as Gumbel distribution is used for its simplicity and publicity. It is the most used distribution for rainfall and runoff data analysis especially for annual records (Chow et al, 1988).

Hydrological systems are sometimes impacted by extreme events, such as severe storms, floods, and droughts. The magnitude of an extreme event is inversely related to its frequency of occurrence, very severe events occurring less frequently than more moderate events. One way of analyzing the rainfall data is using frequency analysis. The objective of the frequency analysis of hydrologic data is to relate the magnitude of extreme events to their frequency of occurrence through the use of probability distribution (Chow et al., 1988).

4.3.1 Gumbel Distribution

For the purpose of extreme value analysis, the following procedure has been followed:

1. The annual rainfall values were arranged in descending order over the recorded period and each value was given a rank, r.

2. For each value of rainfall, denoted by x, the probability of exceedance, P(x) was calculated using the Gringorten formula which is appropriate for the analysis of extremes (Chow et al., 1988):

$$P(x) = \frac{(r-0.44)}{(n+0.12)} \qquad \mathbf{7}$$

where:

x: annual rainfall

P(x): the probability of exceedance

r: the rank of x

n: the total number of recorded years

3. The probability of non-exceedance was calculated using the following relation:

$$F(x) = 1 - P(x) = 1 - \frac{(r-0.44)}{(n+0.12)} \qquad \mathbf{8}$$

where:

F(x): the probability of non-exceedance

x and P(x): as defined previously

4. The Gumbel probability distribution is defined as:

$$F(x) = \exp\left(-\exp(-b_g\,(x - a_g))\right) \qquad \mathbf{9}$$

Where:

$$b_g = \frac{\pi}{\sigma\sqrt{6}} \quad \text{and,} \quad a_g = \mu - \frac{\gamma}{b_g} \qquad (\gamma = 0.5772)$$

μ : the mean of all rainfall values

σ : the standard deviation of the rainfall values

5. The estimated Gumbel value of rainfall is defined as follows:

$$\hat{x} = \frac{\left[-Ln\left(-Ln\left(F(x)\right)\right)\right]}{b_g} + a_g \qquad \mathbf{10}$$

Annual rainfall values for the six stations in the Faria catchment were substituted in the above equations of the Gumbel distribution and parameters were calculated and listed in **Table 11**. The square values of the correlation coefficient r^2, are also determined. The Gumbel plots for one station are presented in **Figure 25**. The Gumbel plots for all stations are presented in **Appendix B2**. From the figures and tabulated results it is confirmed that Gumbel distribution can be applied to model the annual rainfall for the rainfall stations of the Faria catchment. From a statistical point of view, all values of r^2 are high, about 0.94, such that the suitability of Gumbel distribution is assumed.

Table 11: Parameters of Gumbel Distribution for the Six Stations of the Faria Catchment

Rainfall Station	μ	σ	$\mathbf{b_g}$	$\mathbf{a_g}$	$\mathbf{r^2}$
Nablus Meteorological Station	642.6	203.3	0.0063	551	0.955
Taluza Primary School	630.5	196	0.0065	542.3	0.941
Tubas Secondary School	415.2	143.9	0.0089	350.5	0.935
Beit Dajan Station	379.1	134.8	0.0095	318.4	0.95
Tammon Primary School	322.3	106.4	0.012	274.4	0.945
Al Faria Meteorological Station	198.6	83	0.0154	161.2	0.944
Standardized of all Stations	0	1	1.282	-0.45	1

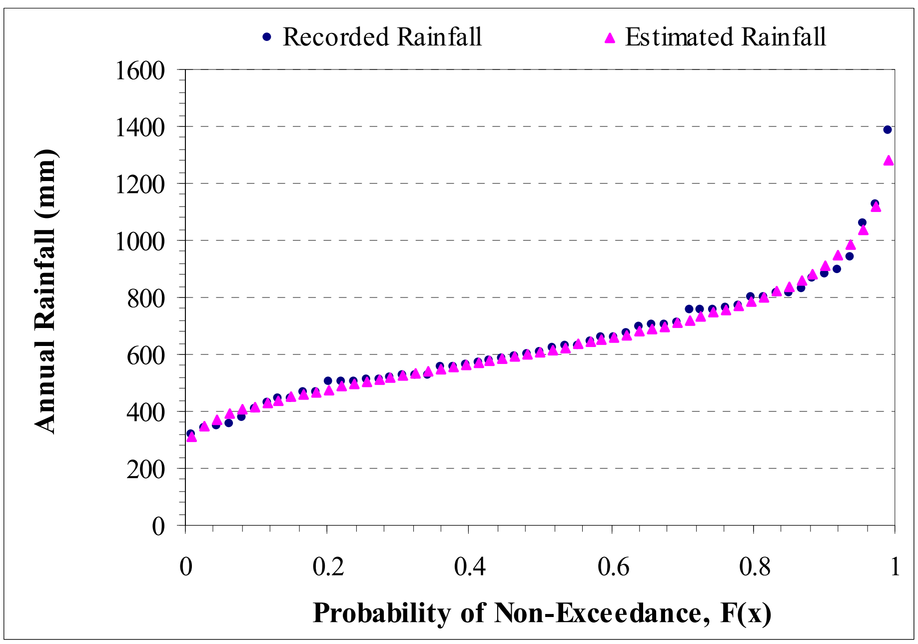

Figure 25: Gumbel Plots of Annual Rainfall for Nablus Station

To generalize things, the standardized variable $[(X-\mu)/\sigma]$ is calculated for the six stations. Gumbel distribution was applied to the standardized variable and is plotted in **Figure 26**. From the figure it is clear that Gumbel distribution is a good representative of the annual rainfall of the Faria catchment.

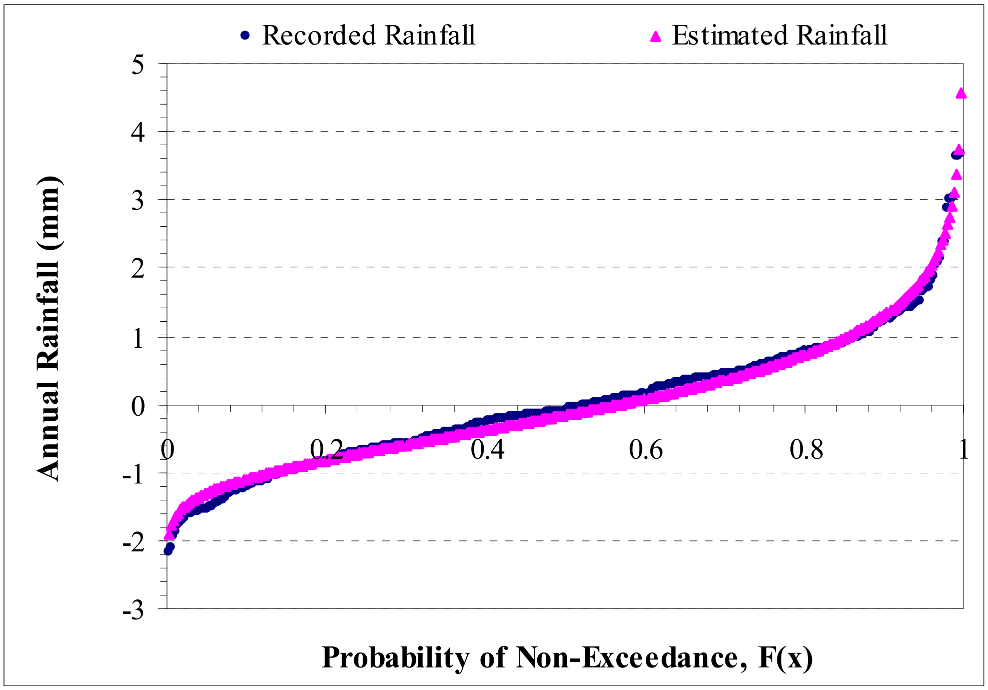

Figure 26: Gumbel Plots of the Standardized Variable of the Six Stations of Faria Catchment

4.4 Areal Rainfall

A rain gauge records rainfall at a geographical point. In most of the hydrologic analysis, average depth of precipitation over the area under consideration ought to be computed. To calculate the spatially distributed rainfall for an area, the point rainfall needs to be converted to areal rainfall. There are several methods available in literature to estimate areal rainfall. However, depending on the accuracy and the objective of the analysis, any of the following methods can be used: arithmetic average, Thiessen polygon, isohyetal, grid point, orthographic or isopercental method (Patra, 2001). In this study Thiessen polygon method has been used as explained in the following section.

4.4.1 Thiessen Polygon Method

The first step in the Thiessen polygon method is to connect all the rain gauges by straight lines so that no lines form an angle greater than 90 degrees. Next, perpendicular bisectors are constructed on the first lines. The bisectors should intersect within the triangular areas. The area of each polygon within the catchment is divided by the total area and expressed as a percentage. The area percent multiplied by the rainfall amount for each polygon gives an estimation of the rainfall over the catchment.

The relative area weight for six polygons enclosing the corresponding stations of Faria catchment in percentages is presented in **Table 12**. **Figure 27** shows the constructed Thiessen polygons in the study area. Areal Rain Extension that works under ArcView GIS environment has been used to delineate the Thiessen polygons and to calculate the areal rainfall.

Table 12: Areal Rainfall Using the Thiessen Polygon Method

Rainfall Station	**Polygon Area (km^2)**	**Weight%**	**Rainfall (mm)**	**Weighted Rainfall (mm)**
Nablus Meteorological Station	36.2	0.11	642.6	69.6
Taluza Primary School	52.2	0.16	630.5	98.4
Tubas Secondary School	19.0	0.06	415.2	23.7
Beit Dajan Station	75.4	0.23	379.1	85.5
Tammon Primary School	48.5	0.15	322.3	46.8
Al Faria Meteorological Station	102.9	0.31	198.6	61.1
Total	334.3	1.00		385.2

The results indicate that the areal average rainfall for the whole Faria catchment extending from Nablus Mountains to the Jordan River is 385 mm; which nearly equals the long term average rainfall of Beit Dajan station.

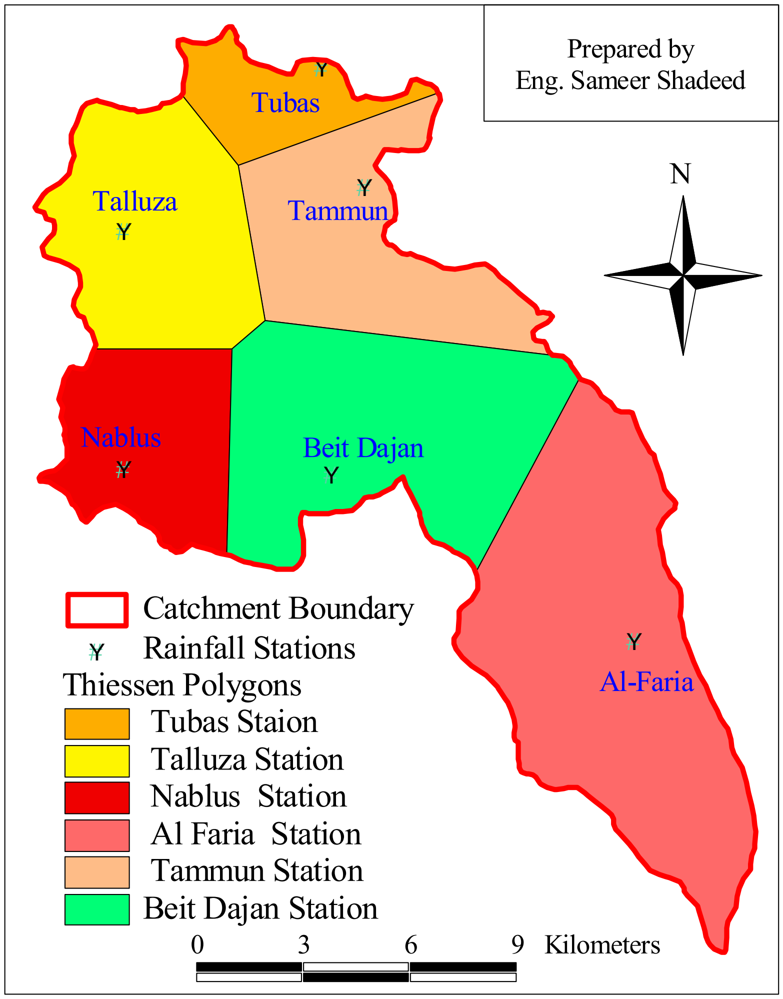

Figure 27: Thiessen Polygon Map for the Faria Catchment

4.5 Correlation Analysis between Stations

The spatiality of rainfall distribution within the Faria catchment is investigated by using the multiple regression analysis. **Table 13** gives the average annual rainfall, the x, y coordinates and the elevation of the six stations. A relation between the average annual rainfall and the coordinates and elevations of the rainfall are developed for five of the stations. The sixth station, Taluza, was left to be used in verifying the results of the regression analysis and to test the resulted regression equation. The resulting equation due to regression analysis of the five stations is:

$$R = 8308 - 39.5X - 2.6Y - 0.3H \quad (11)$$

where:-

R: is the annual average rainfall in mm

X: is the x-coordinate in km

Y: is the y-coordinate in km

H: is the elevation in m

The square value of the correlation coefficient r^2, was determined at about 0.985 which indicates a high correlation between rainfall, coordinates and elevations. The developed relation was used to calculate the annual average rainfall for the stations and the outcome are tabulated as in **Table 13**.

Table 13: Coordinates, Elevations, Rainfall Averages and Estimated Averages for the Six Stations

Station Name	**X Coord. (km)**	**Y Coord. (km)**	**Elev. (m)**	**AVG (mm)**	**Estimated AVG (mm)**
Nablus Meteorological Station	178	178	570	642.6	643.2
Taluza Primary School	178	186	500	630.5	642.6
Tubas Secondary School	185	192	375	415.2	388.8
Beit Dajan Station	185	178	520	379.1	370.4
Tammon Primary School	187	188	340	322.3	351.0
Al Faria Meteorological Station	196	172	-237	198.6	189.9

From the table it is clear that the estimated average annual rainfall is close to the recorded one for Taluza station which is a verification of the results with an error of about 2%. It is then to assume the suitability of the developed relation.

CHAPTER FIVE

RUNOFF MODELING

5.1 Introduction

The computation of flow hydrograph is of great importance to water resources engineers and scientists. Among the most basic challenges of hydrology are the quantitative understanding of the processes of runoff generation and prediction of the flow hydrographs and their transmission to the outlet. The high spatial variability in rainfall intensities and amounts combined with variability in soil properties makes prediction of runoff generation very difficult especially for ungauged catchments. Even in cases where catchments are gauged, the period of record is often too short to allow accurate estimates of the different hydraulic parameters.

Traditional techniques have been widely applied for the estimation of runoff hydrographs at the outlets of gauged catchments using historical rainfall runoff data and unit hydrographs derived from them. Such procedures are questioned for their reliability due to the climatic and physical changes in the catchment and their application to ungauged, arid and semiarid catchments.

In the unit hydrograph theory it is assumed that the potential abstractions are fully met before runoff occurs. This assumption is applicable to humid regions, but is doubtful in arid and semiarid regions. For arid and semiarid regions, the infiltration portion is higher than for humid regions due to higher infiltration rates and dry soil antecedent moisture condition. The infiltrability of the soil is high and the infiltration process will continue significantly during the rainfall event. The amount of actual infiltration may not satisfy the infiltrability of the soil. The evaporation losses are also high in arid and semiarid regions and the evaporation process may occur during the storm. Therefore the applicability of the unit hydrograph approach in semiarid regions should be investigated as to its basic assumption of satisfying the abstraction and neglecting the surface and subsurface flow interaction during the rainfall-runoff process (Shaheen, 2001).

In the West Bank, which is characterized as semiarid region, hydrological modeling has not been given enough care and no intensive studies have been done. However, this study is an attempt to hydrologically investigate and to derive the unit hydrograph for the Faria catchment as one of the most important catchments of the West Bank, since the catchment has not been modeled using appropriate rainfall-runoff model so far. The KW-GIUH model that was developed for ungauged catchments is to be used in the modeling.

5.2 GIUH Model

Hydrological simulation models can take the form of theoretical linkage between the geomorphology and hydrology. The geomorphological instantaneous unit hydrograph (GIUH) is one approach of these kinds of models. The GIUH focuses on finding the catchment response given its geomorphological features. The model uses catchment characteristics to predict flow rates. GIUH can be applied to any excess rainfall through convolution to produce the direct runoff hydrograph.

GIUH approach has been applied by several engineers to predict runoff from rainfall for ungauged catchments. They have been proposed to estimate floods for ungauged streams by using the information obtainable from topographic maps or remote sensing possibly linked with the

Geographic Information Systems (GIS) and Digital Elevation Models (DEM) (Snell and Sivapalan, 1994; Jain et al., 2000; and Hall et al., 2001).

Lee and Chang (2005) reviewed the development of GIUH approach and concluded that the significant advance in research on the topographic runoff approaches was the development of the geomorphologic instantaneous unit hydrograph model (GIUH) proposed by Rodriguez-Iturbe and Valdes (1979). During the last two decades, the use of catchment geomorphologic characteristics in runoff simulations has received a great deal of attention from hydrologists (e.g. Gupta et al., 1980; Rodriguez-Iturbe et al., 1982; Kirshen and Bras, 1983; Karlinger and Troutman, 1985; Agnese et al., 1988; Chutha and Dooge, 1990; Lee and Yen, 1997; Yen and Lee, 1997; Olivera and Maidment, 1999; Berod et al., 1999; Brooks and McDonnell, 2000).

The concept of the Geomorphological unit hydrograph is introduced by Rodriguez-Iturbe and Valdes in 1979. This method is based on the Horton-Strahler ordering law.

In the Strahler system for stream ordering and catchment ranking a stream segment with no tributaries is called a first order segment. When two stream segments of the same order meet, the order of the downstream stream segment is raised with one. When two stream segments of a different order meet, the order of the downstream segment is equal to the highest order upstream.

In the GIUH approach, Rainfall excess is assumed to follow different paths on overland areas and in channels of different stream orders probabilistically, according to the drainage pattern to reach the catchment outlet. The travel time of the rainfall excess is assumed to follow a probability distribution in a channel of a given order. The exponential and uniform distributions have been proposed by Gupta et al. (1980). Jin (1992) suggested gamma distribution to get better results. Various methods have been used to determine the time scale to be used with the probability distribution. Rodriguez-Iturbe and Valdes (1979) gave the time parameters as regression equations from discharge records. Agnese et al. (1988) obtained the time scale formula from experimental data. Rodriguez-Iturbe et al. (1982) estimated the first order channel travel time by using a kinematic wave approximation. The travel times of higher order channels were then related to the first order channels through geomorphologic laws. An alternative approach was provided by Lee and Yen (1997). The travel times for different orders of overland areas and channels were derived using the kinematic wave theory and then substituted into the GIUH model to develop a kinematic wave based GIUH model (KW-GIUH) for catchment runoff simulation. The available KW-GIUH program (version 1.2) can be applied to catchments with stream network of up to the seventh order. The program has been developed by Kwan Tun Lee and Chin-Hisn Chang, Watershed Hydrology and Hydraulics Laboratory, Department of River and Harbor Engineering and National Taiwan Ocean University. The KW-GIUH model is applied in this study to predict the runoff hydrographs of the Faria catchment.

5.3 Travel Time Estimation of the KW-GIUH Model

The travel time of the surface flow on a hillslope depends on the slope, surface roughness, and flow depth. The travel times for different orders of overland areas and channels were derived using the kinematic-wave theory and then substituted into the GIUH model to develop a kinematic-wave based GIUH model (KW-GIUH) for watershed runoff simulation. The following is a discussion of the approach applied.

An ith-order sub-basin of the catchment is conceptually simplified as consisting of two identical rectangular form V-shape overland flow planes. Each plane contributes a lateral discharge into a channel of constant cross section and slope as shown in **Figure 28**.

The mean length of the ith-order V-shape overland flow plane is

$$\bar{L}_{o_i} = \frac{AP_{OA_i}}{2N_i \bar{L}_{c_c}} \qquad \textbf{12}$$

Where A is the total area of the catchment, P_{OA_i} is the ratio of ith-order overland area to the total catchment area, N_i is the number of the ith-order channels and $\bar{L}_{c_i}$ is the mean channel length of the ith-order sub-basin.

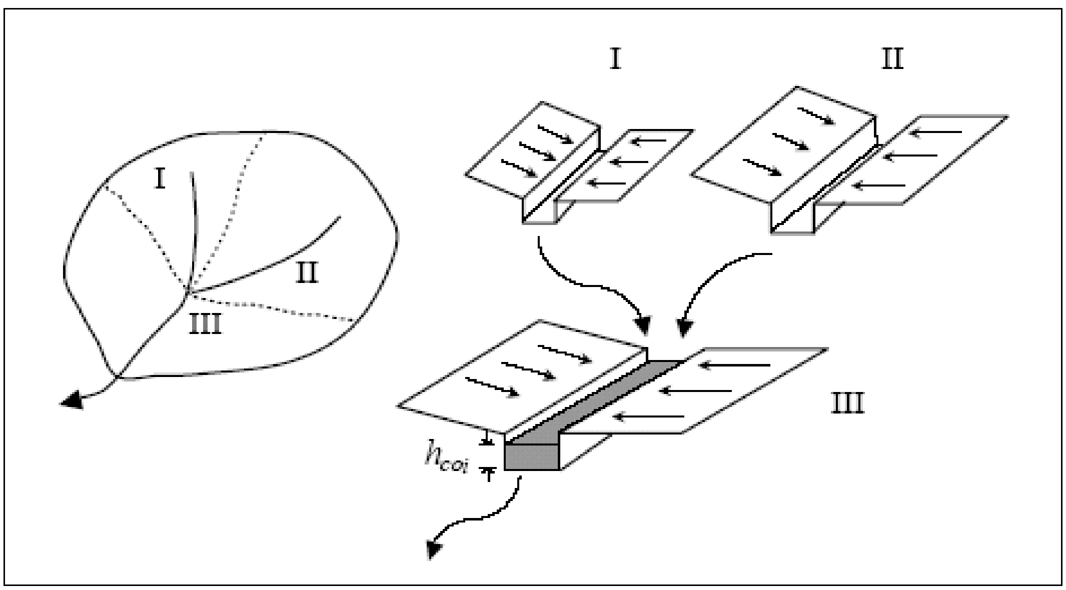

Figure 28: Runoff Structure for a second-Order Catchment (Lee and Chang, 2005)

The flow rate at the end of a plane increase with time until it reaches equilibrium. The longest time for a raindrop to travel through the ith-order overland plane $T_{x_{oi}}$ is the time for the flow to reach equilibrium in the plane. Thus, the discharge for the ith-order overland sub-basin at any time, $t < T_{x_{oi}}$, is

$$q_{o_i} = \frac{\overline{S}_{o_i}^{1/2}}{n_o}(q_L t)^m \qquad 13$$

Where q_{o_i} is the ith-order overland flow discharge per unit width, $\overline{S}_{o_i}$ is the mean ith-order overland slope, n_o is the overland flow roughness coefficient, m is a constant and q_L is the lateral flow rate joining the main flow q_{o_i}.

Once the flow equilibrium state reached, the discharge afterward, $t > T_{x_{oi}}$, is

$$q_{o_i} = q_{os_1} = q_L \overline{L}_{o_i} = \frac{\overline{S}_{o_i}^{1/2}}{n_o} h_{os_i}^m \qquad 14$$

Where q_{os_i} and h_{os_i} represent the ith-order overland discharge and water depth at equilibrium, respectively. The travel time for the ith-order overland plane is

$$T_{x_{oi}} = \frac{h_{os_i}}{q_L} = \left(\frac{n_o \overline{L}_{o_i}}{\overline{S}_{o_i}^{1/2} q_L^{m-1}} \right)^{1/m} \qquad 15$$

Since the sub-basin model is conceptually composed of two identical rectangular planes, the lateral discharge into the central channel is contributed from both side planes. Thus, the lateral discharge becomes $2q_L \overline{L}_{o_i}$. The amount of rain that falls directly onto the channels is small compared to that falling on overland planes and can therefore be neglected. As the flow in the ith-order overland planes gradually increases with time to reach equilibrium, an additional time T_{x_i} is needed for the ith-order channel to reach its equilibrium. A first order channel conveys only the lateral discharge contributed by two first order overland slopes. Thus, the discharge of the first order channel at any $t < T_{x_1}$ is

$$Q_{c_1} = \frac{B_1 \overline{S}_{c_1}^{1/2}}{n_c} \left(\frac{2q_L \overline{L}_{o_1}}{B_1} t \right)^m \tag{16}$$

Where B_1 is the first order channel width, $\overline{S}_{c_1}$ is the mean slope of the first order channel and n_c is the roughness coefficient of the channel flow. And for $t \geq T_{x_1}$

$$Q_{c_1} = Q_{cs_1} = 2q_L \overline{L}_{o_1} \overline{L}_{c_1} = \frac{B_1 \overline{S}_{c_1}^{1/2}}{n_c} h_{cs_1}^m \tag{17}$$

Where Q_{cs_1} and h_{cs_1} represent the first order channel discharge and water depth at equilibrium, respectively. Therefore, the rainwater travel time for the first order channel is

$$T_{x_1} = \frac{B_1 h_{cs_1}}{2q_L \overline{L}_{o_1}} = \frac{B_1}{2q_L \overline{L}_{o_1}} \left(\frac{2q_L n_c \overline{L}_{o_1} \overline{L}_{c_1}}{B_1 \overline{S}_{c_1}^{1/2}} \right)^{1/m} \tag{18}$$

Since the catchment is considered as a multiple sub-basin system, the water is transported successively from lower order to higher order channels. Thus, the discharge for an ith-order (i>1) channel at any time $t < T_{x_i}$ is

$$Q_{c_1} = \frac{B_i \overline{S}_{c_i}^{1/2}}{n_c} \left(h_{co_1} + \frac{2q_L \overline{L}_{o_i}}{B_i} t \right)^m \tag{19}$$

Where h_{co_i} is the water depth at the entrance of the ith-order channel. By considering that the rainwater travels from upstream sub-basins through different paths towards the ith-order sub-basins, h_{co_i} can be expressed as

$$h_{co_i} = \left[\frac{q_L n_c \left(N_i \overline{A}_i - AP_{OA_i} \right)}{N_i B_i \overline{S}_{c_i}^{1/2}} \right]^{1/m} \tag{20}$$

Likewise, for $t \geq T_{x_i}$, the channel discharge at equilibrium is

$$Q_{ci} = Q_{csi} = \frac{B_i \overline{S}_{c_i}^{1/2}}{n_c} h_{co_i}^m + 2q_L \overline{L}_{oi} \overline{L}_{c_{i1}} = \frac{B_i \overline{S}_{c_i}^{1/2}}{n_c} h_{cs_i}^m \qquad \textbf{21}$$

Where Q_{cs_i} and h_{cs_i} represent the ith-order channel discharge and water depth at equilibrium, respectively. Hence, by replacing the h_{cs_1} with $h_{cs_i} - h_{co_1}$ (which represents the increase in flow resulting from lateral flow) and deriving h_{cs_i} from (10), the travel time for the ith-order channel become

$$T_{x_i} = \frac{B_i}{2q_L \overline{L}_{o_i}} \left(h_{cs_i} - h_{co_i} \right) = \frac{B_i}{2q_L \overline{L}_{o_i}} \left[\left(h_{co_i}^m + \frac{2q_L n_c \overline{L}_{o_i} \overline{L}_{c_i}}{B_i \overline{S_{c_i}^{1/\ 2}}} \right)^{1/m} - h_{co_i} \right] \qquad \textbf{22}$$

From the equations presented, the travel times for different order sub-basins can be estimated analytically from overland and channel hydraulics instead of relaying on the catchment specified empirical formulas.

5.4 Structure of the KW-GIUH Model

Overland flow over a permeable soil surface can occur when the rainfall rate is greater than the infiltration capacity or when surface saturation exists in regions near the stream (Lee and Chang, 2005).

When a unit depth of rain excess falls uniformly and instantaneously onto a catchment, the unit rainfall excess is assumed to consist of a large number of independent, noninteraction raindrops. Thus, the whole rainfall-runoff process can be represented by tracing the rainfall excess moving along different paths towards the catchment outlet to produce the outflow hydrograph (Lee and Yen, 1997).

Based on the Strahler ordering scheme, a catchment of order Ω can be divided into different states. For example, **Figure 29** shows the possible travel paths of the rain drops for a third-order catchment. Most of the surface flow occurs on the low portions of the catchment (the shaded area in **Figure 29**); after that, it goes into the adjacent channel and then flows through the stream network to the outlet. Each raindrop falling on the overland region will move successively from lower to higher order channels until it reaches the outlet. The catchment geomorphology is represented probabilistically based on the stream order, instead of simulating the overland surfaces and channels by their individually actual geometry as in the deterministic modeling. The ith-order overland regions is denoted by x_{oi} and x_i represents the ith-order channel, in which i = 1, 2,…, Ω. If w denotes a specified runoff path $x_{oi} \rightarrow x_i \rightarrow x_j \rightarrow ..... \rightarrow x_\Omega$,the probability of a drop of rainfall excess adopting this path can be expressed as

$P(w) = P_{OA_i} . P_{x_{oi} x_i} ... P_{x_i x_j} ... P_{x_k x_\Omega}$,where $P_{x_{oi} x_i}$ is the transitional probability of the raindrop moving from the ith-order overland region to the ith-order channel and $P_{x_i x_j}$ is the transitional probability of the raindrop moving from an ith-order channel to a jth-order channel and is computed as

$$P_{x_i x_j} = \frac{N_{i,j}}{N_i} \qquad \mathbf{23}$$

Where N_{ij} is the number of ith-order channels contributing to the jth-order channels and P_{OA_i} is the ratio of ith-order overland area to the total catchment and is computed as

$$P_{OA_i} = \frac{1}{A}\left(N_i \overline{A}_i - \sum_{i=1}^{i-1} N \overline{A}_i P_{x_i x_j} \right) \qquad \mathbf{24}$$

Where $\overline{A_i}$ is the mean of the drainage area of order i. and is estimated as

$$\overline{A}_i = \frac{1}{N_i}\sum_{j=1}^{N_i} A_{ji} \quad \textbf{25}$$

It should be noted that A_{ji} denotes not only the areas of the overland flow regions that drains directly into the *j*th channel of order i, but it also includes overland areas draining into the lower order channels tributary to this *j*th channel of order i.

The travel time for the overland flow region and for the storage component of a channel are assumed to follow an exponential distribution, but the translation component of a channel is assumed to follow a uniform distribution. For the state x_k, the travel time for the channel storage component and channel translation component are $T_{x_{rk}}$ and $T_{x_{ck}}$, respectively, and the total travel time is $T_{x_k} = T_{x_{rk}} + T_{x_{ck}}$

The IUH can be represented by the convolution of two groups of the probability density functions and is given by:

$$u(t) = \sum_{w} \left\{ \left[f_{x_{oi}}(t) * f_{x_{ri}}(t) * f_{x_{rj}}(t) * \ldots\ldots * f_{x_{r\Omega}}(t) \right] * \left[f_{x_{ci}}(t) * f_{x_{cj}}(t) * \ldots\ldots * f_{x_{c\Omega}}(t) \right] \right\} .P(w) \quad \textbf{26}$$

The first part of equation (25) represents the overland flow region (x_{ok}) and the channel storage component (x_{rk}). The exponential distribution with a mean travel time of T_{xk} is

$$f_{x_k}(t) = \frac{1}{T_{x_k}} \exp\left(\frac{-t}{T_{x_k}}\right), \text{ for all t} \quad \textbf{27}$$

The second part of equation (25) represents the channel translation component (x_{ck}). The uniform distribution with a men travel time of T_{xk} over an interval (0, 2T_{xk}) is

$$f_{x_k}(t) = \begin{Bmatrix} \dfrac{1}{2T_{x_k}}; & 0 \le t \le 2T_{x_k} \\ 0; & otherwise \end{Bmatrix} \quad \textbf{28}$$

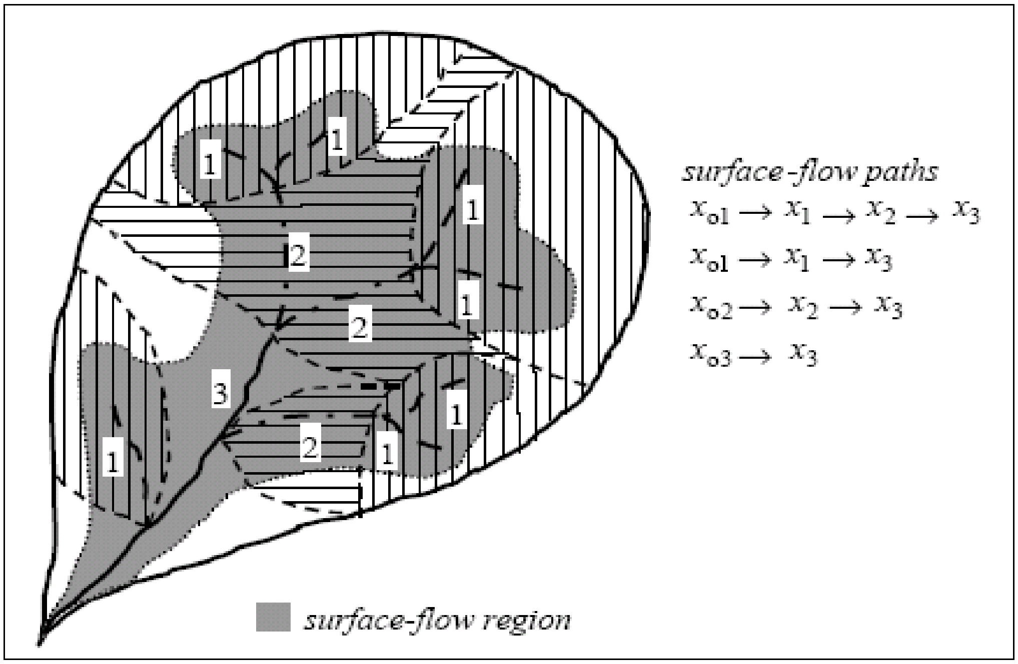

Figure 29: Surface Flow Paths of A third-Order Catchment (Lee and Chang, 2005)

The distribution function bound is set to be from 0 to $2T_{xk}$ because the definition of the mean travel time. Substituting in the previous equation, the IUH can be expressed analytically as:

$$u(t) = \sum_{w \in W} \left\{ \frac{1}{T_M} \left[G(t) + \sum_{k=1}^{N_w} (-1)^k U_{2T_{x_M}}(t).G(t - 2T_{x_M}) \right] \right\}_w .P(w) \quad \textbf{29}$$

Where $U_c(t)$ is a unit step function [$U_c(t)$ = 1 for t $\geq$ c, and $U_c(t)$ = 0 for t < c]; N_w = total number of different order channels in the path w; and

$$T_m = T_{x_{oi}}.T_{x_{ri}}.T_{x_{rj}}...T_{x_{r\Omega}}.(2T_{x_{ci}}).(2T_{x_{cj}})...(2T_{x_{c\Omega}}) \quad \textbf{30}$$

$$G(t) = a_1 + a_2 t + ... + \frac{1}{(N_w - 1)!} a_{N_w} t^{N_w - 1} + b_{oi} \exp\left(\frac{-t}{T_{x_{oi}}}\right) + c_i \exp\left(\frac{-t}{T_{x_{ri}}}\right) + c_j \exp\left(\frac{-t}{T_{x_{rj}}}\right) + ... + c_\Omega \exp\left(\frac{-t}{T_{x_{r\Omega}}}\right) \quad \textbf{31}$$

$$X_M = \{x_{ci}, x_{cj}, ..., x_{ck}\} \in \{x_{ci}, x_{cj}, ..., x_{ck}, ..., x_{c\Omega}\}$$ **32**

$$T_{x_M} = \sum_{i=1}^{M} T_{x_{ci}}$$ **33**

Where M denotes the size of X_M ; and $a_1, a_2, ..., a_{N_w}, b_{oi}, c_i, c_j, ..., c_\Omega = coefficients.$

The coefficients are determined by comparing coefficients in partial fractions after applying the Laplace transformation.

5.5 KW-GIUH Model Input Parameters

In the following sections the input parameters for the application of the KW-GIUH model on the Faria catchment.

5.5.1 Hydraulic parameters

The following notations are used

- Catchment area (km^2)
- Rainfall duration (hr)
- Flow duration (hr)
- Baseflow (m^3/s) or Φ index (mm/hr)
- Hourly rainfall intensity i (mm/hr)
- Hourly discharge (m^3/s)

5.5.2 Geomorphic parameters

- Stream network order Ω

- Overland flow roughness n_o
- Channel flow roughness n_c
- ith-order stream number N_i
- Mean ith-order stream length $\overline{L_{c\,i}}$ (km)
- ith-order sub catchment contributing area $\overline{A_i}$ (km^2)
- Ratio of ith-order overland area to the catchment area P_{OA_i}
- Mean ith-order overland slope $\overline{S_{o\,i}}$ (m/m)
- Mean ith-order channel slope $\overline{S_{c\,i}}$ (m/m)
- Stream network transitional probability $P_{x_i x_j}$
- Channel width at catchment outlet B_Ω (m)

5.5.3 Parameter Estimation Using GIS

The Geographical Information System (GIS) techniques were used to shape the geomorphological features of the catchment. In this study, GIS ArcView 3.2 software was used for geomorphological parameter determinations. The catchment stream networks, sub-catchments area, stream lengths and others were produced by using 1:50,000 scanned topography map under the GIS environment. A Digital Elevations Model (DEM) with a 20-m resolution has been used to derive flow directions and stream slopes. The DEM of the Faria catchment is shown in **Figure 30**. The hydraulic parameters have been derived from the available rainfall and runoff data.

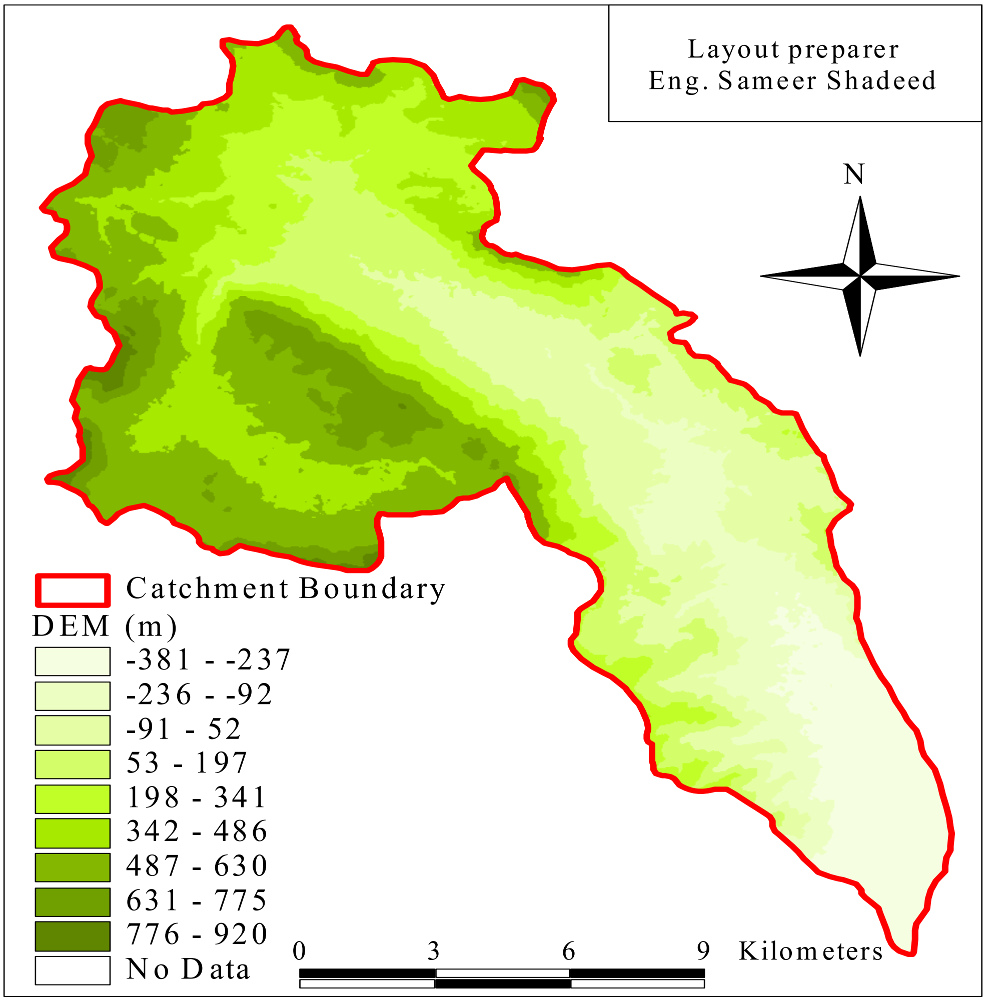

Figure 30: Digital Elevations Model (DEM) for the Faria Catchment

Studying the catchment area and delineating all possible flow paths and streams, it can be shown that there is no uniformity of the catchment characteristics. Therefore; the catchment under study is divided into two parts, the upper and lower Faria catchment. The upper part of the catchment is composed of two sub-catchments which are Al-Faria sub-catchment and Al-Badan sub-catchment. The areas of the sub-catchments are 64 km^2 and 85 km^2, respectively. The lower part of the catchment is named Al-Malaqi sub-catchment and has an area of about 185 km^2 as shown in **Figure 31**. Strahler's stream ordering system has been applied and has indicated that the

Al-Faria and Al-Badan sub-catchments are both of fourth order, while Al-Malaqi sub-catchment is of third order.

Figure 32 shows the drainage network map and the stream orders of the three sub-catchments. The maps in their digital forms have been used to estimate the input parameters needed for the application of the KW-GIUH model. These input parameters for the application of the model on the three sub-catchments are listed in **Tables 14** through **17**.

Table 14 gives the stream network transitional probability for the three sub-catchments, whereas table 18 is the input parameters of the GIUH model for Al-Badan sub-catchment. Those input parameters for Al-Faria and Al-Malaqi sub-catchments are presented in **Table 19** and **20** respectively.

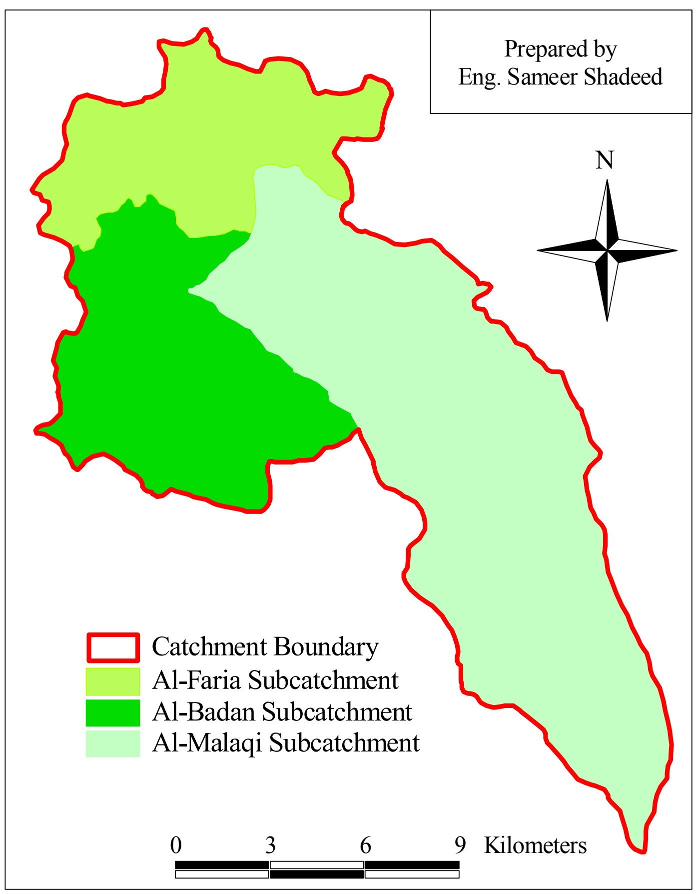

Figure 31: The Three Sub-catchments of the Faria Catchment

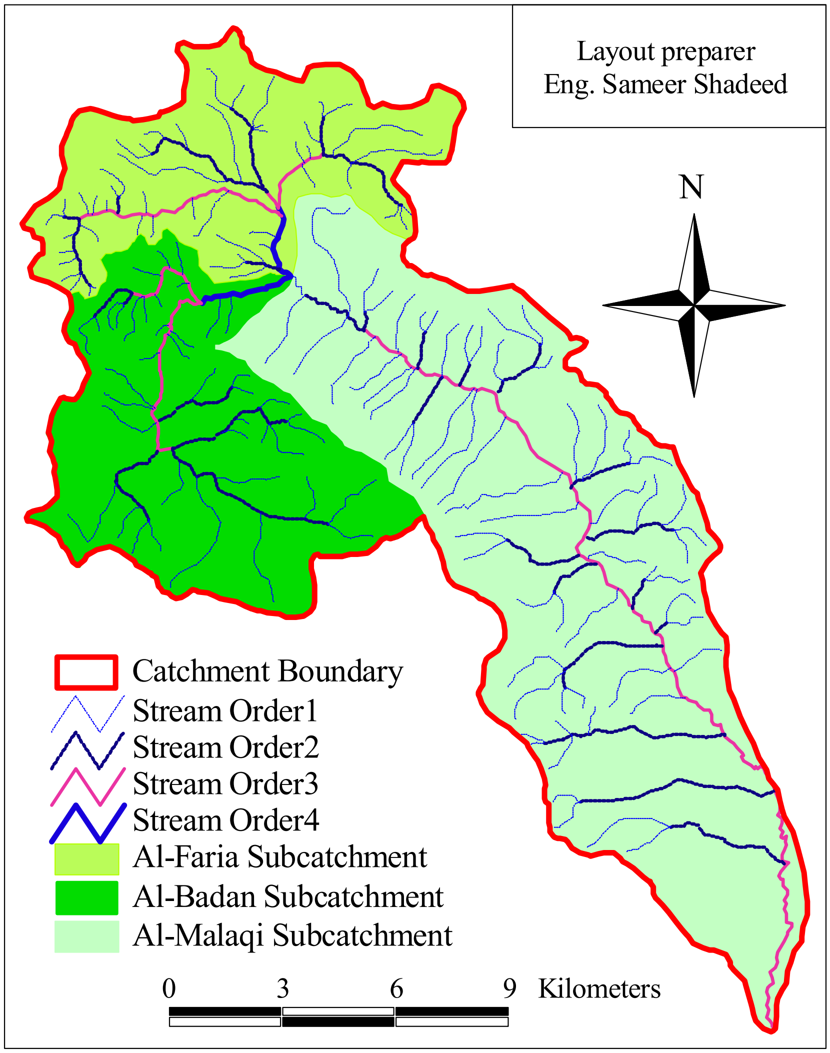

Figure 32: The Stream Order Networks for the Three Sub-catchments of the Faria Catchment

Table 14: $P_{x_i x_j}$ For the Three Sub-catchments

Description	Al-Badan	Al-Faria	Al-Malaqi
$P_{1,2}$	25/41	36/49	45/62
$P_{1,3}$	14/41	11/49	17/62
$P_{1,4}$	2/41	2/49	0
$P_{2,3}$	6/6	7/8	1
$P_{2,4}$	0/6	1/8	0
$P_{3,4}$	2/2	3/3	0

Table 15: KW-GIUH Input Parameters for Al-Badan Sub-catchment

Parameter	**Al-Badan Sub-catchment**			
	Order			
	1	2	3	4
N_i	41	6	2	1
$\overline{L}_{ci\,(m)}$	1379	3202	5027	3172
$\overline{A}_i\,(km^2)$	1.370	10.12	40.73	85.28
P_{OA_i}	0.66	0.186	0.126	0.028
$\overline{S}_{ci\,(m/m)}$	0.14	0.062	0.051	0.029
$\overline{S_{o\,i}}\ (m/m)$	0.17	0.092	0.14	0.135
Area (km^2)	85.28			
n_o	0.3			
n_c	0.03			
$B_\Omega\,(m)$	4.57			

Table 16: KW-GIUH Input Parameters for Al-Faria Sub-catchment

Parameter	**Al-Faria Sub-catchment**			
	Order			
	1	2	3	4
N_i	49	8	3	1
$\overline{L}_{ci\,(m)}$	1031	2120	3496	2621
$\overline{A}_i\,(km^2)$	0.937	6.099	19.365	64.0
P_{OA_i}	0.717	0.153	0.102	0.028
$\overline{S}_{ci\,(m/m)}$	0.117	0.058	0.033	0.031
$\overline{S_{o\,i}}\ (m/m)$	0.154	0.085	0.161	0.125
Area (km^2)	64.0			
n_o	0.3			
n_c	0.03			
$B_\Omega\,(m)$	3.66			

Table 17: KW-GIUH Input Parameters for Al-Malaqi Sub-catchment

Parameter	Al-Malaqi Sub-catchment		
	Order		
	1	2	3
N_i	62	16	1
$\overline{L}_{ci\ (m)}$	1920	2611	32084
$\overline{A}_i\ (km^2)$	1.81	5.83	184.96
P_{OA_i}	0.606	0.319	0.075
$\overline{S}_{ci\ (m/m)}$	0.14	0.063	0.01
$\overline{S}_{oi}\ (m/m)$	0.146	0.122	0.081
Area (km^2)	184.96		
n_o	0.3		
n_c	0.03		
$B_\Omega\ (m)$	10		

5.6 KW-GIUH Unit Hydrograph Derivation

For the analysis of the Faria catchment and the development of the 1-hr unit hydrograph for Al-Badan, Al-Faria and Al-Malaqi sub-catchments, the following are assumed.

- Rainfall duration = 1 hr
- Flow duration, there is no gauging for discharge
- Φ index = 0.0 mm/hr
- Hourly rainfall intensity i = 1 mm/hr
- Overland and channel flow roughness n_o and n_c were estimated depending upon the features of the catchment and based on the model verification as discussed in section 5.7.

The computer outputs for the three sub-catchments resulting from applying the KW-GIUH model are presented in **Appendix C**. From the outputs the

1mm-GIUH hydrographs for the three sub-catchments are plotted as shown in the **Figures 33** and **34**.

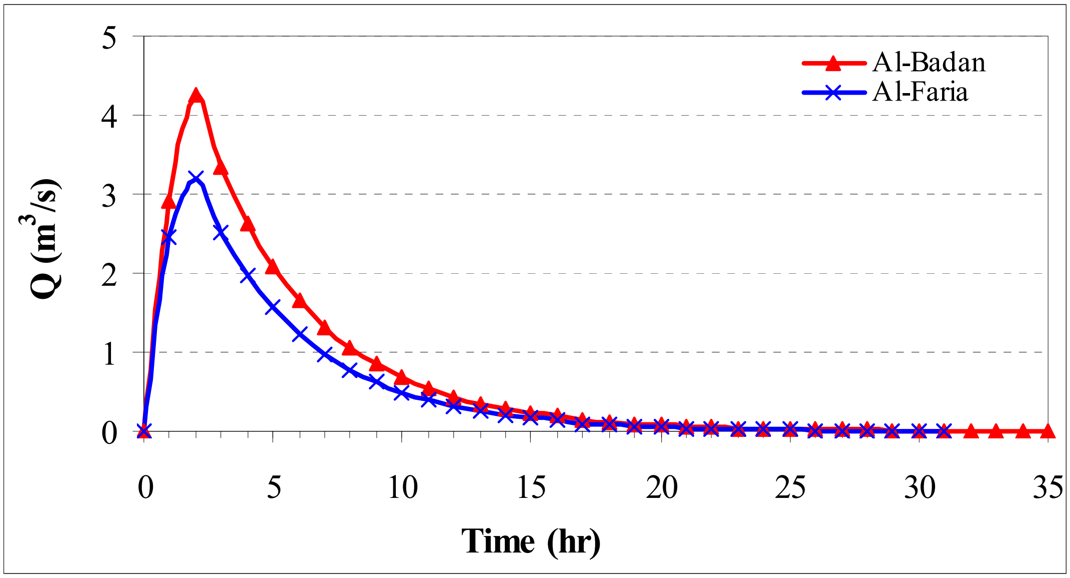

Figure 33: 1mm-GIUH for Al-Faria and Al-Badan Sub-catchments

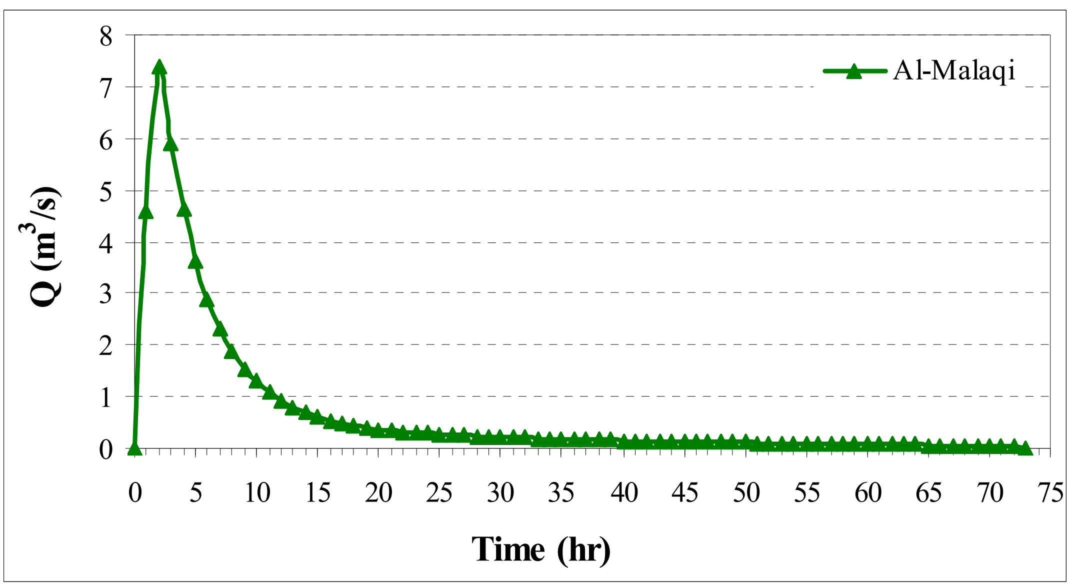

Figure 34: 1mm-GIUH for Al-Malaqi Sub-catchment

Several excess rainfall intensities were applied to Al-Badan sub-catchment, so as to study the effect of excess rainfall amount on the generation of the

GIUH. The results are illustrated in **Figure 35**. From the figure it is clear that the GIUH of a catchment is a function of the excess rainfall and there is a set of GIUHs instead of just one for a certain catchment. The peak value increases with increasing excess rainfall, whereas the time to peak decreases with increasing excess rainfall.

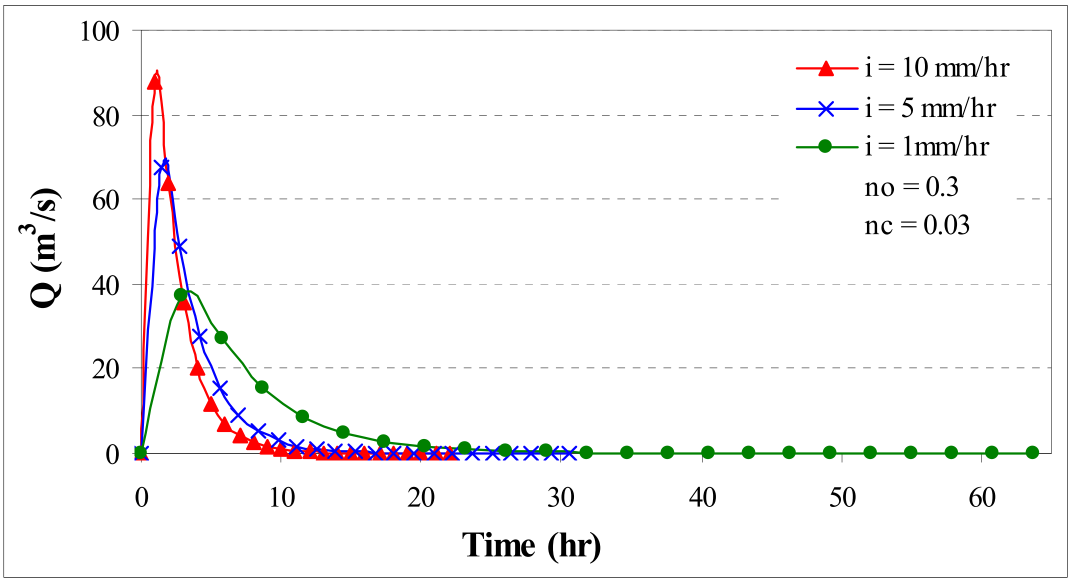

Figure 35: Variation of GIUH with Excess Rainfall

5.7 Sensitivity Analysis

The parameters that contribute to the shape of the KW-GIUH as indicated in the equations mentioned earlier are B_Ω, n_o and n_c. Therefore, it is necessary to perform a sensitivity analysis for these parameters. The sensitivity analysis for these parameters is investigated for the GIUH of Al-Badan sub-catchment. The only geometric parameter that cannot be obtained from a topographic map is the channel width at the catchment outlet. This needs to be measured physically. Therefore, the sensitivity analysis for B_Ω is important. The channel width was tested for the range of $\pm$ 25% from the measured width at the outlet of Al-Badan sub-catchment.

The measured width is 4.6 m. The sensitivity analysis is investigated using three width values; 3.45 m, 4.60 m and 5.75 m. These values are 0.75 of the actual width, actual width and 1.25 of the actual width respectively. The result is shown in **Figure 36**. From the figure it can be concluded that the GIUH is minorly sensitive to the channel width B_{Ω}.

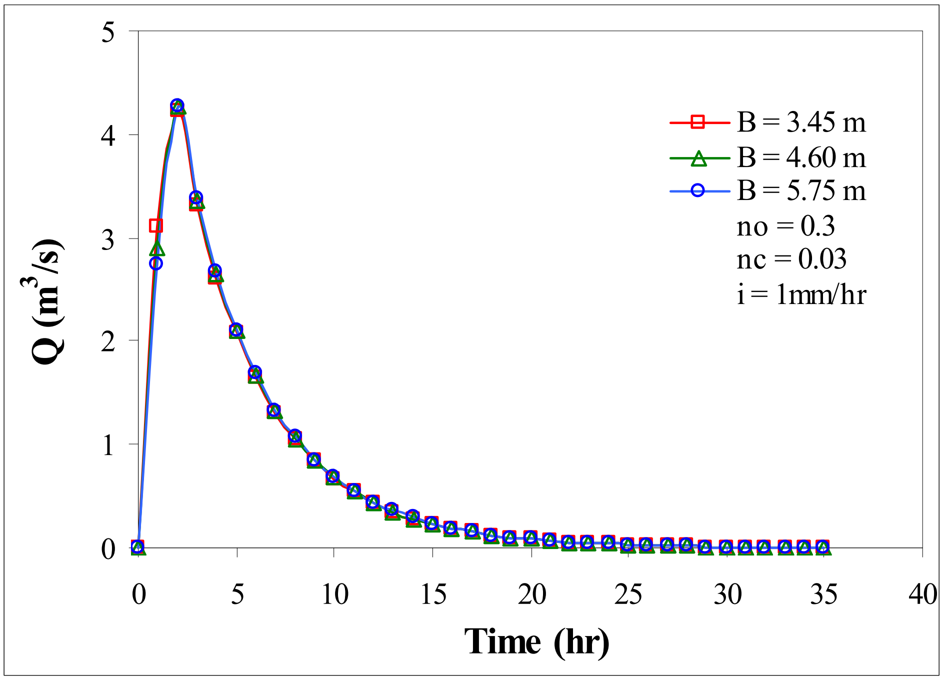

Figure 36: Sensitivity Analysis of Channel Width on GIUH

For the sensitivity analysis of the roughness coefficients, the overland roughness coefficient n_o was tested from 0.1 to 0.5, while the channel roughness n_c was tested from 0.01 to 0.05. The results are shown in **Figure 37** and **38**, respectively. From these figures it can be concluded that the effect of the overland roughness coefficient is significant, while the effect of the channel roughness coefficient is not clear and is very small. In the KW-GIUH model, since the storage effect is mainly incorporated in overland flow routing that is represented by an exponential distribution, GIUH peak is inversely proportional to the value of n_o, while the n_o value has little impact on the time to peak of the GIUH. The recession part of the GIUH graphs is relatively mild for large n_o and is steep for smaller n_o. It is worth mentioning that sensitivity analysis performed in this study is in full agreement with that conducted by Lee and Yen, 1997 for all parameters except for the channel roughness coefficient, n_c. In our study it was found that the GIUH is not sensitive to channel roughness coefficient, whereas in the case of Lee and Yen, 1997 on the Keeling river catchment, Taiwan, the sensitivity to channel roughness was considerable. This can be explained by the variations in the different features between two catchments such as the difference in the geomorphology and the range of the channel roughness coefficient.

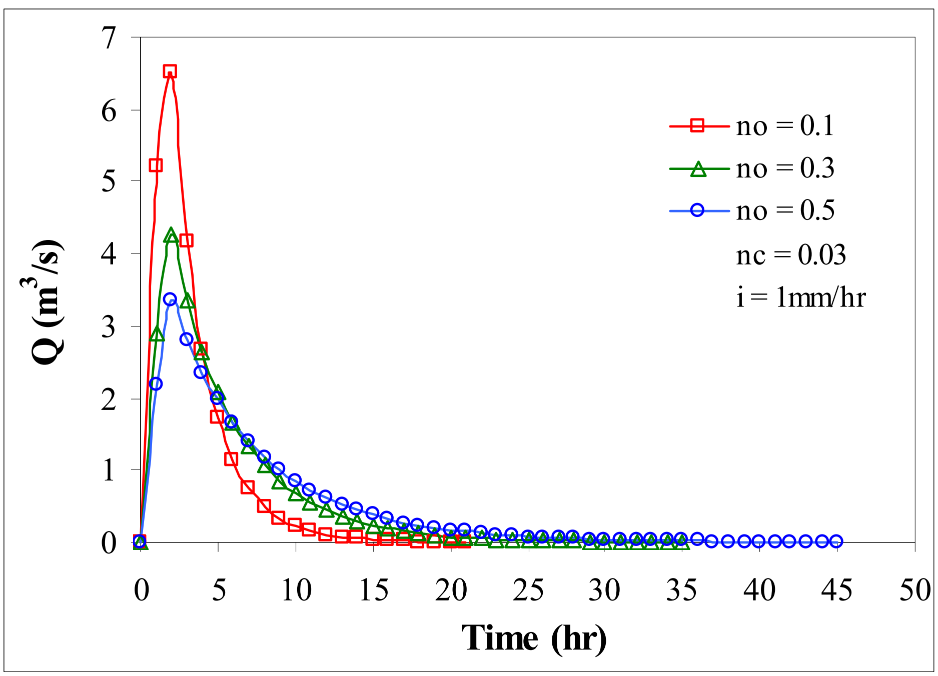

Figure 37: Sensitivity Analysis of Overland Roughness Coefficient on GIUH

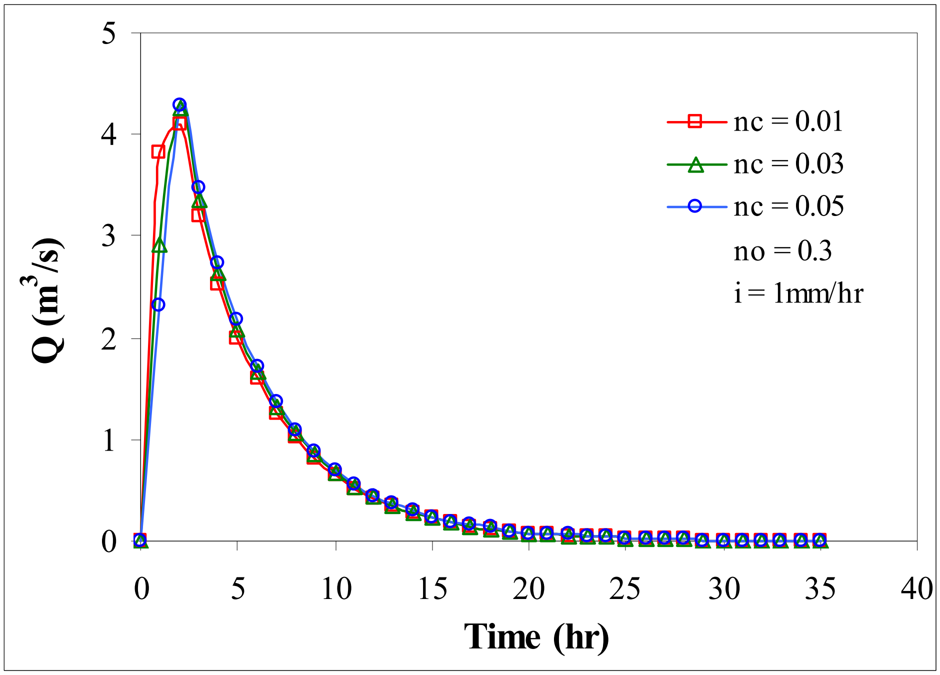

Figure 38: Sensitivity Analysis of Channel Roughness Coefficient on GIUH

5.8 Model Application for Hydrograph Simulation

The primary goal of developing the IUH of a catchment is to apply it for hydrograph generation for design of project storms (Yen and Lee, 1997). Selected rainstorms on Al-Badan sub-catchment have been chosen to test the applicability of the KW-GIUH model to produce the runoff hydrograph of a given rain event and to verify the model output by comparison with observed data for Al-Badan sub-catchment which is shown in **Figure 39**. Two selected rainstorms have been chosen from the last two rainy seasons, 2004-2005. The first event occurred on 14-2-2004 and the second occurred on 5-2-2005.

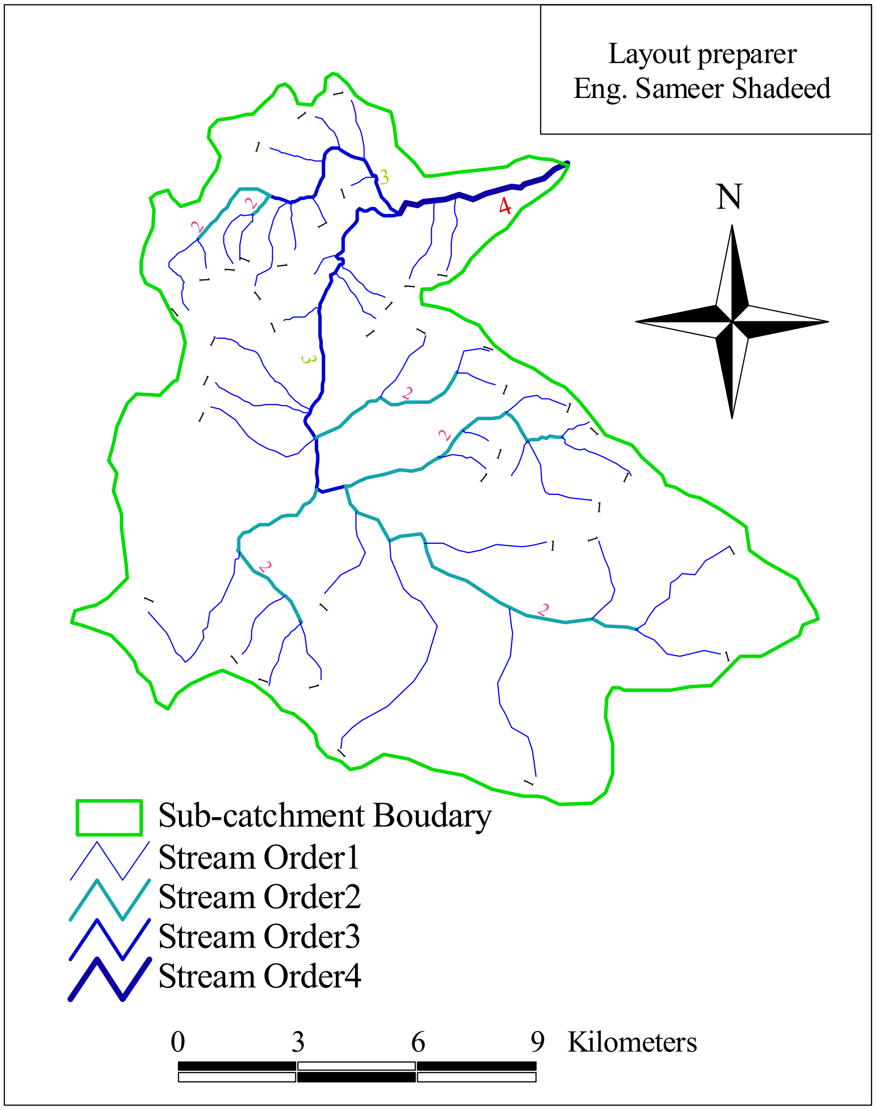

Figure 39: Al-Badan Sub-catchment and its Drainage Network

5.8.1 Event 1, 14-2-2004

During the rainy season of 2004, only one considerable double peak storm was recorded at the fourteen of February which was simulated using the KW-GIUH model. This storm was chosen from the records of the 2004 rainy season, where clear peak of the recorded discharge is obtained. The point rainfall recorded at Nablus meteorological station located near the headwater of Al-Badan sub-catchment was areally averaged over the sub-catchment. This averaging is necessary because the unit hydrograph theory assumed uniform rainfall over the catchment. The total rainfall of this simulated event is about 40 mm and did last for 16 hours. The rainfall excess hyetograph was determined by deducting the abstractions from the rainfall using the Horton infiltration equation (Patra, 2001).

$$f_t = f_c + (f_o - f_c)e^{-kt} \quad \textbf{34}$$

Where f_t is the infiltration capacity at any time t from the beginning of the storm in mm/h, f_c is the infiltration rate in mm/h at the final steady stage when the soil profile becomes fully saturated, f_o is the maximum initial value when t = 0 in mm/h at the beginning of the storm, k is an empirical constant depending on soil cover complex, vegetation and other factors and t is the time lapse from the onset of the storm. Values of f_o, f_c and k are dependent on number of factors such as soil characteristics and climatic conditions. In this study f_o and f_c are taken 4 mm/h and 15 mm/h respectively. These figures are reported by an experimental field study done at similar catchment characteristics near the village of Deir Ibzei, 10 km west of the city of Ramallah, West Bank (Lange et al. 2003). This assumption is reliable since the two locations located in a semiarid region and have nearly the same features and soil characterizations.

The above equation has been applied to estimate the excess rainfall for the selected storm as follows:-

The recorded peak occurs at t = 2 hr from the beginning of storm where the GIUH estimated peak occurs. The recorded and estimated peaks are 4.67 m^3/s and 4.45 m^3/s respectively. This means that the excess rainfall depth equal the recorded peak divided by the estimated one (4.67/4.26 = 1.1). At that time the rainfall depth equal 5.5 mm, as a result f_t equal (5.5-1.1= 4.4).

Substituting in the above equation gives k = 0.66 for the selected storm. This is used to develop the infiltration capacity curve which was applied to calculate the excess rainfall. The infiltration capacity curve is as shown in **Figure 40**. The resulting excess rainfall from the above storm is about 6 mm distributed as shown in **Figure 41**. For the storm of 14/2/2004, the base flow was separated from the recorded discharge.

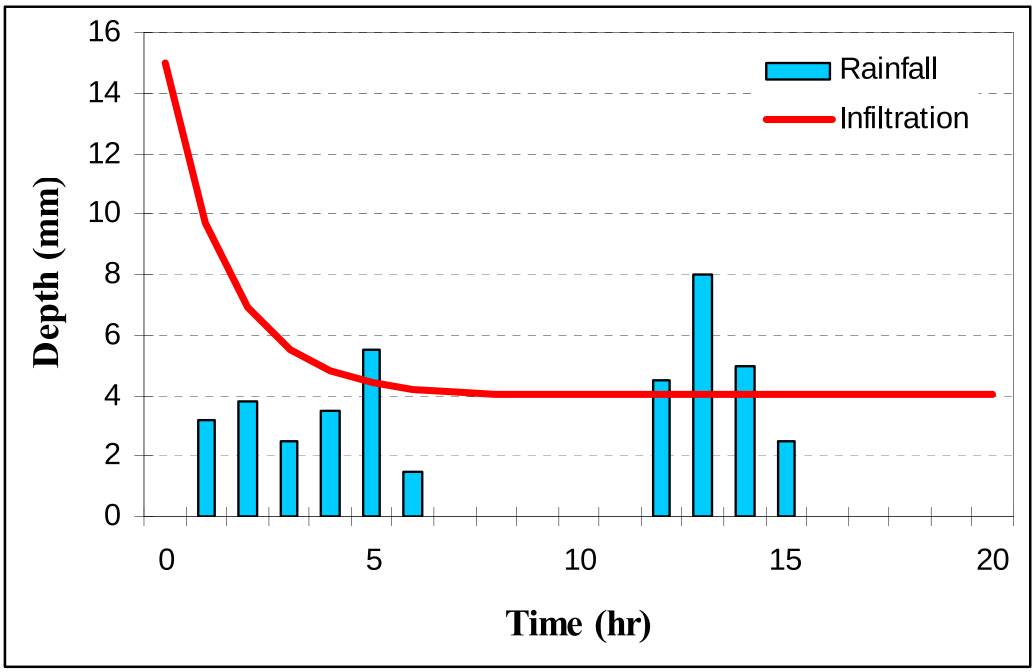

Figure 40: Rainfall Depth and Infiltration Capacity Curve of 14/2/2004 Event

Recorded discharges at Al-Badan Flume for this rainstorm were recorded using the stage flow curve for the Flume. The stage readings were taken manually. The automatic recorder was installed in August 2004 and all events afterwards were recorded automatically. The manual reading produce discrete points and do not cover the whole period of the storm as fewer records are taken during nights. Recorded discharges for this rainstorm were compared with the KW-GIUH generated hydrograph. Recorded and estimated hydrographs were as shown in **Figure 41**. The relative matching between the simulated runoff hydrograph and the recorded flows seems reasonable and within the acceptable limits, which indicates the applicability of the GIUH model to the catchment.

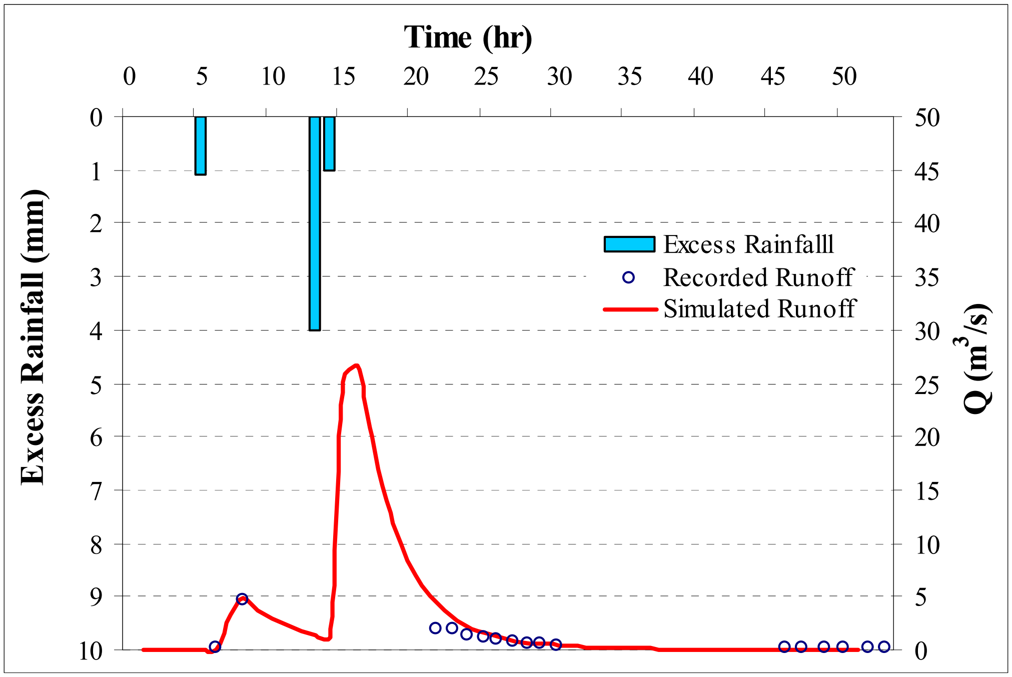

Figure 41: Recorded and Estimated Direct Runoff Hydrograph for Al-Badan Sub-catchment, Event of 14/2/2004

5.8.2 Event 2, 5-2-2005

During the rainy season of 2005, only one double peak considerable event was recorded on the fifth of February is simulated here. The event brought about 100 mm amount of rainfall and lasted 27 hours. Recorded discharges at Al-Badan Flume for this rainstorm were compared with the KW-GIUH generated hydrograph. A complete hourly data were recorded by the automatic divers installed on the Flume. The 5/2/2005 storm was chosen from the records where clear peak of the recorded discharges was produced. The recorded rainfall of the three stations (Nablus, Taluza and Beit Dajan) located within Al-Badan sub-catchment was averaged over the sub-catchment by applying the Thiessen method. The areal averaging of the rainfall over the catchment is necessary because the unit hydrograph theory assumed uniform rainfall.

The excess rainfall hyetograph was determined by deducting the abstractions from the rainfall using the phi-Index method. For the storm of 5/2/2005, the base flow was separated from the recorded discharge. Baseflow for this event was estimated at about 1.8 m^3/s. Using the KW-GIUH model with inputs of rainfall and runoff records and the value of the base flow, as a result the model calculated phi-Index to be 5.32 mm. **Figure 42** shows the storm hyetograph with phi-index. Applying the KW-GIUH results the excess rainfall from this storm at about 4.5 mm distributed as shown in **Figure 43**.

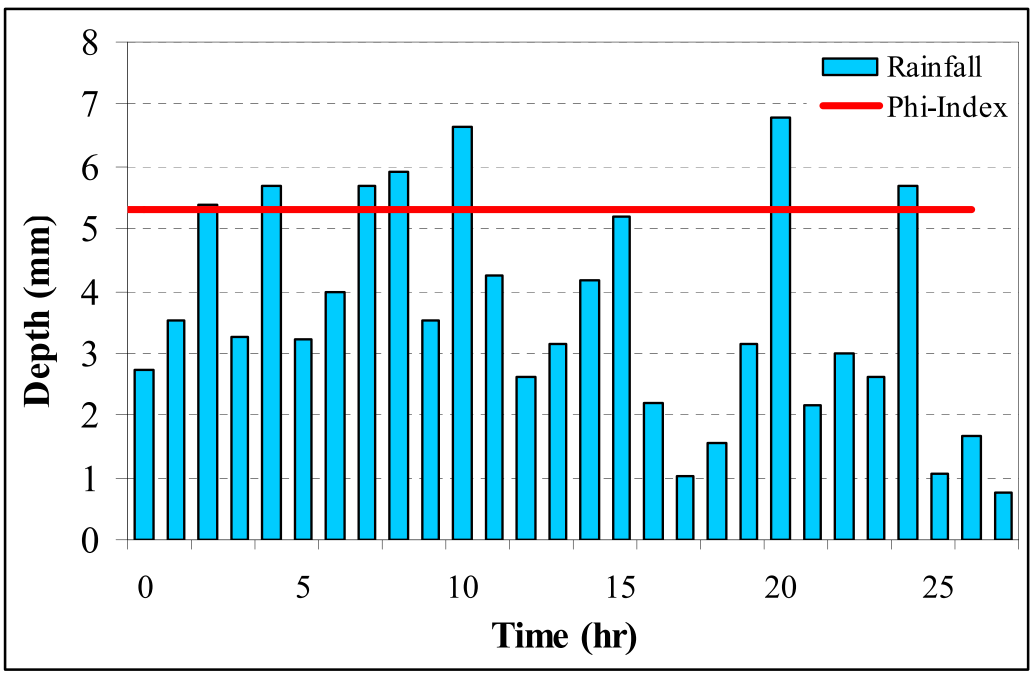

Figure 42: Rainfall Depth and the Phi-Index of Event of 5/2/2005

Recorded discharges for this rainstorm were compared with the simulated GIUH hydrograph to verify the model. Recorded and simulated hydrographs were as shown in **Figure 43**. From the Figure it is noticed that the simulated and observed results are in good agreement to assume the applicability of the KW-GIUH model to Al-Faria catchment.

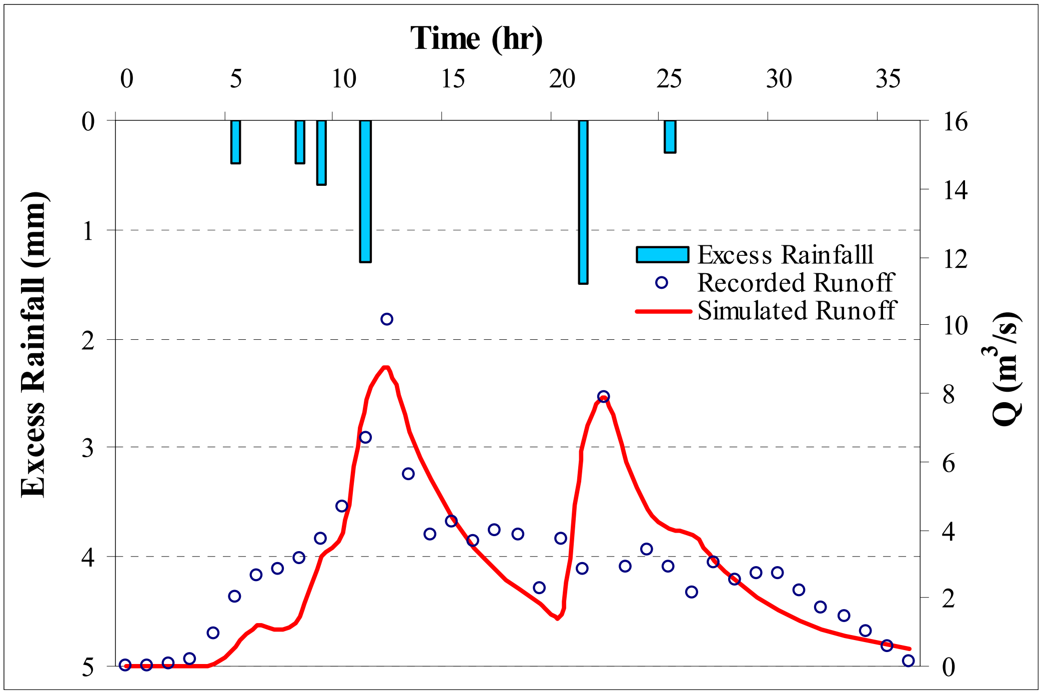

Figure 43: Recorded and Estimated Direct Runoff Hydrograph for Al-Badan Sub-catchment, Event of 5/2/2005

5.9 Analysis and Discussion

The KW-GIUH model that is based on the catchment stream ordering and on network structuring and incorporating with kinematic wave approximation for existing the rainwater travel time estimation demonstrate the high capability to generate instantaneous unit hydrograph without the need for runoff and rainfall data.

The travel time for overland and channel flows in a stream ordering sub basin system were solved analytically from lower to higher order subbasins for known roughness coefficients for both overland areas and channels. The hydraulic response of a catchment was represented by the combination of a series of probability density functions of travel time. The travel time is a function of the amount of water in the flow that is represented by the spatially uniform intensity of excess rainfall to be applied to the KW-GIUH model.

In contrast to the traditional unit hydrograph theory which assumes the linearity as one of its basic assumptions, the KW-GIUH model released this restriction since the produced GIUH is a function of excess rainfall considering the intensity and the interaction between surface flow and subsurface flow intensity. Therefore, a set of GIUHs corresponding to different values of excess rainfall can be obtained.

The critical issue in the KW-GIUH approach is the determination of excess rainfall. In this study two methods were applied. Those are Horton equation method and phi-index method. Results of the two methods are used to investigate the applicability of the KW-GIUH approach to simulate the runoff on the semiarid catchment of Faria.

Two rainstorm events were used to simulate the runoff hydrographs and to verify the applicability of the KW-GIUH model. The first event occurred on February 14^{th}, 2004. The total rainfall of this event is about 40 mm contributing to about 6 mm as excess rainfall. The resulting rainfall-runoff ratio is about 15% for this event. The second event occurred on February 5^{th}, 2005. This event had a total rainfall of about 100 mm and produced 4.5 mm of excess rainfall. The resulting rainfall-runoff ratio for this event is about 4.5%. This indicates that the runoff coefficient in the catchment is in the range of 4.5% to 15% of the annual rainfall. These results are in agreement with those reported results in previous literature such as those in (Husary et al., 1995) and (Takruri, 2003).

In this context, it is to note here that the assumption of uniform distribution of excess rainfall over the catchment is not consistent with the semiarid nature of the Palestinian catchments that behave as variable sources and partially contributing. Nevertheless, the results of the simulation of the events using the GIS-supported KW-GIUH are promising and indicate the applicability of the model to semiarid regions.

CHAPTER SIX

CONCLUSIONS AND RECOMMENDATIONS

6.1 Conclusions

Al-Faria catchment is located in the northern West Bank, which is characterized as semiarid. The catchment is 334 km^2 and extends from the Nablus Mountains in the west to the Jordan River in the east. The rainfall distribution within the Faria catchment ranges from 640 mm at the headwater to 150 mm at the outlet to the Jordan River.

Based on the analysis of the six rainfall stations in Faria catchment, it is noticed that Nablus and Taluza stations have the largest average annual rainfalls whereas Al-Faria station has the lowest average annual rainfall. Tubas station has an average annual rainfall of 415 mm, which nearly equals the arithmetic average of the annual average rainfalls of the six stations of the catchment at about 430 mm.

From the analysis of monthly data it is clear that there is a relatively wet period from November till April and that there is a relatively dry period from May to October. This is associated with the climatic conditions of the catchment.

The internal consistency of the rainfall stations of Faria catchment was examined by using the double mass curve technique. The results proved that all stations are internally consistent.

Significant increasing trend of rainfall averages is noticed in the case of Nablus and Beit Dajan stations. The increasing trend of the elevated stations and the decreasing trend of Al-Faria station, elevated below sea level and located near the Jordan River, can be assumed in relation to the later developments and changes in the climatic conditions of the region. The drying of the Jordan River basin due to the diversion of the head water by the Israeli projects and the Israeli National Water Carrier are assumed among the main reasons for the observed trends. Less water is available for evapotranspiration in the Jordan River basin and thus fewer rainfalls are expected in contradiction to the elevated areas.

Results of probability distribution of rainfall data for the six stations has showed that Gumbel distribution fits the annual rainfall data and can be used for future estimations especially that the correlation coefficient, r^2, was more than 94%. This provides means to understand and evaluate the distribution characteristics of the rainfall in the Faria catchment in particular and of the eastern slopes of the West Bank characterized as semiarid region in general. The obtained results are an important contribution for the design of hydraulic projects and for the assessment of the Palestinian water resources.

The multiple regression analysis was applied to correlate the average annual rainfalls to the location of the stations within the catchment. The coordinates, X and Y, and the elevations, Z, proved to be strongly correlated to average rainfall. A statistical relation is assumed to give the average rainfall as a function of the X, Y and Z of the station's location.

Thiessen polygon method has been used to convert the point rainfall to areal rainfall for the six rainfall stations. The areal average rainfall of the Faria catchment was found at 385 mm. This value is nearly equal to the annual average rainfall of Beit Dajan station which about 379 mm. This indicates that the rainfall in the catchment can be represented by Beit Dajan station.

The rainfall runoff process in the Faria catchment was investigated and modeled. The GIUH model is the model selected for modeling the process as it can be applied incorporating the geomorphological characteristics of the catchment and with less need to highly sophisticated measurements. The KW-GIUH hydrological model supported by the GIS is applied to investigate the rainfall runoff process in the Faria catchment as a case study towards understanding the storm water drainage and rainfall runoff process in the West Bank.

GIUH unit hydrographs were derive for the three sub-catchments of the whole Faria catchment. These sub-catchments are Al-Badan, Al-Faria and Al-Malaqi having areas of about 85 km^2, 64 km^2 and 185 km^2 respectively. Estimated peak discharges of 1-mm excess rainfall for three sub-catchments are 4.26 m^3/s, 3.21 m^3/s and 7.4 m^3/s respectively.

Two rainfall events were simulated on Al-Badan sub-catchment using the generated KW-GIUH hydrograph. Estimated hydrographs were compared with the recorded discharges to verify the results of the model and reasonable matching was obtained. From the obtained results, it can be concluded that the runoff in the Faria catchment is in the range of 4.5% to 15% of the annual rainfall.

6.2 Recommendations

Based on the findings of this work, the following points can be recommended for future research in the field of surface water hydrology in Palestine and in semiarid regions.

1. Use the results of Faria catchment and translate it towards understanding and managing the water resources in Jordan Valley.

2. Flow measuring devices were built at the outlet of Al-Badan and Al-Faria sub-catchments in the context of GLOWA JR project should be maintained to remain working properly. Yearly maintenance is recommended for these stations to insure the quality of obtained data, and thus enhance the evaluation of the applicability of the developed GIUH model.

3. It is recommended to install automatic instruments for measuring other hydrological parameters. These include rainfall intensity, runoff and infiltration in addition to detailed measurement of all meteorological parameters such as evaporation, temperature, humidity, wind speed and others.

4. Available roughness coefficient data is minimal. More extensive data is needed so that assumption concerning this parameter in the model is more realistic.

5. More rainstorm events are required to be investigated in order to calibrate and verify the applicability of the developed GIUH model.

6. The GIUH model should be applied to other catchments in Palestine to evaluate the applicability and reliability of this model and to investigate rainfall runoff process in Palestine representing a semiarid region.

7. Develop the available GIS system in the Palestinian Authorities use it to develop catchment characteristics. These data should be made available to researches for further applications. The GIS

system and data can then be convolved to the GIUH program and other available models.

8. Constructing a dam at Jiser Al-Malaqi to store winter floodwaters will serve the long term objectives of water resources management of Faria catchment.

References

Abrahams, A. D., Parsons, A. J. and Wainwright, J. (1994). Resistance to overland flow on semiarid grassland and shrubland hillslopes, Walnut Gulch, southern Arizona. Journal of Hydrology. Vol. 156, P. 431-46.

Agnese, C. D., Asaro, D. and Giordano, G. (1988). Estimation of the time scale of the geomorphologic instantaneous unit hydrograph from effective streamflow velocity. Water Resource. Vol. 24, No. 7, P. 969-978.

Al-Nubani, N. I. (2000). Rainfall – Runoff Process and Rainfall Analysis for Nablus Basin. M.Sc. Thesis, Faculty of Graduate Studies, An-Najah National University, Nablus, Palestine.

Al-Smadi, M. (1998). Incorporating Spatial and Temporal Variation of Watershed Response in a GIS-Based Hydrologic Model. M.Sc. Thesis, Biological Systems Engineering Department. Virginia Tech, Blcksburg.

Andrew N. S. and Patrick. A. O. (2004). Stormwater Master Planning with GIS, A Case Study of the Blue River Watershed.

Applied Research Institute-Jerusalem (ARIJ). (1996). Environmental Profile for the West Bank, Volume 5, Nablus Profile. Palestine. Caritas Street, Bethlehem.

Barakat, M. H. (2000). Rainfall – Runoff Process and Modeling for Soreq stream near Jerusalem. M.Sc. Thesis, Faculty of Graduate Studies, An-Najah National University, Nablus, Palestine.

Barkhordari, J. (2003). Assessing the Effects of Land use Change on the Hydrologic Regime by RS and GIS. A case Study in the Minab

Catchment. M.Sc. Thesis, International Institute for Geo-information Science and Earth Observation, Hormozgan province, Iran.

Bergström, S., Forsman, A. (1973). Development of A conceptual Deterministic Rainfall Runoff Model. Nordic Hydrology, Vol. 4, P. 147-170.

Berod, D.D., Singh, V.P. and Musy, A. (1999). A geomorphologic kinematic-wave (GKW) model for estimation of floods from small alpine watersheds. Hydrological Process. Vol. 13, P. 1391-1416.

Beven, K. J and Kirkby, M. J. (1979). A physically Based Variable Contributing Area Model of Basin Hydrology. Hydrological Science Bulletin, Vol. 24, No. 1, P. 43-69.

Bhaskar, N. R., James, W. P., and Devulapall, R. S. (1992). Hydrologic Parameter Estimation Using Geographic Information System. Journal of Water Resources Planning and Management, Vol. 118, No. 5, P. 492-512.

Brooks, S.M., McDonnell, R.A., 2000. Research advances geocomputation for hydrological and geomorphological modeling towards the twenty-first century. Hydrological Process. Vol. 14, P. 1899-1907.

Crawford, N.H and Linsley, R.K. (1966). Digital Simulation in Hydrology, Stanford Watershed Model. Technical Report No. 39, Civil Engineering Department, Stanford University.

Chow, V.T, Maidment, David R and Mays, L.W. (1988). Applied Hydrology. McGRAW-HILL, New York.

Chutha, P. and Dooge, J.C.I. (1990). The shape parameters of the geomorphologic unit hydrograph. Journal of Hydrology. Vol. 117, P. 81-97.

Chow, V.T. (1964). Handbook of Applied Hydrology, A Compendium of Water Resources Technology, Mc-Graw Hill book Company, New York.

EQA. (2004). Al-Faria – Jerash Integrated Watershed Management Project (WASMAP), Wadi Al-Faria Baseline Report. Unpublished Report.

FAO (1989). Arid Zone Forestry, A guide for Field Technicians.

Ghanem, M. (1999). Hydrology and Hydrochemistry of the Faria Drainage Basin / West Bank. Ph.D. Thesis, Wissenschaftliche Mitteilungen, Institut Fur Geologie, Technische Universital Bergakademie Freiburg, Germany.

Graf, W. L. (1988). Fluvial Processes in Dryland Rivers. Springer Series in Physical Environment. Springer, Heidelberg.

Grover, S. (2003). Perspectives of GIS Modeling in Hydrology. Natural Resources Management, GIS Development.

Gupta, V.K., Waymire, E. and Wang, C.T. (1980). A representation of an Instantaneous Unit hydrograph From Geomorphology. Water Resources Research, Vol. 16, No. 5, P. 855-862.

Haan, C.T. (1977). Statistical Methods in Hydrology. The Iowa State University Press, Ames, USA.

Hall, M.J., Zaki, A.F. and Shahin, M.A. (2001). Regional Analysis Using the Geomorphoclimatic Instantaneous Unit Hydrograph. Hydrology and Earth System Sciences, Vol. 5, No. 1, P. 93–102.

Hussary, Samar; Najjar, Tagreed; and Aliewi, Amjad. (1995). Analysis of Secondary Source Rainfall Data from the Northern West Bank. Palestinian Hydrology Group and University of New Castle upon type, Jerusalem ,West Bank ,Palestine.

Jain, S.K., Singh, R.D., and Seth, S.M. (2000). Design Flood Estimation Using GIS Supported GIUH Approach, Water Resources Management, Vol. 14, P. 369-376.

Jin, C. (1992). A deterministic gamma-type geomorphological instantaneous unit hydrograph based on path types. Water Resources. Vol. 28, No. 2, P. 479-486.

Karlinger, M.R. and Troutman, B.M. (1985). Assessment of the instantaneous unit hydrograph derived from the theory of topologically random networks. Water Resource. Vol. 21, No, 11, P.1693–1702.

Kirshen, D.M. and Bras, R.L. (1983). The linear channel and its effect on the geomorphologic IUH. Journal of Hydrology. Vol. 65, P.175–208.

Lange, J. (1999). A noncalibrated Rainfall-Runoff Model for Large, Arid Catchments, Nahal Zin, Israel. PhD Thesis, Freiburg University, Institute of Hydrology.

Lange, J and Leibundgut, C. Greenbaum, N and Schick, A.P (1999). A noncalibrated Rainfall-Runoff Model for Large, Arid Catchments, Institute of Hydrology, University of Freiburg, Freiburg, Germany and Department of Geography, Hebrew University. Water Resources Research, Vol. 35, No. 7, P. 2161–2172.

Lange, J., Greenbaum, N., Husary, S., Ghanem, M., Leibundgut, C. and Schick, A. (2003). Runoff Generation from Successive Simulated

Rainfalls on A rocky, Semi-arid, Mediterranean Hillslope. Hydrol. Process. Vol. 17, P. 279–296.

Lee, K.T., and Chang, C.H. (2005). Incorporating Subsurface Flow Mechanism into Geomorphology-Based IUH Modeling. Department of River and Harbor Engineering, National Taiwan Ocean University, 2, Bee-Ning Road, Keelung, Taiwan 202, ROC.

Lim, C. K. (2003). Applying GIS to Hydraulic Analysis. Department of Civil Engineering, Texas University.

Linsly, R.K., Kahler, M.A and Paullus, J.L. (1982). Hydrology for Engineers. Third Edition. McGraw-Hill International Book Company.

Lundin, L.C., Sten Bergström, S., Eriksson, E. and Seibert, J. (1998). Hydrological Models and Modeling.

Maidment, D.R. (1996). GIS and Hydrologic Modeling. An Assessment of Progress, Presented at the Third International Conference on GIS and Environmental Modeling, Santa Fe, New Mexico, 22-26.

Maffini, G. (1997). Using GIS Technology to Advance and Optimize Asset Management. Presentation to Strategic and Profitable Asset Management Conference, London.

MOT. (1998). Palestine Climatic Data Handbook. Metrological Office, Ministry of Transport, Palestinian National Authority.

Nash, J.E. (1958). The Form of the Instantaneous Unit Hydrograph. IAHS-Publ. No. 45, P. 114-121.

Orthor, R., Loibl, W. and Wenl, E. (2001). A Harmonized Water Data Base for the Lower Jordan Valley. ARC Seibersdorf Research Report ARC.S-0157, Ein Untemehment der Austrian Research Centers.

Patra, K.C. (2001). Hydrology and Water Resources Engineering. Alpha Science International Ltd. India.

Petts, G.E. (1995). Changing River Channels. The Geographical Tradition. John Wiley & Sons, Chichester, P. 1-23.

Ponce, V.M. (1989). Engineering Hydrology, Principles and Practices. Prenctice Hall, Englewood Cliffs, New Jersey, USA.

Raghunath H.M. (1985). Hydrology, Principles, Analysis, Design. New Age International Publishers.

Rodriguez-Iturbe, I. and Valdes, J.B. (1979). The Geomorphological Structure of Hydrologic Response. Gradate Program in Hydrology and Water Resources, Universidad Simon Bolivar, Caracas, Venezuela.

Rodriguez-Iturbe, I., Gonzalez-Sanabria, M. and Bras, R.L. (1982). A geomorphoclimatic theory of the instantaneous unit hydrograph. Water Resource. Vol. 18, No. 4, P. 877-886.

Rofe and Rafety Consulting Engineering. (1965). West Bank Hydrology, Analysis 1963-1965, Geological and Hydrological Report, Hashimite Kingdom of Jordan, Central Water Authority, Jordan.

Schick, A.P., Grodek, T. and Lekach, J. (1997). Sediment Management and Flood Protection of Desert Towns: Effects of Small Catchments. Human Impact on Erosion and Sedimentation. IAHS- Wallingford, No. 245.

Shadeed, S.M. and Wahsh, H.F. (2002). Synthetic Modeling of Rainfall-Runoff Process of upper Faria Catchment. B.Sc. thesis, Faculty of Civil Engineering An-Najah National University, Nablus, Palestine.

Shaheen, H.Q. (2002). Storm Water Drainage in Arid and Semiarid Regions: West Bank as A case Study, An-Najah University Journal for Research - Natural Sciences, Vol. 16, No. 12, P. 125-137.

Sherman, L.K. (1932). Stream flow from Rainfall by Unit Hydrograph Method, Engineering News Records, V. 108, P.501-505.

Snell, J.D. and Sivapalan, M. (1994). On Geomorphological Dispersion in Natural Catchments and the Geomorphological Unit Hydrograph, Water Resources Research, Vol. 30, No. 7, P. 2311-2323.

Sorman, A.U. (1995). Estimation of Peak Discharge Using GIUH Model in Saudi Arabia. Journal of Water Resources Planning and Management, Vol. 121, No. 4, P. 287-293.

Strahler, A.N. (1957). Quantitative Analysis of Watershed Geomorphology, Transactions, American Geographical Union.

Takruri, B.B. (2003). Rainfall-Runoff Analysis and the Synthetic Unit Hydrograph for Wadi Faria Catchment. M.Sc. Thesis, Faculty of Graduate Studies, Beir Zeit University, Palestine

Todini, E. (1988). Rainfall Runoff Modeling-Past, Present and Future. Journal of Hydrology, Vol. 100, P 341-352.

Thormählen, A.C. (2003). Hydrological Modeling in A small Hyperarid Catchment. Nahal Yael, Israel. M.Sc. Thesis, Institute of Hydrology, Freiburg University, Germany.

UNESCO. (1984). Map of the world Distribution of Arid Regions. Paris, France.

Viessman, W.J., Lewis, G.L. and Knapp J.W. (2003). Introduction to Hydrology. Fifth Edition, Harper Collins.

Wilson, E.M. (1974). Engineering Hydrology, Second Edition, The Macmillan Press ltd., London Basingstoke Companies.

Yen, B.C., and Lee, K.T. (1997). Unit Hydrograph Derivation for Ungauged Watersheds by Stream-Order Laws, Journal of Hydrologic Engineering, ASCE, Vol. 2, No. 1, P. 1-9.

Appendix A (Tables)

APPENDIX A1

MONTHLY CLIMATIC AVERAGES DATA

Table A1 1: Monthly Climatic Average Data of Al-Farai Station

Element	Jan	Feb	Mar	Apr	May	Jun	Jul	Aug	Sep	Oct	Nov	Dec
Mean Max. Temp. (^{o}C)	19.5	20.2	24.3	29.1	34.6	37.1	39.4	38.5	36.6	33.5	27.9	21.5
Mean Min. Temp. (^{o}C)	9.3	9.2	12.1	14.4	19.0	21.1	22.7	24.2	22.9	20.2	16.8	11.9
A bsolute Max. Temp. (^{o}C)**	27	33.1	36	45.1	47.2	49	48	47	43.5	42	38.8	32
A bsolute Min. Temp. (^{o}C)**	0.5	5	3	5	10.5	14.5	16.5	20	17.5	12	6.5	2.7
MeanTemp. (^{o}C)	14.4	14.7	18.2	21.7	26.8	29.1	31.1	31.4	29.8	26.9	22.4	16.7
Mean Wind Speed (Km/h)	4.6	6.5	6.1	3.6	3.3	3.6	6.8	6.5	5.0	2.5	2.5	2.1
Mean Sunshine Duration (h/day)	5.7	6.0	7.5	8.7	10.3	11.6	11.7	11.0	9.9	8.5	7.3	6.2
Mean RH (%)	73	73	63	63	52	51	51	52	43	54	55	67
Total Rainfall (mm)*	55.2	31.9	45	16.7	0	0	0	0	0.3	6.7	23.7	45.1
Max. Monthly Rainfall (mm)	204.1	79	84.4	78.4	0.2	0	0	0	3.6	27.9	51	106.2

* Monthly Total + The period is 1969 - 1981
** The period is 1923 - 1965

Table A1 2: Monthly Climatic Average Data of Nablus Station

Element	**Jan**	**Feb**	**Mar**	**Apr**	**May**	**Jun**	**Jul**	**Aug**	**sep**	**Oct**	**Nov**	**Dec**
Mean Max. Temp. (^{o}C)	13.1	14.4	17.2	22.2	25.7	27.9	29.1	29.4	28.4	25.8	20.2	14.6
Mean Min. Temp. (^{o}C)	6.2	6.7	8.8	12.1	14.9	17.4	19.3	19.5	18.5	16.2	12.1	7.8
A bsolute Max. Temp. (^{o}C)	22.9	28.1	30.4	35	38.6	38	38.1	38.6	38.8	35.3	30.7	28
A bsolute Min. Temp. (^{o}C)	-0.6	-2.8	-1	0.6	6.9	11.4	12.3	15.9	13	9.3	1.4	0.3
MeanTemp. (^{o}C)	9.6	10.5	13	17.1	20.3	22.6	24.2	24.4	23.4	21	16.1	11.2
Mean Wind Speed (Km/h)	8.7	9.5	10	10.2	10.7	12	12.4	11.7	10.3	7.7	7.8	7.7
Pressure (mbar)	953	952	951	949	948	946	944	945	948	951	953	953
Mean Sunshine Duration (h/day)	4.7	4.8	6.4	8.2	8.9	8.4	9.6	10.9	10.2	9.8	7	4.5
Mean RH (%)	67	67	62	53	51	55	61	65	64	57	57	67
Total Rainfall (mm)*	141.1	146.9	104	20.2	7.8	0	0	0	1.8	20.7	77.1	140.5
Total Evaporation (mm)*	49	67	99	149	203	226	238	218	178	131	75	49
Total PET (mm)*	36	36	55	82	106	112	117	112	105	103	72	36
Max. Monthly Rainfall (mm)	389	389	220	225	65	3	0	1	22	83	249	472

* Monthly Total

APPENDIX A2

CROPWAT 4 OUTPUT RESULTS FOR NABLUS AND AL-FARIA STATIONS

Table A2 1: CROPWAT 4 Output Results for Nablus Station

Climate Data Table

Country: Palestine | Station: Nablus | Altitude: 530 (m)

Month	Max Temp. (C)	Min Temp. (C)	Humidity (%)	WindSpeed (km/d)	SunShine (hours)	Solar Radiation (MJ/m2/d)	ETo (mm/d)
January	13.1	6.2	67.0	208.8	4.7	9.6	1.8
February	14.4	6.7	67.0	228.0	4.8	11.6	2.2
March	17.2	8.8	62.0	240.0	6.4	16.0	3.2
April	22.2	12.1	53.0	244.8	8.2	20.8	4.7
May	25.7	14.9	51.0	256.8	8.9	23.1	5.7
June	27.9	17.4	55.0	288.0	8.4	22.7	6.1
July	29.1	19.3	61.0	297.6	9.6	24.2	6.2
August	29.4	19.5	65.0	280.8	10.9	25.1	6.0
September	28.4	18.5	64.0	247.2	10.2	21.9	5.1
October	25.8	16.2	57.0	184.8	9.8	18.3	3.9
November	20.3	12.1	57.0	187.2	7.0	12.4	2.6
December	14.6	7.8	67.0	184.8	4.5	8.8	1.7
Average	22.3	13.3	60.5	237.4	7.8	17.9	4.1

Report... Close

Table A2 2: CROPWAT 4 Output Results for Al-Faria Station

Climate Data Table

Country: Palestine | Station: Al-Jeftlik | Altitude: -237 (m)

Month	Max Temp. (C)	Min Temp. (C)	Humidity (%)	WindSpeed (km/d)	SunShine (hours)	Solar Radiation (MJ/m2/d)	ETo (mm/d)
January	19.5	9.3	73.0	110.4	5.7	10.6	1.7
February	20.2	9.2	73.0	156.0	6.0	12.9	2.3
March	24.3	12.1	63.0	146.4	7.5	17.4	3.5
April	29.1	14.4	63.0	86.4	8.7	21.5	4.3
May	34.6	19.0	52.0	79.2	10.3	25.1	5.5
June	37.1	21.1	51.0	86.4	11.6	27.4	6.3
July	39.4	22.7	51.0	163.2	11.7	27.3	7.6
August	38.5	24.2	52.0	156.0	11.0	25.2	6.9
September	36.6	22.9	43.0	120.0	9.9	21.5	5.5
October	33.5	20.2	54.0	60.0	8.5	16.7	3.3
November	27.9	16.8	55.0	60.0	7.3	12.7	2.2
December	21.5	11.9	67.0	50.4	6.2	10.4	1.4
Average	30.2	17.0	58.1	106.2	8.7	19.1	4.2

Report... Close

APPENDIX A3

GROUNDWATER WELLS IN THE FARIA CATCHMENT

Table A3 1: Basic Information of Wells Located within the Faria Catchment

No	ID	X (km)	Y (km)	Z(m)	Name	Aquifer	Basin	Locality	Governate	Water use
1	18-18/001	181.050	188.620	220.00	Yunes Swadi & Partners	Eocene	North Eastern	Ras Al-Faria	Nablus	Agricultural
2	18-18/002	182.200	188.350	180.00	'Abed Al Ra'uf Faris	Eocene	North Eastern	Ras Al-Faria	Tubas	Agricultural
3	18-18/004	181.910	188.710	180.00	Ref'at Al Fares	Eocene	North Eastern	Ras Al-Faria	Tubas	Agricultural
4	18-18/016	182.370	188.890	175.00	Mustafa Abu Khayzaran	Eocene	North Eastern	Ras Al-Faria	Tubas	Agricultural
5	18-18/017	182.300	189.650	223.00	Tubas Water Project	Eocene	North Eastern	Ras Al-Faria	Tubas	Domestic
6	18-18/025A	181.650	189.540	220.00	Muhammad 'Ali 'Abdallah	Eocene	North Eastern	Ras Al-Faria	Nablus	Agricultural
7	18-18/032	182.120	188.950	197.28	Ahmad Shanti & Partners	Eocene	North Eastern	Ras Al-Faria	Tubas	Agricultural
8	18-18/033	182.140	189.770	213.32	Sulayman Saleh	Eocene	North Eastern	Ras Al-Faria	Tubas	Agricultural
9	18-18/005	181.750	188.300	200.00	Ref'at Al Fares	Eocene	North Eastern	Ras Al-Faria	Nablus	Agricultural
10	18-18/011	187.040	183.140	-30.00	Ameen & Marwan Masri	Neogene	North Eastern	Ras Al-Faria	Nablus	Agricultural
11	18-18/011A	187.040	183.400	-15.00	Marwan & Ameen Masri	Neogene	North Eastern	Ras Al-Faria	Nablus	Agricultural
12	18-18/011B	187.040	183.140	-30.00	Marwan & Ameen Masri	Neogene	Eastern	Wadi Al-Faria	Nablus	Agricultural
13	18-18/013	187.290	182.440	-36.09	'Abdallah 'Abed Al Hadi	Neogene	Eastern	Wadi Al-Faria	Nablus	Agricultural
14	18-18/014	186.610	182.950	-30.00	Sukaynah 'Abed Al Hadi	Neogene	Eastern	Wadi Al-Faria	Tubas	Agricultural
15	18-18/019	188.730	181.150	-40.00	'Abed Al Kareem Salem	Upper Cenomanian	Eastern	Wadi Al-Faria	Nablus	Agricultural
16	18-18/019A	188.570	181.320	-40.00	'Adel & Sa'di Al Shak'ah	Neogene	Eastern	Wadi Al-Faria	Nablus	Agricultural
17	18-18/023	187.210	183.070	-28.83	'Azmi 'Abed Al Majeed	Neogene	Eastern	Wadi Al-Faria	Nablus	Agricultural
18	18-18/026	186.800	182.500	-15.00	Fayez Ahmad 'Isa	Neogene	Eastern	Wadi Al-Faria	Nablus	Agricultural

19	18-18/027	186.060	183.610	-18.39	Nader 'Abed Al Hadi	Neogene	Eastern	Wadi Al-Faria	Nablus	Agricultural
20	18-18/027A	186.090	183.540	-19.28	Ibraheem Dhyab	Neogene	Eastern	Wadi Al-Faria	Nablus	Agricultural
21	18-18/030	186.240	183.350	-23.51	Qasem 'Abed Al Hadi	Neogene	Eastern	Wadi Al-Faria	Nablus	Agricultural
22	18-18/031	186.410	183.120	-29.16	Nader 'Abed Al Hadi	Neogene	North Eastern	Wadi Al-Faria	Nablus	Agricultural
23	18-18/031A	186.650	183.120	-28.00	Samirah 'Abed Al Hadi	Neogene	North Eastern	Wadi Al-Faria	Nablus	Agricultural
24	18-18/034	185.500	183.900	-10.00	Qasem 'Abed Al Hadi	Neogene	North Eastern	Wadi Al-Faria	Nablus	Agricultural
25	18-18/035	186.450	183.350	-15.00	Hafedh 'Abdallah	Neogene	North Eastern	Wadi Al-Faria	Nablus	Agricultural
26	18-18/036	187.600	182.550	-50.00	Khaleel 'Abed Al Hadi	Neogene	North Eastern	Wadi Al-Faria	Nablus	Agricultural
27	18-18/037	180.150	185.400	210.86	Nablus Municipality	Upper Cenomanian	North Eastern	Wadi Al-Faria	Nablus	Domestic
28	18-18/038	182.750	185.750	90.00	Nablus Municipality	Upper Cenomanian	North Eastern	Wadi Al-Faria	Nablus	Domestic
29	18-18/039	187.900	182.350	-58.00	Ibraheem Hamdan	Neogene	North Eastern	Wadi Al-Faria	Nablus	Agricultural
30	19-17/034	192.740	178.370	-148.88	Rajeh Shak'ah	Upper Cenomanian	Eastern	Furush Beit Dajan	Jericho	Agricultural
31	19-17/043	192.920	176.760	-178.63	'Abed Al Qader 'Abed Al Jaleel	Neogene	Eastern	Furush Beit Dajan	Jericho	Agricultural
32	19-17/044	192.000	179.030	-125.56	Muhammad Yusef Shaheen	Upper Cenomanian	Eastern	Furush Beit Dajan	Jericho	Agricultural
33	19-17/045	191.940	179.520	-132.20	Hasan I'baisi	Lower Cenomanian	Eastern	Furush Beit Dajan	Jericho	Agricultural
34	19-17/046	192.560	176.230	-167.02	Nash'at Al Masri	Neogene	Eastern	Furush Beit Dajan	Jericho	Agricultural
35	19-17/047	192.410	178.970	-137.31	Hasan 'Abed Al Jaleel	Upper Cenomanian	Eastern	Furush Beit Dajan	Jericho	Agricultural
36	19-17/050	192.790	179.120	-125.05	Muhammad Ahmad 'Abed Al Jabbar	Upper Cenomanian	Eastern	Furush Beit Dajan	Jericho	Agricultural

37	19-17/051	192.170	179.300	-127.49	Tawfeeq Yazdi	Upper Cenomanian	Eastern	Furush Beit Dajan	Jericho	Agricultural
38	19-17/057	192.180	179.000	-135.00	'Atara -Mekorot No.1	Upper Cenomanian	Eastern	Furush Beit Dajan	Jericho	Israeli
39	19-17/058	193.370	176.660	-160.00	Masawa No. 1	Lower+Upper	Eastern	Furush Beit Dajan	Jericho	Israeli
40	19-17/059	191.560	173.370	19.21	Geteet No.3	Lower Cenomanian	Eastern	Furush Beit Dajan	Jericho	Israeli
41	19-17/060	189.980	178.240	50.00	'Atara No.2	Lower Cenomanian	Eastern	Furush Beit Dajan	Jericho	Israeli
42	19-16/001	196.770	169.900	-260.00	'Ali 'Abdallah Damen	Alluvium	Eastern	Al Jiftlik	Jericho	Agricultural
43	19-16/003	198.460	169.650	-280.00	Ahmad Hashem Al Zghayyer	Alluvium	Eastern	Al Jiftlik	Jericho	Agricultural
44	19-16/004	198.200	169.300	-273.00	Ahmad Hashem Al Zghayyer	Alluvium	Eastern	Al Jiftlik	Jericho	Agricultural
45	19-16/005	199.590	168.850	-290.00	'Abed Al'azeez Lubbad Sarrees	Alluvium	Eastern	Al Jiftlik	Jericho	Agricultural
46	19-16/008	196.780	169.670	-260.00	Burhan Damen	Alluvium	Eastern	Al Jiftlik	Jericho	Agricultural
47	19-16/009	196.970	169.220	-265.00	Nawwaf Al Damen	Alluvium	Eastern	Al Jiftlik	Jericho	Agricultural
48	19-16/010	196.850	169.730	-260.00	Shaher Al Damen	Alluvium	Eastern	Al Jiftlik	Jericho	Agricultural
49	19-17/001	196.900	170.740	-255.00	'Inad Al Masri	Alluvium	Eastern	Al Jiftlik	Jericho	Agricultural
50	19-17/002	196.520	171.240	-252.60	Waheed Al Masri	Eocene	Eastern	Al Jiftlik	Jericho	Agricultural
51	19-17/004	197.220	170.560	-260.00	Al Jiftlik Nursery No. 3	Alluvium	Eastern	Al Jiftlik	Jericho	Agricultural
52	19-17/005	197.220	170.560	-260.00	Al Jiftlik Nursery No.5	Alluvium	Eastern	Al Jiftlik	Jericho	Agricultural
53	19-17/006	196.780	170.000	-260.00	Adham Al Damen	Alluvium	Eastern	Al Jiftlik	Jericho	Agricultural
54	19-17/007	196.640	172.290	-243.65	Fathalla Al Masri	Eocene	Eastern	Al Jiftlik	Jericho	Agricultural

55	19-17/008	196.250	170.250	-250.65	'Allan Al Damen & Partners	Alluvium	Eastern	Al Jiftlik	Jericho	Agricultural
56	19-17/009	197.470	170.230	-263.85	Rafeeq Qamhawi	Alluvium	Eastern	Al Jiftlik	Jericho	Agricultural
57	19-17/010	197.060	170.150	-262.42	Husain Drai'i	Alluvium	Eastern	Al Jiftlik	Jericho	Agricultural
58	19-17/021	196.520	170.560	-256.16	Mahmud Damen	Alluvium	Eastern	Al Jiftlik	Jericho	Agricultural
59	19-17/023	194.200	175.230	-195.94	Burhan Al Damen	Eocene	Eastern	Al Jiftlik	Jericho	Agricultural
60	19-17/024	196.560	171.550	-250.61	Basel Kan'an	Alluvium	Eastern	Al Jiftlik	Jericho	Agricultural
61	19-17/027	196.250	171.470	-248.92	Hassan Smadi	Alluvium	Eastern	Al Jiftlik	Jericho	Agricultural
62	19-17/028	198.150	170.500	-267.91	Fareed Abu Shamat	Alluvium+Eocene	Eastern	Al Jiftlik	Jericho	Agricultural
63	19-17/031	197.680	171.060	-264.65	'Abed Al Lateef Haydar	Alluvium	Eastern	Al Jiftlik	Jericho	Agricultural
64	19-17/033	196.510	172.910	-237.89	Deya' Saleh 'Abdu	Alluvium	Eastern	Al Jiftlik	Jericho	Agricultural
65	19-17/052	195.932	171.613	-240.00	Araih No.1	Eocene	Eastern	Al Jiftlik	Jericho	Israeli
66	19-17/053	196.790	170.570	-258.73	Al Jiftlik Nursery	Alluvium	Eastern	Al Jiftlik	Jericho	Agricultural
67	19-17/054	197.600	169.150	-273.00	Ma'ruf Abu Samrah	Alluvium	Eastern	Al Jiftlik	Jericho	Agricultural
68	19-17/055	196.150	173.400	-230.00	Jawad Al Masri	Eocene	Eastern	Al Jiftlik	Jericho	Agricultural
69	19-17/056	194.600	174.100	-205.00	Mahmud Damen	Eocene	Eastern	Al Jiftlik	Jericho	Agricultural

Appendix A4

Monthly Flow Discharge of the Springs in the Faria Catchment

Table A4 1: Monthly Flow Discharge of Shibli Spring

Coordinates: 189.90/181.90											**Elevation: -80**
Year	**Oct**	**Nov**	**Dec**	**Jan**	**Feb**	**Mar**	**Apr**	**May**	**June**	**July**	**Aug**	**Sep**
70/71	26	26	26	26	25	25	26	27	27	25	25	25
71/72	25	25	26	25	27	27	27	26	26	26	25	25
72/73	25	25	25	26	27	27	28	26	24	25	25	24
73/74	23	24	26	30	_	30	29	30	30	29	31	28
74/75	17	28	28	28	28	28	30	29	27	27	26	26
75/76	26	26	28	26	26	_	28	42	40	36	35	35
76/77	36	41	35	34	41	37	38	36	32	34	36	37
77/78	38	37	37	37	37	37	38	37	35	34	33	34
78/79	_	32	36	34	34	33	32	33	33	30	32	31
79/80	29	30	33	30	27	35	34	34	34	29	32	32
80/81	36	_	35	38	31	29	35	35	34	36	34	27
81/82	29	27	34	37	36	36	34	34	27	29	31	28
82/83	27	30	28	31	29	38	35	38	38	42	33	33
83/84	35	36	39	39	34	36	36	37	38	37	35	37
84/85	34	35	37	35	39	36	39	35	33	33	30	30
85/86	29	31	33	30	34	29	33	29	29	28	27	26
86/87	27	41	29	29	29	27	26	27	26	27	29	25
87/88	24	26	39	31	27	33	29	29	31	30	28	27
88/89	31	31	31	30	32	27	29	28	28	26	29	24
89/90	25	28	23	27	25	26	26	25	22	27	26	27
90/91	20	24	22	21	22	22	26	26	22	23	23	18
91/92	16	18	19	_	34	31	49	41	38	52	53	40
92/93	37	32	42	29	24	23	24	23	23	21	24	18
93/94	26	23	23	24	23	22	26	19	21	19	22	21
94/95	20	22	22	20	21	24	26	24	27	25	22	27
95/96	25	27	25	29	21	23	19	25	20	19	22	24
96/97	25	28	26	24	33	25	30	21	21	23	30	22
97/98	22	20	22	20	24	30	29	27	23	25	25	
98/99	28	23	26	23	22	20	_	_	_	_	_	_

- No Data

Table A4 2: Monthly Flow Discharge of Faria Spring

Coordinates: 182.40/188.40												**Elevation: +160**
Year	**Oct**	**Nov**	**Dec**	**Jan**	**Feb**	**Mar**	**Apr**	**May**	**June**	**July**	**Aug**	**Sep**
70/71	172	172	172	170	163	161	145	136	137	105	103	128
71/72	130	121	140	134	158	172	191	_	181	175	171	169
72/73	138	132	154	151	158	154	143	138	114	133	131	139
73/74	110	140	141	182	238	251	228	232	214	226	198	192
74/75	188	188	184	182	123	169	174	166	129	160	160	166
75/76	_	135	159	153	152	171	181	158	151	141	138	138
76/77	138	142	_	143	143	144	147	131	129	142	120	125
77/78	139	136	145	141	133	124	125	97	103	97	84	73
78/79	81	86	86	83	72	55	52	38	29	29	16	24
79/80	23	37	113	154	231	235	231	244	229	218	196	203
80/81	_	179	194	200	198	208	201	204	216	214	197	199
81/82	191	192	178	176	169	154	141	151	138	147	124	112
82/83	112	116	126	131	137	229	274	280	260	268	249	236
83/84	233	235	214	228	209	211	201	174	178	153	178	146
84/85	154	136	147	162	143	157	154	151	141	140	128	124
85/86	112	116	118	115	119	118	102	82	68	72	51	41
86/87	28	91	109	147	180	199	167	181	187	159	115	105
87/88	_	102	105	117	148	_	165	197	179	190	162	140
88/89	139	_	191	208	195	175	179	160	143	163	116	122
89/90	104	138	139	139	160	121	105	115	138	128	128	97
90/91	120	105	90	_	119	112	110	89	80	65	67	77
91/92	59	50	121	255	570	577	380	471	441	338	385	358
92/93	340	331	389	409	410	339	294	335	232	252	273	212
93/94	_	256	256	274	250	276	189	185	170	163	171	152
94/95	151	150	191	247	438	_	210	213	186	190	201	149
95/96	149	126	174	_	180	162	155	163	127	101	135	115
96/97	115	126	137	170	160	232	251	260	217	186	150	165
97/98	165	190	231	170	210	228	259	263	189	203	160	179
98/99	179	_	169	174	213	161	_	_	_	_	_	_

- No Data

Table A4 3: Monthly Flow Discharge of Miska Spring

Coordinates: 187.03/182.90											**Elevation: -38**
Year	**Oct**	**Nov**	**Dec**	**Jan**	**Feb**	**Mar**	**Apr**	**May**	**June**	**July**	**Aug**	**Sep**
70/71	67	67	73	75	77	69	74	81	69	66	64	54
71/72	54	57	67	54	65	76	78	75	66	68	62	66
72/73	62		68	70	67	70	62	50	52	46	49	40
73/74	43	42	57	72	_	75	76	78	71	71	69	56
74/75	68	53	69	44	66	44	63	59	49	44	50	49
75/76	57	63	67	61	71	_	72	61	61	61	63	54
76/77	44	50	63	63	62	67	68	53	48	39	_	41
77/78	38	35	40	56	62	70	56	42	31	26	24	22
78/79	18	20	23	19	22	24	20	15	8	6	6	3
79/80	4	5	11	15	11	49	30	62	59	65	62	45
80/81	42	_	51	54	51	50	60	65	57	55	55	41
81/82	36	38	68	65	60	52	50	35	28	30	19	14
82/83	13	10	22	44	43	58	70	77	81	97	73	75
83/84	72	80	72	76	92	88	75	76	59	59	47	43
84/85	38	38	40	56	61	64	61	40	23	21	17	13
85/86	6	13	17	29	28	31	24	9	6	1	0	0
86/87	0	3	5	12	9	20	14	21	6	7	4	1
87/88	0	8	6	11	14	27	34	28	23	31	22	14
88/89	11	36	41	32	28	27	33	5	5	5	2	1
89/90	0	2	7	12	12	9	16	5	0	0	0	0
90/91	0	0	0	0	2	3	2	0	0	0	0	0
91/92	0	0	2	_	43	61	71	76	67	75	63	56
92/93	51	67	76	83	72	76	62	57	47	53	55	51
93/94	53	61	58	52	50	52	59	50	44	41	42	35
94/95	44	53	51	41	42	30	53	39	48	47	45	38
95/96	38	49	49	39	50	53	45	39	35	35	35	19
96/97	15	30	45	45	51	49	59	42	51	40	48	41
97/98	38	43	49	59	49	55	60	45	46	43	45	34
98/99	27	34	41	44	41	32	_	_	_	_	_	_

- No Data

Table A4 4: Monthly Flow Discharge of Dafna Spring

Coordinates: 176.20/179.90											**Elevation: +560**
Year	**Oct**	**Nov**	**Dec**	**Jan**	**Feb**	**Mar**	**Apr**	**May**	**June**	**July**	**Aug**	**Sep**
70/71	1.4	1.2	1.1	1.2	1.4	3.3	3.9	10	3.9	2.8	2.2	1.7
71/72	1.4	1.4	1.3	3.3	7.2	11.1	10	6.7	3.3	2.8	1.9	1.8
72/73	1.5	1.4	1.7	1.5	3.3	2.5	2.9	2.5	2.2	1.8	1.4	1.3
73/74	1.1	1.1	1.3	2.8	_	_	11.1	5	3	2.5	2.5	2.2
74/75	1.9	1.7	1.7	2.5	_	_	8.9	3.3	2.8	2.2	1.9	1.7
75/76	0.5	0.4	0.4	0.4	0.4	_	1.6	0.8	0.8	0.7	0.5	0.4
76/77	0.5	0.4	0.4	1.4	_	_	0.8	0.7	0.5	0.4	1.5	0.2
77/78	0.2	0.2	0.2	0.9	1.9	0.8	0.5	_	_	0.3	0.3	0.3
78/79	1	_	_	_	_	_	_	1.4	_	_	_	_
79/80	0.4	4	6.7	22.2	20	41.7	13.3	5	_	2.8	2.8	2.5
80/81	2.9	2.8	2.8	3.9	_	_	10	6.7	1.1	4.2	3.3	2.8
81/82	2.8	1.9	2.8	2.5	5	10	5	3.9	3.9	3.3	3.3	3.3
82/83	3	3	3	_	_	_	_	13	7	7	7	5
83/84	4	4	4	3	5	7	7	5	5	4	3	3
84/85	3	3	3	2	7	6	5	4	3	2	2	2
85/86	2	2	3	3	3	4	1	4		3	3	2
86/87	2	2	4	5	7	6	8	4	4	4	4	4
87/88	4	4	4	5	_	_	7	5	5	5	4	4
88/89	4	4	4	5	7	5	7	7	5	5	5	4
89/90	4	4	5	4	7	10	10	10	5	4	3	3
90/91	3	3	3	3	5	5	7	5	4	4	3	3
91/92	3	3	_	_	_	_	_	7		7	6	6
92/93	19	15	14	_	_	_	_	30	28	7	6	5
93/94	4		4		10		7	6		4	3	2
94/95	_	_	_	_	_	_	_	_	_	_	_	_
95/96	_	_	_	_	_	_	_	_	_	_	_	_
96/97	_	_	_	2	4	17	17	13	8	5	4	3
97/98	3	3	3	3	5	20	20	8	7	3		3
98/99	3	3	2	2	1	1	_	_	_	_	_	_

- No Data

Table A4 5: Monthly Flow Discharge of Balata Spring

Coordinates: 176.84/179.77											**Elevation: +510**
Year	**Oct**	**Nov**	**Dec**	**Jan**	**Feb**	**Mar**	**Apr**	**May**	**June**	**July**	**Aug**	**Sep**
70/71	1	1	1	1	2	5	5	10	7	4	2	2
71/72	2	1	1	3	16	6	10	2	3	2	2	2
72/73	1	_	1	3	3	9	4	3	2	2	1	2
73/74	1	2	2	13	_	20	10	5	2	2	3	2
74/75	_	2	1	1	8	14	3	2	3	_	2	2
75/76	2	_	2	3	3	_	9	_	3	3	2	2
76/77	2	_	2	5	6	17	3	2	4	2	1	1
77/78	1	1	2	3	_	2	1	2	_	2	2	2
78/79	_	2	2	2	2	2	2	3	3	3	2	1
79/80	1	1	12	14	23	25	15	10	10	7	5	3
80/81	2	2	6	10	30	33	20	10	8	5	3	3
81/82	3	3	2	2	14	23	12	5	5	2	2	2
82/83	2	2	3	24	30	30	30	10	7	3	3	3
83/84	3	2	2	2	4	8	4	3	3	2	2	2
84/85	2	2	1	1	8	15	3	2	2	2	1	1
85/86	1	1	1	1	4	2	2	2	1	1	_	1
86/87	1	1	3	20	23	15	15	7	4	4	3	2
87/88	2	2	2	6	25	30	12	6	6	6	6	4
88/89	4	4	15	15	_	9	20	15	5	4	4	5
89/90	4	3	3	4	13	15	17	5	3	3	3	3
90/91	3	4	3	_	3	8	_	4	3	2	2	2
91/92	1	2	25	30	_	38	30	25	13	13	9	6
92/93	4	3	8	30	30	23	15	9	6	6	6	3
93/94	2	3	5	4	3	17	9	6	6	4	3	1
94/95	2.15	1.34	20	23.07	20	10.01	5.46	4.01	3	3	3	1.04
95/96	1.5	1.41	2.4	2.12	18.75	30	33.33	13.05	3.33	3.25	4.29	1.91
96/97	2.15	1.79	1.91	3.12	2.55	37.5	30	13.64	9.1	4.68	4.29	3
97/98	2.44	2.4	8.33	6.86	15	11.11	12.5	10.71	9.38	5.26	4	3.7
98/99	3.33	2.86	2.7	4.55	4	3.03	_	_	_	_	_	_

- No Data

Table A4 6: Monthly Flow Discharge of Asubian Spring

Coordinates: 180.44/184.42												**Elevation: +130**
Year	**Oct**	**Nov**	**Dec**	**Jan**	**Feb**	**Mar**	**Apr**	**May**	**June**	**July**	**Aug**	**Sep**
70/71	5	5	6	_	6	5	5	6	6	6	6	6
71/72	5	6	6	6	5	6	6	6	7	_	6	_
72/73	_	6	5	5	5	5	5	6	6	5	6	
73/74	5	5	5	6	7	6	8	6	7	7	6	6
74/75	6	6	5	6	5	5	6	6	6	6	6	6
75/76	6	6	5	6	6	6	6	7	6	6	6	5
76/77	5	5	5	5	5	5	6	6	6	6	6	7
77/78	6	6	5	5	5	5	5	5	5	5	5	5
78/79	4	4	5	5	4	4	4	4	5	5	4	4
79/80	4	4	5	5	5	6	7	6	6	6	7	6
80/81	6	6	5	5	6	5	6	6	6	7	6	6
81/82	7	6	5	5	5	5	5	6	7	7	7	7
82/83	7	6	6	6	6	8	7	9	8	9	9	8
83/84	8	8	7	7	7	7	7	7	8	7	8	8
84/85	7	8	7	7	6	7	6	7	7	7	7	6
85/86	7	7	7	6	6	6	6	6	6	6	6	6
86/87	6	6	6	7	7	7	7	7	9	7	8	7
87/88	8	7	6	6	7	_	6	7	7	7	8	7
88/89	7	_	6	6	6	6	6	6	6	6	7	7
89/90	7	7	6	6	6	6	7	7	7	6	6	6
90/91	6	7	6		6	6	6	6	6	6	6	6
91/92	6	6	6	7	8	8	8	8	7	7	7	6
92/93	7	6	7	7	7	7	8	7	7	7	7	7
93/94	_	6	6	6	6	6	7	7	6	6	7	7
94/95	7	7	6	6	6	6	6	6	6	6	7	7
95/96	7	7	7	6	6	6	6	7	7	8	8	7
96/97	7	6	6	6	6	6	7	6	8	8	8	7
97/98	8	8	7	6	6	6	6	8	8	7	7	8
98/99	7	5	5	5	5	5	_	_	_	_	_	_

- No Data

Table A4 7: Monthly Flow Discharge of Duleib Spring

Coordinates: 182.00/187.95											**Elevation: +155**
Year	**Oct**	**Nov**	**Dec**	**Jan**	**Feb**	**Mar**	**Apr**	**May**	**June**	**July**	**Aug**	**Sep**
70/71	28	25	25	17	15	16	18	18	_	19	18	14
71/72	16	16	10	23	60	54	58	54	48	30	28	34
72/73	28	24	25	23	21	19	21	20	13	_	7	7
73/74	5	_	_	25	138	144	112	112	68	66	44	34
74/75	31	31	20	31	22	35	29	22	24	27	19	20
75/76	_	15	13	11	7	18	20	17	17	16	14	9
76/77	_	11	8	7	10	12	16	12	13	14	_	9
77/78	9	7	6	5	5	4	4	3	2	1	1	1
78/79	0	0	0	0	0	0	0	0	0	0	0	0
79/80	0	0	0	7	41	_	119	72	52	37	35	32
80/81	_	28	25	29	39	49	37	35	29	31	33	22
81/82	19	19	15	13	11	19	10	6	7	5	4	2
82/83	2	1	1	1	5	155	172	164	142	127	91	62
83/84	62	46	42	42	31	36	34	30	25	20	15	14
84/85	14	8	8	6	7	7	14	16	10	7	6	4
85/86	3	2	2	1	0	1	1	0	0	0	0	0
86/87	0	0	0	11	27	24	28	23	25	20	14	11
87/88	_	11	8	7	26		79	50	57	48	25	33
88/89	29	_	28	29	36	27	24	22	18	22	14	16
89/90	11	8	8	12	14	15	14	12	18	16	16	8
90/91	8	6	4	_	4	3	4	4	3	2	1	_
91/92	0	0	2	161	580	733	542	396	261	220	215	164
92/93	175	170	225	275	255	183	156	165	139	127	98	81
93/94	_	50	46	42	30	32	25	25	18	21	19	16
94/95	16	13	23	28	_	84	46	42	41	40	34	26
95/96	27	16	18	20	23	18	22	_	_	15	15	14
96/97	8	9	8	7	8	35	132	130	65	70	48	36
97/98	38	34	34	28	32	34	85	77	74	56	43	29
98/99	372	22	28	27	20	17	_	_	_	_	_	_

- No Data

Table A4 8: Monthly Flow Discharge of Qudeira Spring

Coordinates: 180.13/185.28											**Elevation: +215**
Year	**Oct**	**Nov**	**Dec**	**Jan**	**Feb**	**Mar**	**Apr**	**May**	**June**	**July**	**Aug**	**Sep**
70/71	_	_	_	_	_	_	_	_	_	_	_	_
71/72	_	_	_	_	_	_	_	_	_	_	_	_
72/73	_	_	_	_	_	_	_	_	_	_	_	_
73/74	0	0	0	67	70	70	64	59	53	52	50	48
74/75	45	42	42	34	44	51	51	48	43	41	33	_
75/76	26	21	14	6	9	51	_	46	43	40	39	35
76/77	23	18	11	0	38	49	48	45	46	38	33	_
77/78	20	11	11	15	12	12	10	6	0	0	0	0
78/79	0	0	0	0	0	0	0	0	0	0	0	0
79/80	0	0	0	53	70	110	106	90	87	78	68	60
80/81	_	57	60	75	82	80	69	67	64	61	58	55
81/82	51	49	47	46	43	48	42	41	36	22	10	10
82/83	1	0	0	0	66	109	120	103	85	75	64	59
83/84	57	56	57	57	64	63	78	69	64	61	57	38
84/85	27	25	7	1	0	43	42	43	37	10	3	0
85/86	0	0	0	0	0	0	0	0	0	0	0	0
86/87	0	0	0	68	93	129	129	127	116	104	93	82
87/88	71	64	51	61	94	_	99	98	95	88	68	64
88/89	62	0	57	59	61	63	78	76	71	68	65	51
89/90	42	37	24	22	55	59	61	59	58	55	51	44
90/91	38	25	14	_	16	26	39	37	30	24	18	4
91/92	0	0	30	128	130	109	99	90	88	66	80	66
92/93	47	40	54	54	64	55	51	39	43	37	39	34
93/94	_	29	31	29	24	34	32	26	23	20	15	14
94/95	14	9	33	40	24	34	32	26	23	20	15	14
95/96	_	29	31	29	33	36	41	37	35	34	29	30
96/97	33	24	19	16	22	29	42	32	39	28	25	18
97/98	14	10	6	3	10	45	44	42	43	32	42	21
98/99	38	34	35	29	37	40	49	46	45	39	34	27

- No Data

Table A4 9: Monthly Flow Discharge of Hamad & Beida Spring

Coordinates: 180.12/185.32												**Elevation: +215**
Year	**Oct**	**Nov**	**Dec**	**Jan**	**Feb**	**Mar**	**Apr**	**May**	**June**	**July**	**Aug**	**Sep**
70/71	25	23	19	18	21	21	38	36	35	31	30	26
71/72	22	19	19	42	42	43	42	41	40	39	37	34
72/73	_	28	27	26	25	31	30	25	24	24	24	23
73/74	17	9	7	41	37	38	36	37	37	35	33	33
74/75	28	25	23	25	25	28	30	28	21	30	23	_
75/76	22	25	22	14	17	46	_	34	33	33	30	29
76/77	24	17	16	14	30	37	33	33	35	30	23	_
77/78	19	20	17	19	17	15	15	19	14	12	10	11
78/79	4	1	0	0	0	0	0	0	0	0	0	0
79/80	0	0	29	24	28	37	35	31	34	27	30	27
80/81	_	23	27	28	30	31	34	22	29	30	28	26
81/82	18	16	19	21	15	19	24	18	18	15	11	11
82/83	10	8	9	12	36	43	37	33	32	36	29	25
83/84	25	25	29	30	32	34	43	38	41	32	26	24
84/85	23	17	17	16	12	26	25	30	22	20	17	14
85/86	10	7	3	0	0	0	6	5	4	1	0	0
86/87	0	7	18	43	48	38	33	38	35	34	32	32
87/88	25	21	22	23	37	_	35	30	29	25	25	24
88/89	24	_	24	25	30	31	41	42	32	32	29	22
89/90	20	17	15	17	28	29	27	32	29	22	17	15
90/91	13	11	6	_	14	15	21	18	17	14	13	11
91/92	8	4	29	65	80	113	74	82	63	54	54	40
92/93	32	39	48	42	48	47	45	38	37	34	38	34
93/94	_	34	27	32	27	33	29	33	26	21	20	18
94/95	_	_	_	13	22	33	53	53	50	44	30	34
95/96	34	32	24	33	30	36	41	45	45	44	37	30
96/97	30		35	27	26	23	_	_	_	_	_	_
97/98	25	23	19	18	21	21	38	36	35	31	30	26
98/99	22	19	19	42	42	43	42	41	40	39	37	34

- No Data

Table A4 10: Monthly Flow Discharge of Al-Jiser Spring

Coordinates: 180.37/185.10										**Elevation: +170**	
Year	**Oct**	**Nov**	**Dec**	**Jan**	**Feb**	**Mar**	**Apr**	**May**	**June**	**July**	**Aug**	**Sep**
70/71	_	_	_	_	_	_	_	_	_	_	_	_
71/72	_	_	_	_	_	_	_	_	_	_	_	_
72/73	_	_	_	_	_	_	_	_	_	_	_	_
73/74	_	_	_	_	_	_	_	_	_	_	_	_
74/75	_	_	_	_	_	_	_	_	_	_	_	_
75/76	5	4	4	5	5	7	_	5	6	5	5	5
76/77	5	5	5	6	6	6	7	6	6	5	6	_
77/78	5	5	5	5	5	5	5	5	5	5	4	3
78/79	3	3	2	2	1	1	1	1	0	0	0	0
79/80	0	0	0	7	8	10	10	9	8	8	6	5
80/81	_	5	5	5	5	6	6	5	5	5	4	5
81/82	4	4	3	4	4	4	5	4	4	4	4	3
82/83	3	3	3	3	4	8	7	9	7	6	6	6
83/84	6	5	5	4	4	6	6	5	5	4	4	3
84/85	2	2	2	2	2	3	3	3	3	2	2	2
85/86	1	1	1	1	1	1	1	2	1	1	1	0
86/87	0	1	1	3	3	4	4	4	4	3	2	2
87/88	2	2	2	2	6	_	6	6	6	5	5	4
88/89	4	_	3	3	4	4	4	6	5	5	4	4
89/90	3	3	3	3	4	4	6	5	5	5	5	4
90/91	3	3	3	_	3	3	3	3	3	3	3	2
91/92	2	2	3	8	10	11	11	8	10	9	8	6
92/93	7	6	7	7	7	7	8	7	6	6	5	5
93/94	_	4	5	5	4	5	6	5	5	4	4	4
94/95	4	3	5	5	5	6	6	5	5	5	4	4
95/96	4	5	4	4	4	5	4	6	6	5	5	4
96/97	4	3	3	3	3	4	5	4	6	8	7	7
97/98	6	7	6	8	7	7	10	9	8	9	7	8
98/99	9	6	6	5	6	5	_	_	_	_	_	_

- No Data

Table A4 11: Monthly Flow Discharge of Sidreh Spring

Coordinates: 179.95/185.49											**Elevation: +240**
Year	**Oct**	**Nov**	**Dec**	**Jan**	**Feb**	**Mar**	**Apr**	**May**	**June**	**July**	**Aug**	**Sep**
70/71	0	0	0	0	0	0	0	57	35	146	0	0
71/72	0	0	0	0	171	145	163	126	110	73	54	10
72/73	3	0	0	0	0	0	0	0	0	0	0	0
73/74	0	0	0	242	251	259	200	163	105	78	47	31
74/75	16	0	0	0	8	72	54	39	24	8	0	0
75/76	0	0	0	0	0	37	26	11	0	0	0	0
76/77	0	0	0	0	0	41	31	15	0	0	0	0
77/78	0	0	0	0	0	0	0	0	0	0	0	0
78/79	0	0	0	0	0	0	0	0	0	0	0	0
79/80	0	0	23	0	96	214	181	141	112	80	47	29
80/81	22	_	0	0	70	83	78	81	43	30	13	0
81/82	0	0	0	0	0	0	0	0	0	0	0	0
82/83	0	0	0	0	0	242	282	251	213	139	102	68
83/84	36	31	12	0	0	0	11	0	0	0	0	0
84/85	0	0	0	0	0	0	0	0	0	0	0	0
85/86	0	0	0	0	0	0	0	0	0	0	0	0
86/87	0	0	0	6	30	139	52	27	7	0	0	0
87/88	0	0	0	0	236	_	180	163	114	96	31	18
88/89	3	0	0	0	0	0	40	17	11	0	0	0
89/90	0	0	0	0	0	0	0	0	0	0	0	0
90/91	0	0	0	0	0	0	0	0	0	0	0	0
91/92	0	0	0	251	405	557	461	400	300	300	251	163
92/93	132	89	310	320	303	290	233	163	155	117	58	41
93/94	0	27	8	0	0	36	15	0	0	0	0	0
94/95	0	0	19	83	89	132	132	89	57	36	23	0
95/96	0	0	0	0	0	0	58	36	19	0	0	0
96/97	0	0	0	0	0	132	340	299	280	235	181	53
97/98	31	18	0	0	15	27	190	165	131	95	57	36
98/99	18	5	0	0	0	_	_	_	_	_	_	_

- No Data

Table A4 12: Monthly Flow Discharge of Tabban Spring

Coordinates: 180.42/184.82											**Elevation:+160**
Year	**Oct**	**Nov**	**Dec**	**Jan**	**Feb**	**Mar**	**Apr**	**May**	**June**	**July**	**Aug**	**Sep**
70/71	30	28	28	29	29	31	31	32	35	35	35	35
71/72	26	29	28	30	30	30	33	32	35	_	35	_
72/73	_	33	32	33	35	35	37	38	38	39	38	38
73/74	38	37	37	40	42	42	44	42	43	44	42	42
74/75	42	42	41	41	41	42	42	42	42	41	42	41
75/76	40	41	41	41	41	42	_	43	42	42	42	41
76/77	_	41	40	40	42	42	42	43	42	41	44	41
77/78	41	41	41	41	40	41	40	41	41	41	40	40
78/79	40	40	40	39	38	38	38	38	38	36	35	35
79/80	35	35	41	44	51	42	52	48	44	48	50	46
80/81	41	42	49	46	48	46	48	45	42	47	40	44
81/82	44	45	43	47	46	49	54	48	39	41	54	47
82/83	47	45	37	43	44	44	58	50	51	48	48	59
83/84	55	53	56	56	54	59	57	47	58	51	51	47
84/85	54	51	48	48	52	43	53	51	53	57	47	44
85/86	49	57	52	53	48	48	56	52	51	46	46	46
86/87	55	48	48	47	54	48	55	50	53	53	43	43
87/88	41	52	46	42	48	_	40	46	41	56	48	41
88/89	48	_	46	42	41	39	51	38	42	49	43	48
89/90	56	48	31	37	39	30	41	32	38	40	40	46
90/91	46	36	39	_	39	46	51	53	49	49	47	51
91/92	51	54	56	53	48	46	57	62	57	44	50	42
92/93	42	41	39	43	53	49	47	49	52	47	53	53
93/94	_	44	58	58	38	47	39	41	45	42	36	37
94/95	37.12	34.7	36.4	34	41	36	38	40	38.6	41.4	38	41
95/96	39.3	41	38	40	39	41	41	41	41	43	38	42
96/97	44	40	37	33	38	36	43	44	38	49	45	48
97/98	35	37	33	32	41	40	37	36	42	38	39	38
98/99	51	35	40	48	34	5	_	_	_	_	_	_

- No Data

Table A4 13: Monthly Flow Discharge of Abu Saleh Spring

Coordinates: 186.26/183.57											**Elevation: +510**
Year	**Oct**	**Nov**	**Dec**	**Jan**	**Feb**	**Mar**	**Apr**	**May**	**June**	**July**	**Aug**	**Sep**
70/71	12.3	11.6	12.9	18	14.4	11.3	10.4	11.7	10	8.8	_	_
71/72	7.4	6.7	8.4	8.3	12.1	12.5	11.4	11.9	15.4	15.7	11.6	11.4
72/73	10.6	9.4	9.6	7.1	13.8	8.8	6.5	5.4	5.4	12.3	8.8	8.1
73/74	8	_	_	_	_	_	_	_	_	41	_	_
74/75	_	_	_	_	_	_	_	18.8	20.5	15.7	15.2	14.4
75/76	11.8	12.2	18.2	31.4	_	_	_	12.3	8.9	6.8	5.1	1.5
76/77	1.9	1	2.6	5	_	_	8	4.8	2.2	0.7	0	_
77/78	0	_	0	4.43		2.7	0	0	_	0	0	0
78/79	_	0	0	0	0	0	0	0	0	0	0	0
79/80	0	0	0	0	0	0	_	_	_	_	_	_
80/81	_	_	_	_	_	_	_	_	_	_	_	_
81/82	_	_	_	_	_	_	_	_	_	_	_	_
82/83	_	_	_	_	_	_	_	_	_	_	_	_
83/84	_	_	_	_	_	_	_	_	_	_	_	_
84/85	_	_	_	_	_	_	_	_	_	_	_	_
85/86	_	_	_	_	_	_	_	_	_	_	_	_
86/87	_	_	_	_	_	_	_	_	_	_	_	_
87/88	_	_	_	_	_	_	_	_	_	_	_	_
88/89	_	_	_	_	_	_	_	_	_	_	_	_
89/90	_	_	_	_	_	_	_	_	_	_	_	_
90/91	_	_	_	_	_	_	_	_	_	_	_	_
91/92	_	_	_	_	_	_	_	_	_	_	_	_
92/93	_	_	_	_	_	_	_	_	_	_	_	_
93/94	12.4	14.3	11.5	11.2	9	6.5	8.2	5.3	3.8	3.2	3.3	1.7
94/95	1.1	2.8	1.4	1.9	1	2	4.8	4.9	4.9	3.6	2.7	2.2
95/96	1.4	2.6	1.6	2	1.47	2.6	2.83	2	5	3.33	2.63	1.39
96/97	0.68	2.08	4.01	2.08	_	2.5	3.03	1.43	2.08	2.8	2.5	0.4
97/98	0.16	1.3	_	0.43	4.7	7.1	1	2.3	4	2.3	0.8	1.2
98/99	1	0.6	1.8	1.2	0.6	_	_	_	_	_	_	_

- No Data

APPENDIX A5

FLOW MEASUREMENTS AT WADI AL-BADAN AND WADI AL-FARIA

Table A5 1: Flow Records of Al-Badan and Al-Faria Flumes

Al-Badan			Al-Faria	
Date	**Time**	**Q(m^3/s)**	**Time**	**Q(m^3/s)**
11/11/2003	1:25PM	0.11	1:35PM	0.09
02/12/2003	8:30AM	0.09	8:40AM	0.07
02/12/2003	10:05AM	0.09	10:14AM	0.09
02/12/2003	3:18PM	0.12	3:25PM	0.09
03/12/2003	10:35AM	0.12	10:40AM	0.09
03/12/2003	5:30PM	0.14	5:35PM	0.11
04/12/2003	10:57AM	0.13	11:02AM	0.11
04/12/2003	5:22PM	0.16	5:16PM	0.13
05/12/2003	10:41AM	0.12	10:36AM	0.12
05/12/2003	4:36PM	0.12	4:33PM	0.12
06/12/2003	10:35AM	0.15	10:30AM	0.10
06/12/2003	2:44PM	0.13	2:50PM	0.10
07/12/2003	9:31AM	0.14	9:36AM	0.11
07/12/2003	3:38PM	0.13	3:50PM	0.11
08/12/2003	8:50AM	0.14	9:02AM	0.11
08/12/2003	4:05PM	0.15	4:15PM	0.11
09/12/2003	8:10AM	0.15	8:20AM	0.12
09/12/2003	4:00PM	0.15	4:12PM	0.12
10/12/2003	8:45AM	0.15	8:50AM	0.12
10/12/2003	4:00PM	0.15	4:10PM	0.12
11/12/2003	10:25AM	0.15	10:05AM	0.10
12/12/2003	8:10AM	0.15	8:20AM	0.11
12/12/2003	4:00PM	0.15	4:12PM	0.09
13/12/2003	9:00AM	0.15	9:12AM	0.09
13/12/2003	4:00PM	0.15	4:10PM	0.10
14/12/2003	9:00AM	0.15	9:10AM	0.10
15/12/2003	8:10AM	0.15	8:20AM	0.10
16/12/2003	8:40AM	0.15	8:55AM	0.11
18/12/2003	12:50PM	0.15	1:00PM	0.13
18/12/2003	1:30PM	0.16	1:35PM	0.14
18/12/2003	2:45PM	0.17	3:00PM	0.16
18/12/2003	4:00PM	0.19	4:05PM	0.17
18/12/2003	4:45PM	0.19	5:00PM	0.19
19/12/2003	7:45AM	0.19	7:50AM	0.20
19/12/2003	9:00AM	0.19	9:10AM	0.17
19/12/2003	10:10AM	0.19	10:20AM	0.18
19/12/2003	12:30PM	0.16	12:40PM	0.18
19/12/2003	3:15PM	0.17	3:20PM	0.17
19/12/2003	5:00PM	0.17	4:50PM	0.17
22/12/2003	9:00AM	0.16	9:15AM	0.16

24/12/2003	10:00AM	0.16	9:50AM	0.17
26/12/2003	10:30AM	0.16	10:45AM	0.16
28/12/2003	11:00AM	0.17	10:30AM	0.19
30/12/2003	12:15PM	0.17	12:20PM	0.14
01/01/2004	10:35AM	0.17	10:40AM	0.14
03/01/2004	9:00AM	0.14	9:10AM	0.11
05/01/2004	12:15PM	0.14	12:20PM	0.11
07/01/2004	9:05AM	0.14	8:50AM	0.13
07/01/2004	10:15AM	0.15	10:05AM	0.14
07/01/2004	11:20AM	0.16	11:30AM	0.14
07/01/2004	12:30PM	0.16	12:45PM	0.15
07/01/2004	1:45PM	0.17	1:35PM	0.16
07/01/2004	3:05PM	0.17	2:55PM	0.16
07/01/2004	4:20PM	0.19	4:30PM	0.17
08/01/2004	8:45AM	0.20	8:40AM	0.17
08/01/2004	10:00AM	0.21	9:50AM	0.17
08/01/2004	12:10PM	0.22	12:03PM	0.16
08/01/2004	2:05PM	0.22	2:00PM	0.16
08/01/2004	4:05PM	0.21	4:10PM	0.14
09/01/2004	9:00AM	0.17	8:50AM	0.14
09/01/2004	11:05AM	0.17	11:10AM	0.14
09/01/2004	3:30PM	0.16	3:20PM	0.14
11/01/2004	10:00AM	0.17	10:10AM	0.13
13/01/2004	11:15AM	0.17	11:20AM	0.14
15/01/2004	3:05PM	0.17	3:00PM	0.14
17/01/2004	2:30PM	0.16	2:20PM	0.13
19/01/2004	1:17PM	0.16	1:25PM	0.14
21/01/2004	9:25AM	0.17	9:30AM	0.14
22/01/2004	12:40PM	0.20	12:35PM	0.16
22/01/2004	1:50PM	0.21	1:40PM	0.20
22/01/2004	3:15PM	0.23	3:20PM	0.20
22/01/2004	9:20AM	0.22	4:30PM	0.16
24/01/2004	2:20AM	0.19	2:25PM	0.16
25/01/2004	1:10PM	0.19	1:00PM	0.16
26/01/2004	7:30AM	0.21	7:25AM	0.17
26/01/2004	8:20AM	0.21	8:30AM	0.17
26/01/2004	9:30AM	0.22	9:35AM	0.18
26/01/2004	10:40AM	0.23	10:37AM	0.19
26/01/2004	11:30AM	0.23	11:22AM	0.17
26/01/2004	12:40PM	0.23	12:45PM	0.17
26/01/2004	1:53PM	0.23	1:48PM	0.17
26/01/2004	3:05PM	0.25	3:00PM	0.16
26/01/2004	4:15PM	0.21	4:10PM	0.16

26/01/2004	5:07PM	0.21	5:15PM	0.15
27/01/2004	9:00AM	0.25	8:45AM	0.22
27/01/2004	11:15AM	0.25	11:20AM	0.23
27/01/2004	12:30PM	0.23	12:25PM	0.22
27/01/2004	2:05PM	0.21	2:00PM	0.21
27/01/2004	3:15PM	0.20	3:10PM	0.20
27/01/2004	4:20PM	0.19	4:30PM	0.19
28/01/2004	12:30PM	0.19	2:40PM	0.16
30/01/2004	3:15PM	0.19	3:20PM	0.16
02/02/2004	9:15AM	0.34	9:20AM	0.16
02/02/2004	3:05PM	0.34	3:10PM	0.16
02/02/2004	4:20PM	0.29	4:30PM	0.17
04/02/2004	11:15AM	0.28	11:10AM	0.18
06/02/2004	9:30AM	0.28	9:40AM	0.17
08/02/2004	2:15PM	0.25	2:25PM	0.17
10/02/2004	4:05PM	0.25	4:00PM	0.17
12/02/2004	3:30PM	0.25	3:42PM	0.16
14/02/2004	2:24PM	0.28	2:18PM	0.16
14/02/2004	3:45PM	0.30	3:50PM	0.17
14/02/2004	4:30PM	0.32	4:40PM	0.17
14/02/2004	7:30PM	4.84	*	*
15/02/2004	8:05AM	2.04	8:15AM	0.38
15/02/2004	9:15AM	2.04	9:20AM	0.40
15/02/2004	10:20AM	1.60	10:30AM	0.40
15/02/2004	11:30AM	1.43	11:40AM	0.40
15/02/2004	12:20PM	1.19	12:15PM	0.39
15/02/2004	1:35PM	0.90	1:30PM	0.38
15/02/2004	2:32PM	0.71	2:25PM	0.36
15/02/2004	3:28PM	0.67	3:32PM	0.34
15/02/2004	4:40PM	0.64	4:48PM	0.30
16/02/2004	8:45AM	0.37	8:50AM	0.22
16/02/2004	9:53AM	0.37	10:00AM	0.24
16/02/2004	11:20AM	0.36	11:27AM	0.26
16/02/2004	12:45PM	0.34	1:05PM	0.27
16/02/2004	2:30PM	0.34	2:25PM	0.28
16/02/2004	3:45PM	0.33	3:50PM	0.30
17/02/2004	10:11AM	0.34	10:15AM	0.26
17/02/2004	12:45PM	0.37	12:55PM	0.25
17/02/2004	2:55PM	0.37	2:45PM	0.24
17/02/2004	4:30PM	0.38	4:37PM	0.22
19/02/2004	3:15PM	0.32	3:20PM	0.30
21/02/2004	10:32AM	0.28	10:28AM	0.17
23/02/2004	3:15PM	0.25	3:30PM	0.16

25/02/2004	2:18PM	0.21	2:25PM	0.14
27/02/2004	1:57PM	0.20	2:05PM	0.13
29/02/2004	3:10PM	0.19	3:22PM	0.13
02/03/2004	4:25PM	0.19	4:30PM	0.13
04/03/2004	3:50PM	0.23	3:40PM	0.1
06/03/2004	2:15PM	0.25	2:20PM	0.11
08/03/2004	11:05AM	0.25	11:00AM	0.11
10/03/2004	3:30PM	0.25	3:20PM	0.10
12/03/2004	4:15PM	0.23	4:25PM	0.10
14/03/2004	9:05AM	0.23	9:15AM	0.10
16/03/2004	11:15AM	0.22	11:33AM	0.10
18/03/2004	3:15PM	0.21	3:25PM	0.09
20/03/2004	2:30PM	0.22	2:20PM	0.10
04/04/2004	12:00AM	0.14	12:10PM	0.04
02/05/2004	1:25PM	0.14	1:35PM	0.03
01/12/2004	2:33PM	0.04	2:45PM	0.03
02/12/2004	10:00AM	0.04	10:10AM	0.02
02/12/2004	9:25AM	0.06	9:10AM	0.03
03/12/2004	2:10PM	0.04	2:20PM	0.02
04/12/2004	1:30PM	0.05	1:20PM	0.02
05/12/2004	4:15PM	0.05	4:25PM	0.02
06/12/2004	4:40PM	0.05	4:30PM	0.02
07/12/2004	9:12AM	0.05	9:20PM	0.02
08/12/2004	2:35PM	0.05	2:45PM	0.02
09/12/2004	1:00PM	0.05	1:20PM	0.02
09/12/2004	9:55AM	0.09	9:38AM	0.05
10/12/2004	11:15AM	0.05	11:25AM	0.02
11/12/2004	3:05PM	0.05	3:00PM	0.02
12/12/2004	2:00PM	0.05	1:50PM	0.02
13/12/2004	9:45AM	0.05	9:35AM	0.02
14/12/2004	7:13AM	0.05	7:20AM	0.03
14/12/2004	8:25AM	0.06	8:35AM	0.03
14/12/2004	9:35AM	0.06	9:30AM	0.04
14/12/2004	10:40AM	0.07	10:50AM	0.04
15/12/2004	2:40PM	0.08	2:50PM	0.04
16/12/2004	10:15AM	0.09	10:30AM	0.05
17/12/2004	4:20PM	0.08	4:30PM	0.05
18/12/2004	2:40PM	0.07	2:45PM	0.05
19/12/2004	1:40PM	0.06	1:20PM	0.04
20/12/2004	9:30AM	0.01	9:45AM	0.05
21/12/2004	11:20AM	0.01	11:10AM	0.05
22/12/2004	2:00PM	0.01	2:20PM	0.05
23/12/2004	4:20PM	0.00	4:30PM	0.04

24/12/2004	3:50PM	0.00	4:00PM	0.04
25/12/2004	6:20AM	0.01	6:30AM	0.05
25/12/2004	7:30AM	0.01	7:40AM	0.06
25/12/2004	8:45AM	0.01	8:35AM	0.06
25/12/2004	9:55AM	0.01	9:40AM	0.06
25/12/2004	10:45AM	0.01	10:55AM	0.07
25/12/2004	11:50AM	0.01	11:55AM	0.07
25/12/2004	12:50PM	0.01	1:00PM	0.07
26/12/2004	3:20P	0.01	3:30PM	0.07
27/12/2004	2:20PM	0.01	2:30PM	0.06
27/12/2004	10:20AM	0.01	11:20AM	0.05
28/12/2004	3:40PM	0.01	3:50PM	0.05
29/12/2004	2:20PM	0.01	2:00PM	0.05
30/12/2004	1:15PM	0.01	1:00PM	0.05
31/12/2004	12:00AM	0.01	12:20PM	0.05
01/01/2005	3:40PM	0.06	3:50PM	0.07
02/01/2005	3:00PM	0.08	3:10PM	0.07
02/01/2005	4:15PM	0.08	4:00PM	0.08
02/01/2005	5:00PM	0.09	5:10PM	0.09
03/01/2005	6:30AM	0.11	6:40AM	0.09
03/01/2005	7:50AM	0.12	8:00AM	0.09
03/01/2005	8:55AM	0.12	9:00AM	0.09
03/01/2005	10:40AM	0.12	10:50AM	0.07
04/01/2005	10:45AM	0.12	11:15AM	0.06
05/01/2005	10:30AM	0.13	10:20AM	0.07
05/01/2005	11:45AM	0.14	11:35	0.07
05/01/2005	12:20PM	0.12	12:40PM	0.06
05/01/2005	12:35PM	0.14	12:40PM	0.08
05/01/2005	1:50PM	0.14	1:40PM	0.08
05/01/2005	2:40PM	0.14	2:30PM	0.08
05/01/2005	3:55PM	0.14	3:40PM	0.09
05/01/2005	4:30PM	0.15	4:35PM	0.10
06/01/2005	10:20AM	0.14	10:30AM	0.09
07/01/2005	7:15AM	0.15	7:00AM	0.07
08/01/2005	3:20PM	0.16	3:30PM	0.07
09/01/2005	2:00PM	0.16	1:40PM	0.06
10/01/2005	10:15AM	0.16	10:20AM	0.06
11/01/2005	11:40AM	0.16	11:30AM	0.06
12/01/2005	3:00PM	0.14	3:20PM	0.06
13/01/2005	9:00AM	0.14	9:15AM	0.06
14/01/2005	12:00PM	0.14	12:30PM	0.06
15/01/2005	11:14AM	0.16	11:25PM	0.07
15/01/2005	12:20PM	0.16	12:25AM	0.07

15/01/2005	1:30PM	0.16	1:40PM	0.07
15/01/2005	2:40PM	0.17	2:50PM	0.07
15/01/2005	4:00PM	0.17	3:45PM	0.10
15/01/2005	5:10PM	0.17	5:00PM	0.11
16/01/2005	3:15PM	0.17	3:35PM	0.10
17/01/2005	2:30PM	0.17	2:40PM	0.10
18/01/2005	10:00AM	0.17	10:20AM	0.10
19/01/2005	12:30PM	0.17	12:20PM	0.10
19/01/2005	1:40PM	0.18	1:30PM	0.11
19/01/2005	2:30PM	0.18	2:35PM	0.11
19/01/2005	3:20P	0.19	3:30PM	0.12
19/01/2005	4:45PM	0.19	4:40PM	0.11
20/01/2005	10:00AM	0.19	10:15AM	0.10
21/01/2005	3:20PM	0.19	3:30PM	0.10
22/01/2005	11:00AM	0.21	10:50AM	0.10
22/01/2005	12:10PM	0.23	12:00PM	0.11
22/01/2005	1:20PM	0.28	1:00PM	0.12
22/01/2005	2:15PM	0.37	2:00PM	0.13
22/01/2005	3:30PM	0.53	3:35PM	0.16
22/01/2005	4:30PM	0.58	4:40PM	0.17
22/01/2005	8:00PM	7.67	8:20PM	0.19
23/01/2005	7:30AM	0.30	8:00AM	0.09
24/01/2005	9:00AM	0.67	9:20AM	0.10
25/01/2005	11:00AM	0.23	11:10AM	0.09
26/01/2005	2:00PM	0.23	2:15PM	0.08
27/01/2005	4:00PM	0.24	4:20PM	0.08
28/01/2005	10:00AM	0.23	10:10AM	0.07
29/01/2005	2:30PM	0.23	2:40PM	0.07
30/01/2005	9:55AM	0.21	10:00AM	0.07
31/01/2005	2:50PM	0.19	3:00PM	0.07
01/02/2005	8:20AM	0.19	8:30PM	0.13
01/02/2005	9:40AM	0.19	9:35PM	0.13
01/02/2005	10:50AM	0.19	10:40PM	0.13
01/02/2005	11:40AM	0.20	11:50PM	0.14
01/02/2005	12:55AM	0.21	1:00AM	0.14
01/02/2005	2:00AM	0.21	2:20AM	0.15
01/02/2005	3:30AM	0.21	3:35AM	0.16
01/02/2005	4:40AM	0.21	4:50AM	0.16
02/02/2005	7:40PM	0.23	7:30PM	0.11
02/02/2005	8:50PM	0.23	8:35PM	0.13
02/02/2005	9:40PM	0.25	9:30PM	0.13
02/02/2005	10:45PM	0.25	10:35PM	0.13
02/02/2005	11:40PM	0.25	11:30PM	0.14

02/02/2005	12:50PM	0.25	12:40PM	0.14
02/02/2005	1:45AM	0.25	1:55AM	0.14
02/02/2005	2:50AM	0.28	3:00AM	0.14
02/02/2005	4:00AM	0.28	4:20AM	0.14
04/02/2005	8:30PM	0.28	8:20PM	0.13
04/02/2005	9:40PM	0.28	9:45PM	0.13
04/02/2005	10:50PM	0.30	10:40PM	0.13
04/02/2005	11:55PM	0.31	12:00PM	0.13
04/02/2005	1:10AM	0.32	1:20AM	0.14
04/02/2005	2:25AM	0.34	2:35AM	0.15
04/02/2005	3:30AM	0.34	3:40AM	0.16
04/02/2005	4:40AM	0.36	4:50AM	0.17
05/02/2005	8:00PM	2.53	7:40PM	0.22
05/02/2005	9:00PM	3.05	8:50PM	0.24
05/02/2005	10:00PM	3.39	10:00PM	0.26
05/02/2005	10:30PM	3.62	11:30PM	0.28
05/02/2005	11:40PM	4.21	12:40PM	0.32
05/02/2005	12:50PM	4.33	2:00AM	0.38
05/02/2005	2:10AM	4.84	3:40AM	0.52
05/02/2005	3:30AM	5.50	4:40AM	0.67
06/02/2005	*	*	8:00PM	1.65
07/02/2005	*	*	10:00PM	0.43
07/02/2005	*	*	11:00PM	0.43
07/02/2005	*	*	12:20PM	0.45
07/02/2005	*	*	1:30AM	0.47
07/02/2005	*	*	2:40AM	0.47
07/02/2005	*	*	4:00AM	0.54
08/02/2005	*	*	2:00AM	0.19
09/02/2005	*	*	3:00AM	0.16
10/02/2005	*	*	1:30AM	0.16
11/02/2005	*	*	10:15PM	0.16
12/02/2005	*	*	9:20PM	0.17
13/02/2005	1:15AM	0.53	1:45PM	0.14
14/02/2005	12:20PM	0.47	12:00PM	0.17
15/02/2005	1:10AM	0.47	1:00AM	0.16
16/02/2005	2:50AM	0.42	3:00AM	0.16
17/02/2005	4:00AM	0.42	4:10AM	0.16
18/02/2005	11:20PM	0.42	11:30PM	0.19
19/02/2005	2:15AM	0.42	2:00AM	0.19
20/02/2005	2:30PM	0.42	2:35PM	0.16
21/02/2005	4:00PM	0.42	4:20PM	0.16
22/02/2005	11:20AM	0.42	11:35AM	0.17
23/02/2005	10:40AM	0.39	10:50AM	0.17

24/02/2005	12:50PM	0.37	1:00PM	0.19
25/02/2005	2:10PM	0.37	2:20PM	0.19
26/02/2005	1:40PM	0.32	1:30PM	0.17
27/02/2005	10:25AM	0.30	10:35AM	0.16
28/02/2005	4:20PM	0.28	4:00PM	0.16
01/03/2005	9:20AM	0.28	9:30AM	0.16
02/03/2005	3:00PM	0.28	3:10PM	0.16
03/03/2005	2:10PM	0.28	2:20PM	0.16
04/03/2005	4:00PM	0.32	4:20PM	0.16
05/03/2005	11:30AM	0.32	11:20AM	0.17
06/03/2005	10:15AM	0.32	10:25AM	0.17
07/03/2005	1:05PM	0.32	1:15PM	0.17
08/03/2005	8:40AM	0.32	9:00AM	0.17
09/03/2005	11:00AM	0.32	11:15PM	0.19
10/03/2005	12:10PM	0.32	12:30PM	0.19
11/03/2005	3:20PM	0.32	3:30PM	0.19
12/03/2005	2:10PM	0.37	2:20PM	0.19
13/03/2005	4:00PM	0.37	4:20PM	0.19
14/03/2005	1:00PM	14.0	1:20PM	0.19
15/03/2005	3:00PM	14.0	2:50PM	0.19
16/03/2005	5:20PM	14.0	5:00PM	0.19
17/03/2005	2:00PM	14.0	1:40PM	0.19
18/03/2005	3:00PM	14.0	3:20PM	0.19
19/03/2005	1:00PM	12.0	1:15PM	0.16
20/03/2005	12:30PM	12.0	12:15PM	0.16
21/03/2005	4:40PM	12.0	5:00PM	0.16
22/03/2005	2:45PM	12.0	3:00PM	0.14
23/03/2005	11:00AM	12.0	11:30PM	0.14
24/03/2005	4:00PM	12.0	4:20PM	0.14
25/03/2005	11:50AM	12.0	12:00PM	0.13
26/03/2005	3:30PM	12.0	3:40PM	0.13
27/03/2005	1:50PM	12.0	2:00PM	0.13
28/03/2005	5:00PM	12.0	4:50PM	0.13
29/03/2005	3:20PM	12.0	3:30PM	0.13
30/03/2005	1:10PM	12.0	1:20PM	0.13
31/03/2005	2:00PM	12.0	2:15PM	0.13

*Missing records

APPENDIX A6

ANNUAL RAINFALL FOR THE SIX STATIONS WITHIN THE FARIA CATCHMENT

Table A6 1: Annual Rainfall Data of the Faria Catchment Stations

Years	Rainfall (mm)					
	Nablus Meteorological Station	Al Faria Meteorological station	Beit Dajan	Tubas secondary school	Taluza Primary School	Tammun Primary School
46-47	595	-	-	-	-	-
47-48	380	-	-	-	-	-
48-49	631	-	-	-	-	-
49-50	708.5	-	-	-	-	-
50-51	812.4	-	-	-	-	-
51-52	315.5	-	-	-	-	-
52-53	884.6	200	354	-	-	-
53-54	755.5	267	421	-	-	-
54-55	470	112	219	-	-	-
55-56	759.7	340	472	-	-	-
56-57	580.5	229	280	-	-	-
57-58	656	190	392	-	-	-
58-59	445.3	160	208	-	-	-
59-60	359.2	80	173	-	-	-
60-61	574	235	370	-	-	-
61-62	677	184	358	-	-	-
62-63	506.6	127	279	-	-	-
63-64	799.6	267	561	-	689	-
64-65	818.2	237	408	-	664	-
65-66	504.6	159	281	-	473	-
66-67	944.3	294	487	-	926	483
67-68	516.5	141	141	274.1	533	358
68-69	658	231	402	467.6	770	267
69-70	525.8	165	287	321	575	279
70-71	602.7	239	322	351	664	419
71-72	619.5	302	438	504	704	378.7
72-73	405.6	168	255	288	565	219
73-74	774	424	575	583	881	529
74-75	528.7	187	319	378	456	307
75-76	630	170	420	459	594	233
76-77	606.2	151	345	391	634	270
77-78	508.7	169	349	285	508	236
78-79	349.2	179	248	219	372	214
79-80	895.6	345	774	638	872	414
80-81	643.7	207	458	345	608	285
81-82	557.7	34	371	459	480	207
82-83	1123.5	78	777	614	815	397
83-84	556.4	198.4	385	460	561	295
84-85	468.3	152.7	317	296	386	258
85-86	526.8	30	293	307	508	287
86-87	757.1	230	466	309	707	218
87-88	829.8	280	237	522	1006	392.3
88-89	566.6	185.5	500	426	507	314.9

89-90	588.7	-	485	293	510	296.5
90-91	504.9	-	355	257	500	130
91-92	1387.6	-	474	899.5	1303.1	616.1
92-93	798.9	-	426	485.5	734.4	330.13
93-94	509.2	-	241	336.5	498.8	276.8
94-95	702.2	-	463	450.5	678.8	398.5
95-96	706.9	-	412	378.5	633.7	337.2
96-97	867.7	-	533	500	775.3	360.3
97-98	758.6	-	413.5	546.1	790.8	460
98-99	341.1	-	145	201.5	292.2	124.2
99-00	696	-	350.9	365.4	492.8	317.6
00-01	431	-	167.7	243.1	324.8	225.4
01-02	446	-	391.5	494	522.3	303.8
02-03	1061.4	-	533.9	599	704.8	487.8
AVG	**642.6**	**198.6**	**379.1**	**415.2**	**630.5**	**322.3**
STD	**203.3**	**83.0**	**134.8**	**143.9**	**196.0**	**106.4**
MAX	**1387.6**	**424.0**	**777.0**	**899.5**	**1303.1**	**616.1**
MIN	**315.5**	**30.0**	**141.0**	**201.5**	**292.2**	**124.2**

- No Data

Appendix B (Figures)

APPENDIX B1

TIME SERIES PLOTS OF ANNUAL RAINFALL FOR THE STATIONS IN THE FARIA CATCHMENT

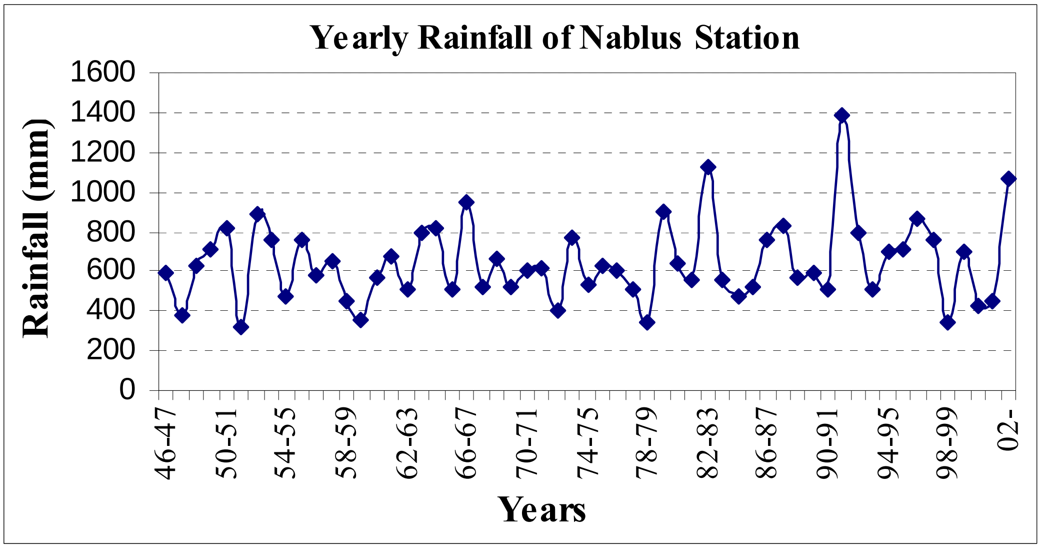

Figure B1 1: Yearly Rainfall of Nablus Station

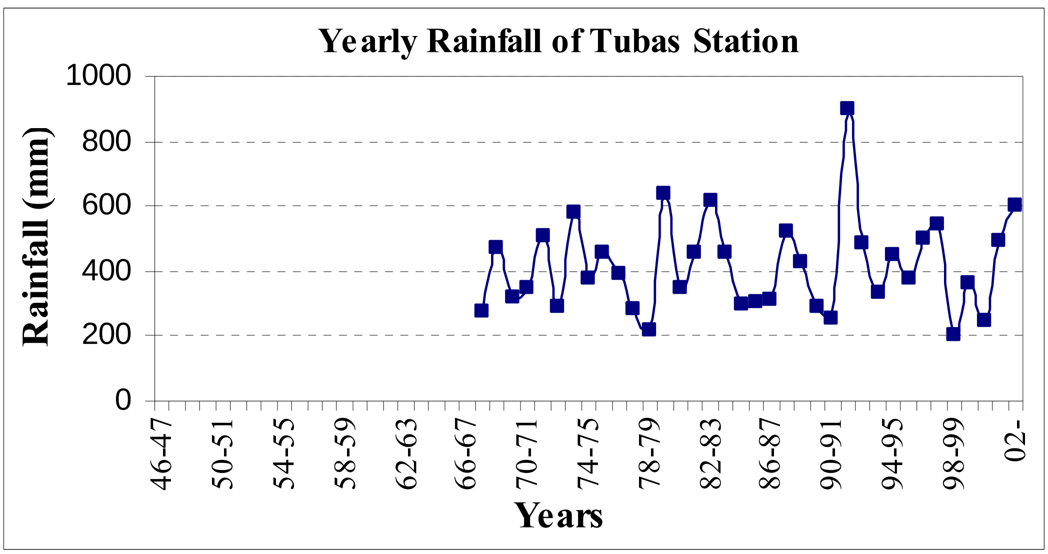

Figure B1 2: Yearly Rainfall of Tubas Station

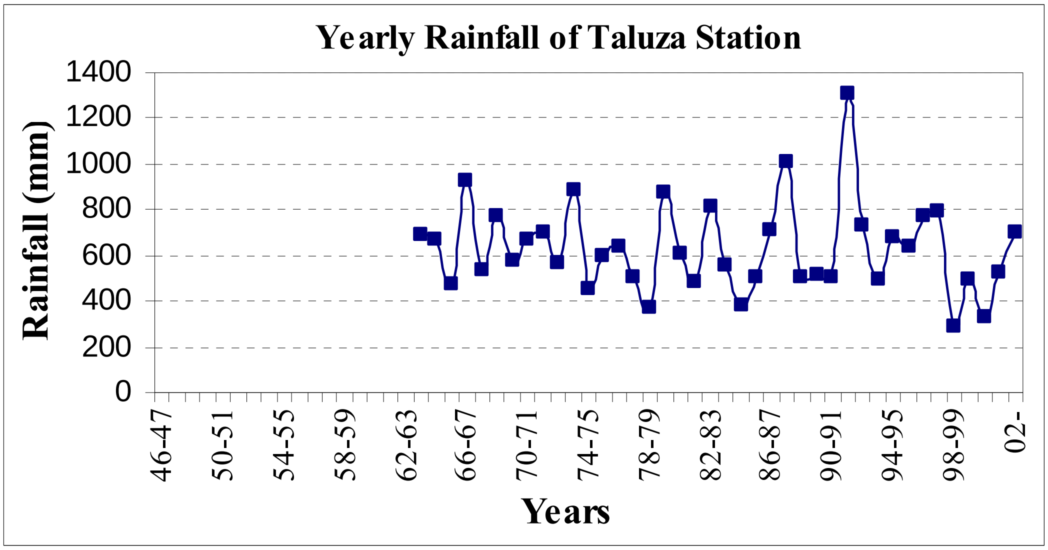

Figure B1 3: Yearly Rainfall of Taluza Station

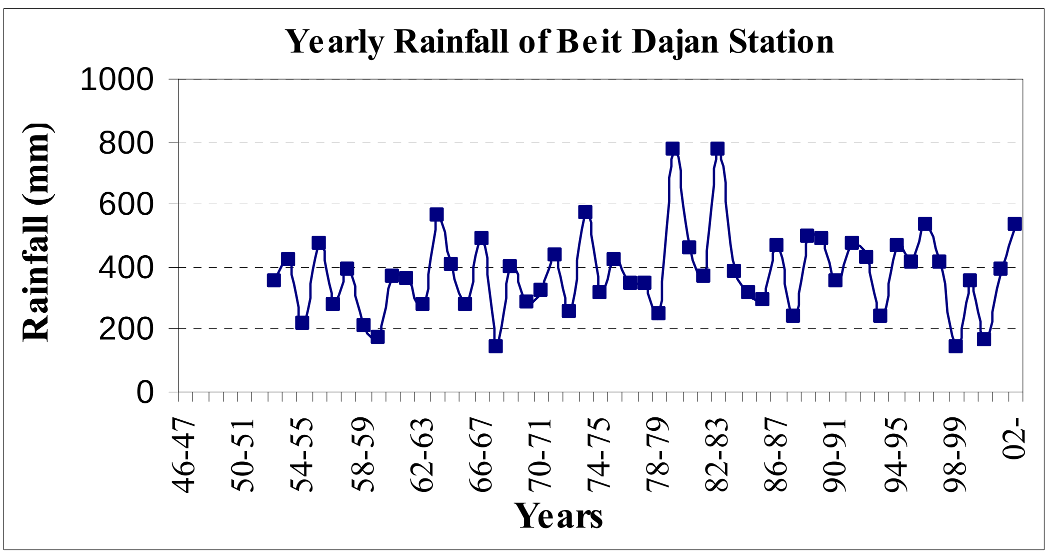

Figure B1 4: Yearly Rainfall of Beit Dajan Station

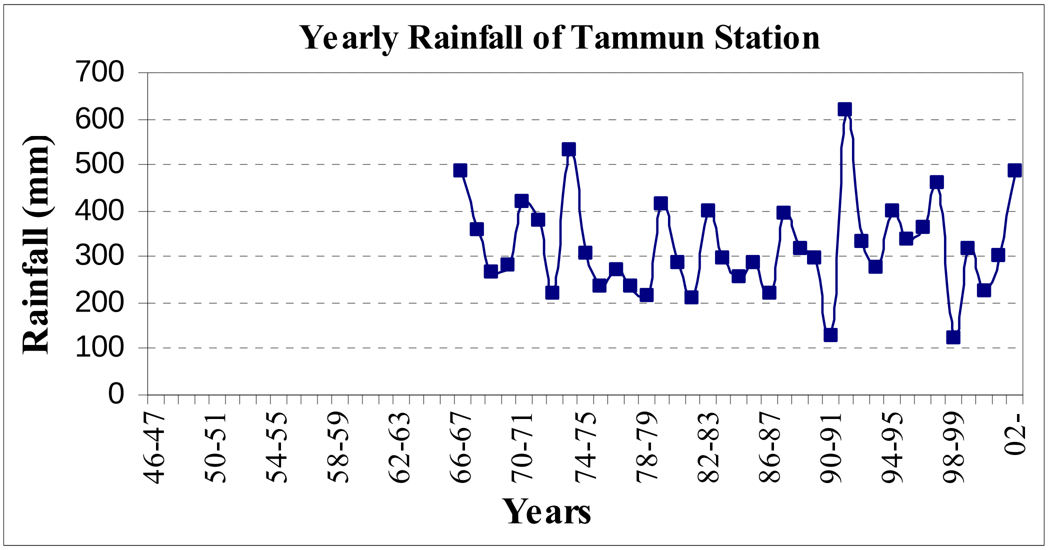

Figure B1 5: Yearly Rainfall of Tammun Station

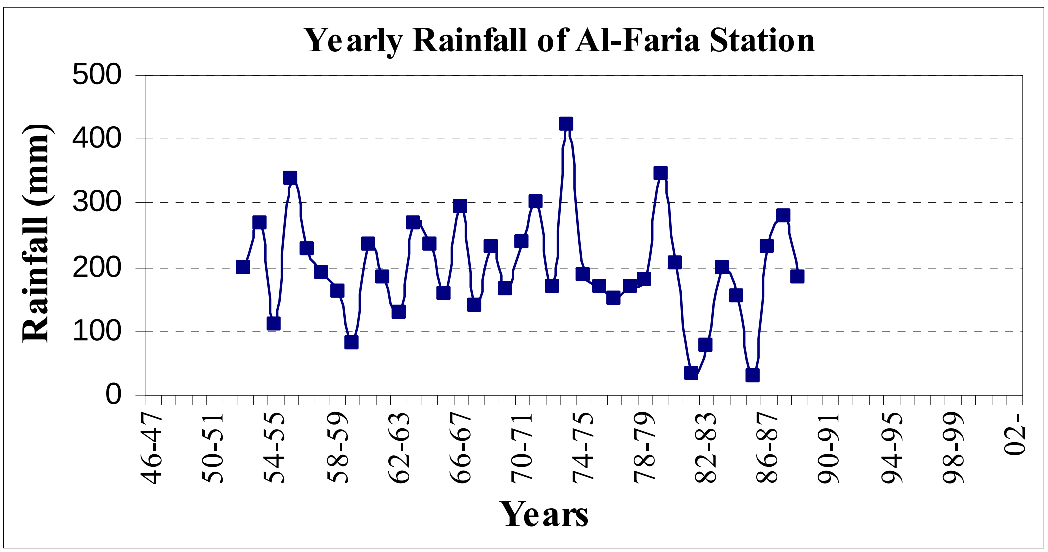

Figure B1 6: Yearly Rainfall of Al-Faria Station

APPENDIX B2

GUMBEL PLOTS OF ANNUAL RAINFALL FOR THE STATIONS IN THE FARIA CATCHMENT

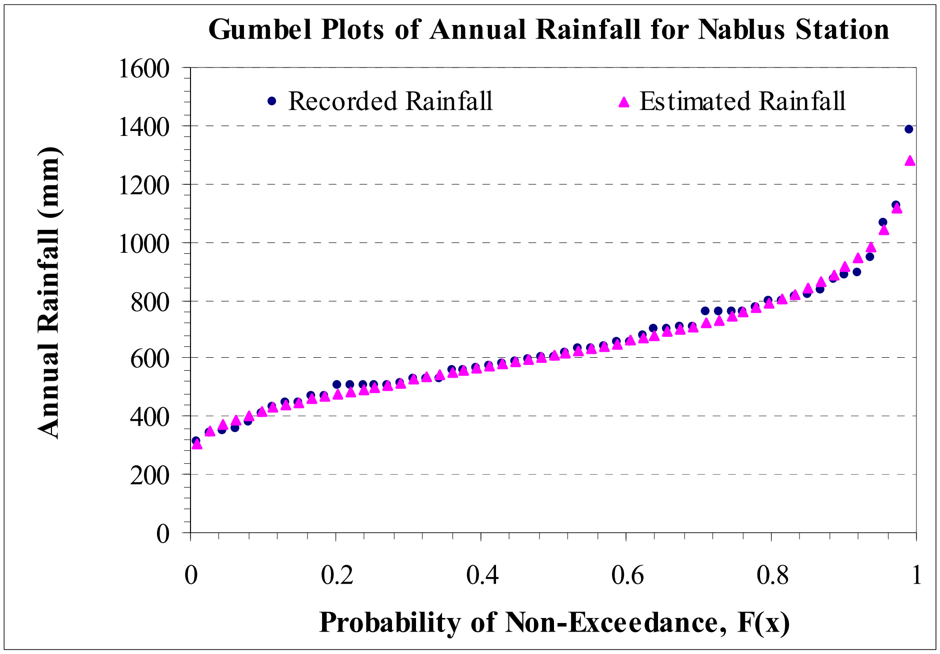

Figure B2 1: Gumbel Plots of Annual Rainfall of Nablus Station

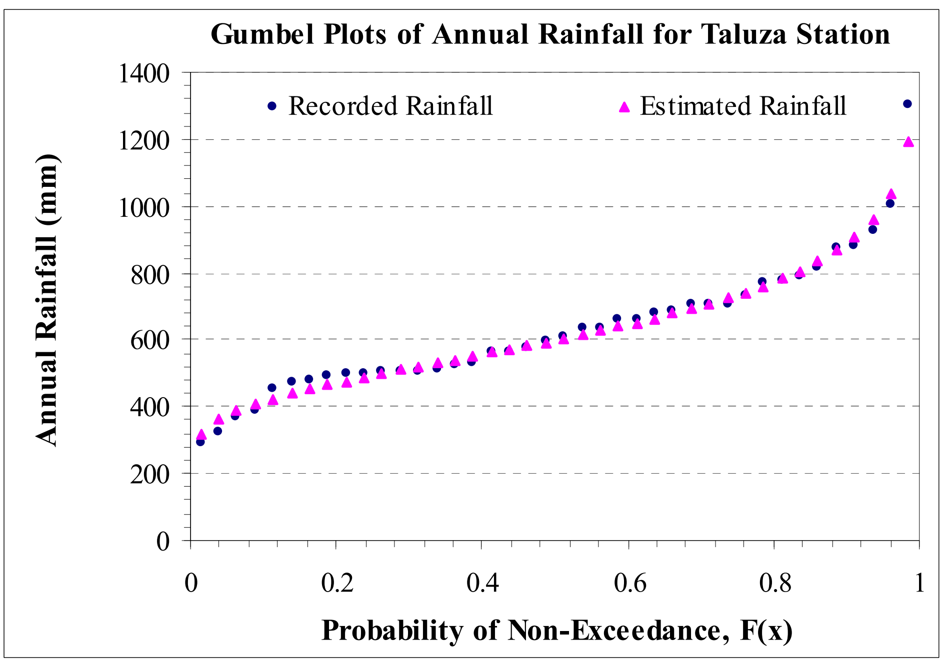

Figure B2 2: Gumbel Plots of Annual Rainfall of Taluza Station

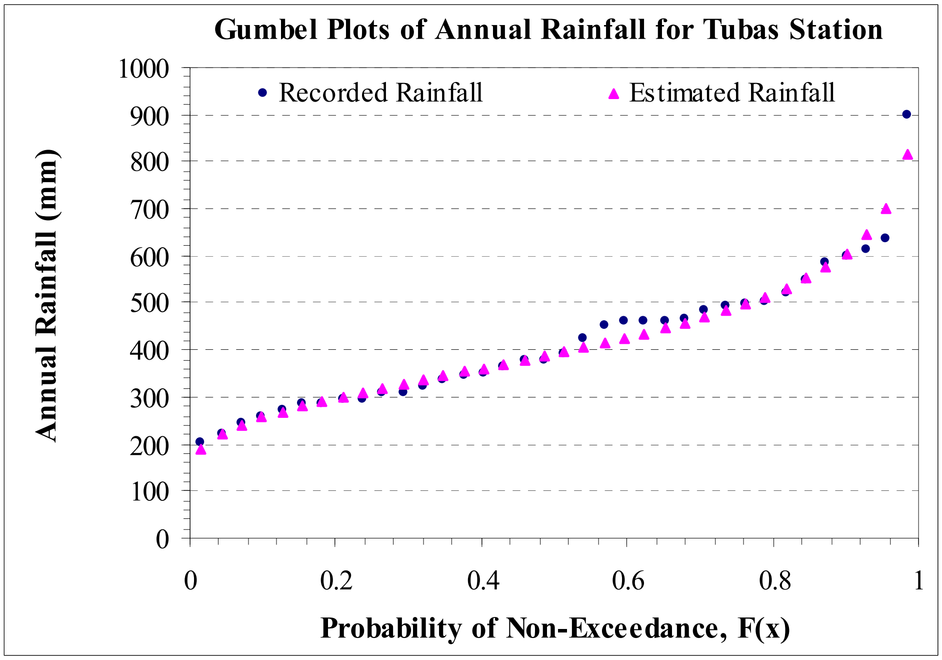

Figure B2 3: Gumbel Plots of Annual Rainfall of Tubas Station

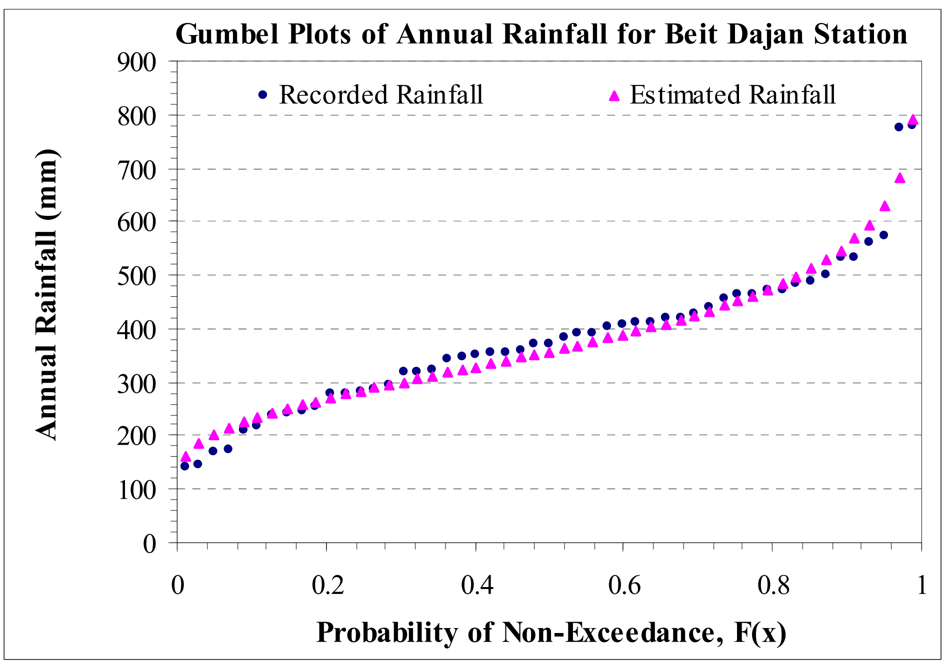

Figure B2 4: Gumbel Plots of Annual Rainfall of Beit Dajan Station

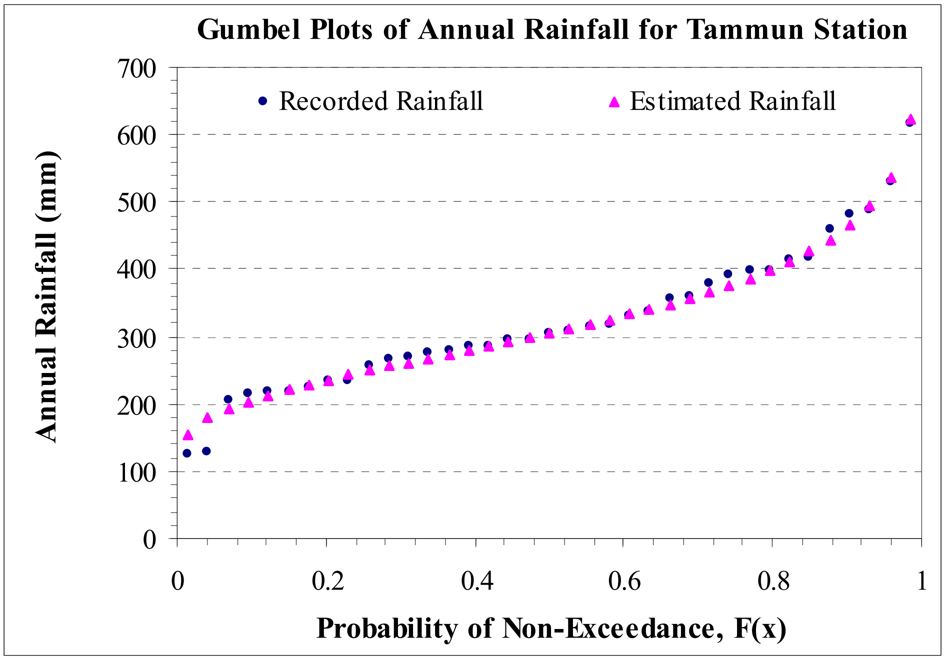

Figure B2 5: Gumbel Plots of Annual Rainfall of Tammun Station

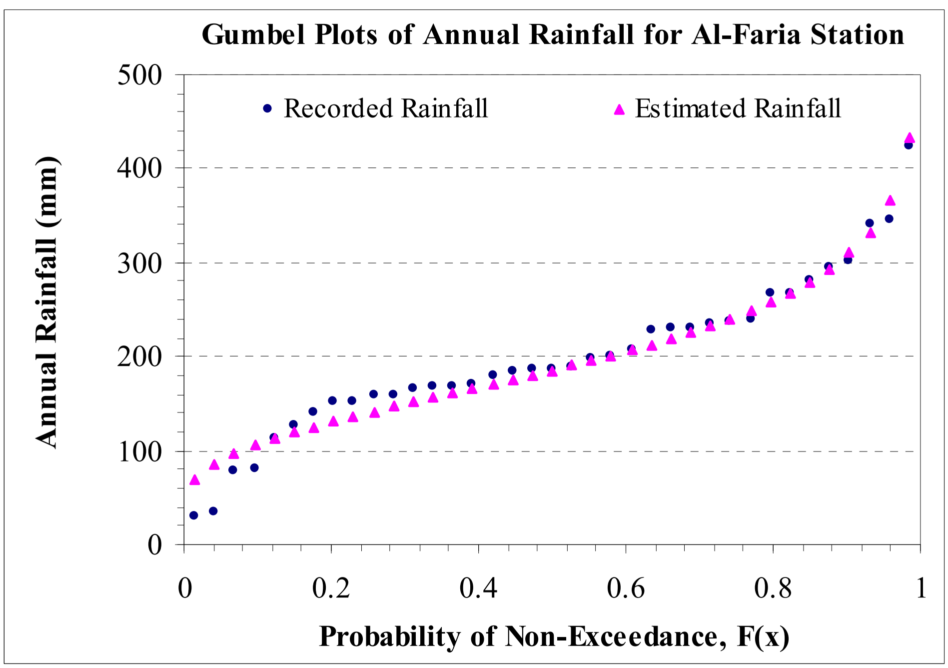

Figure B2 6: Gumbel Plots of Annual Rainfall of Al-Faria Station

APPENDIX C (KW-GIUH Outputs)

Output C 1: KW-GIUH Results of 1-mm Excess Rainfall for Al-Badan Sub-catchment

Kinematic-Wave based Geomorphic Instantaneous Unit Hydrograph
by Kwan Tun Lee and Chin-Hsin Chang
Watershed Hydrology and Hydraulics Laboratory
Department of River and Harbor Engineering
National Taiwan Ocean University
Version 1.2, February 2001, All rights reserved.

Station : Badan
Date : 16/7/2005
Area = 85.28 km*km
Phi index = .00 mm/hr
Based flow = .00 cms

Watershed channel network order: 4
Overland flow roughness coefficient: .300
Channel flow roughness coefficient: .030

Order	Ni	Lci(km)	Ai(km*km)	Poai	Soi	Sci
1	41	1.379	1.370	.660	.1700	.1400
2	6	3.202	10.120	.310	.0920	.0620
3	2	5.027	40.730	.019	.1400	.0510
4	1	3.172	85.280	.011	.1350	.0290

i -> j	Pxixj
1 -> 2	.610
1 -> 3	.340
1 -> 4	.050
2 -> 3	1.000
2 -> 4	.000
3 -> 4	1.000

Rainfall-Runoff Simulation Results:

Time (hr)	Rainfall (mm/hr)	Q-recorded (cms)	Q-simulated (cms)
0	.00	.00	.00
1	1.0	.00	2.91

2	.00	.00	4.26
3	.00	.00	3.35
4	.00	.00	2.64
5	.00	.00	2.09
6	.00	.00	1.66
7	.00	.00	1.32
8	.00	.00	1.06
9	.00	.00	.85
10	.00	.00	.68
11	.00	.00	.54
12	.00	.00	.44
13	.00	.00	.35
14	.00	.00	.28
15	.00	.00	.23
16	.00	.00	.19
17	.00	.00	.15
18	.00	.00	.12
19	.00	.00	.10
20	.00	.00	.08
21	.00	.00	.07
22	.00	.00	.05
23	.00	.00	.04
24	.00	.00	.04
25	.00	.00	.03
26	.00	.00	.02
27	.00	.00	.02
28	.00	.00	.02
29	.00	.00	.01
30	.00	.00	.01
31	.00	.00	.01
32	.00	.00	.01
33	.00	.00	.01
34	.00	.00	.01
35	.00	.00	.00

Output C 2: KW-GIUH Results of 1-mm Excess Rainfall for Al-Faria Sub-catchment

Kinematic-Wave based Geomorphic Instantaneous Unit Hydrograph
by Kwan Tun Lee and Chin-Hsin Chang
Watershed Hydrology and Hydraulics Laboratory
Department of River and Harbor Engineering
National Taiwan Ocean University
Version 1.2, February 2001,

Station : Faria
Date : 16/7/2005
Area = 64.00 km*km
Phi index = .00 mm/hr
Based flow = .00 cms

Watershed channel network order: 4
Overland flow roughness coefficient: .300
Channel flow roughness coefficient: .030

Order	Ni	Lci(km)	Ai(km*km)	Poai	Soi	Sci
1	49	1.031	.937	.717	.1070	.1170
2	8	2.120	6.099	.236	.0850	.0580
3	3	3.496	19.365	.030	.1610	.0330
4	1	2.621	63.997	.017	.0930	.0310

i -> j	Pxixj
1 -> 2	.734
1 -> 3	.224
1 -> 4	.040
2 -> 3	.875
2 -> 4	.125
3 -> 4	1.000

Rainfall-Runoff Simulation Results:

Time (hr)	Rainfall (mm/hr)	Q-recorded (cms)	Q-simulated (cms)
0	.00	.00	.00
1	1.0	.00	2.47

2	.00	.00	3.21
3	.00	.00	2.51
4	.00	.00	1.97
5	.00	.00	1.56
6	.00	.00	1.23
7	.00	.00	.98
8	.00	.00	.78
9	.00	.00	.62
10	.00	.00	.49
11	.00	.00	.39
12	.00	.00	.31
13	.00	.00	.25
14	.00	.00	.20
15	.00	.00	.16
16	.00	.00	.13
17	.00	.00	.10
18	.00	.00	.08
19	.00	.00	.06
20	.00	.00	.05
21	.00	.00	.04
22	.00	.00	.03
23	.00	.00	.03
24	.00	.00	.02
25	.00	.00	.02
26	.00	.00	.01
27	.00	.00	.01
28	.00	.00	.01
29	.00	.00	.01
30	.00	.00	.01
31	.00	.00	.00

Output C 3: KW-GIUH Results of 1-mm Excess Rainfall for Al-Badan Sub-catchment

Kinematic-Wave based Geomorphic Instantaneous Unit Hydrograph
by Kwan Tun Lee and Chin-Hsin Chang
Watershed Hydrology and Hydraulics Laboratory
Department of River and Harbor Engineering
National Taiwan Ocean University
Version 1.2, February 2001, All rights reserved.

Station : Malaqi
Date : 19/07/2005
Area = 184.96 km*km
Phi index = .00 mm/hr
Based flow = .00 cms

Watershed channel network order: 3
Overland flow roughness coefficient: .300
Channel flow roughness coefficient: .030

Order	Ni	Lci(km)	Ai(km*km)	Poai	Soi	Sci
1	62	1.920	1.810	.606	.1460	.1400
2	16	2.611	5.830	.064	.1220	.0630
3	1	3.208	184.960	.330	.0810	.0100

i -> j	Pxixj
1 -> 2	.725
1 -> 3	.274
2 -> 3	1.000

Rainfall-Runoff Simulation Results:

Time (hr)	Rainfall (mm/hr)	Q-recorded (cms)	Q-simulated (cms)
0	.00	.00	.00
1	1.0	.00	4.61
2	.00	.00	7.40
3	.00	.00	5.91
4	.00	.00	4.62
5	.00	.00	3.64

6	.00	.00	2.90
7	.00	.00	2.33
8	.00	.00	1.89
9	.00	.00	1.55
10	.00	.00	1.29
11	.00	.00	1.08
12	.00	.00	.92
13	.00	.00	.79
14	.00	.00	.69
15	.00	.00	.60
16	.00	.00	.54
17	.00	.00	.48
18	.00	.00	.44
19	.00	.00	.40
20	.00	.00	.37
21	.00	.00	.35
22	.00	.00	.32
23	.00	.00	.30
24	.00	.00	.29
25	.00	.00	.27
26	.00	.00	.26
27	.00	.00	.25
28	.00	.00	.24
29	.00	.00	.23
30	.00	.00	.22
31	.00	.00	.21
32	.00	.00	.20
33	.00	.00	.19
34	.00	.00	.19
35	.00	.00	.18
36	.00	.00	.17
37	.00	.00	.17
38	.00	.00	.16
39	.00	.00	.16
40	.00	.00	.15
41	.00	.00	.15
42	.00	.00	.14
43	.00	.00	.14
44	.00	.00	.13
45	.00	.00	.13
46	.00	.00	.12
47	.00	.00	.12
48	.00	.00	.12

49	.00	.00	.11
50	.00	.00	.11
51	.00	.00	.10
52	.00	.00	.10
53	.00	.00	.10
54	.00	.00	.09
55	.00	.00	.09
56	.00	.00	.09
57	.00	.00	.08
58	.00	.00	.08
59	.00	.00	.08
60	.00	.00	.08
61	.00	.00	.07
62	.00	.00	.07
63	.00	.00	.07
64	.00	.00	.07
65	.00	.00	.06
66	.00	.00	.06
67	.00	.00	.06
68	.00	.00	.06
69	.00	.00	.06
70	.00	.00	.05
71	.00	.00	.05
72	.00	.00	.05
73	.00	.00	.00

Appendix D (Pictures)

APPENDIX D1

PHOTOS OF AL-BADAN AND AL-FARIA MEASURING FLUMES

Picture D1 1: Al-Badan Flume

Picture D1 2: Al-Faria Flume

APPENDIX D2

FEATURES BY PHOTOS OF FARIA CATCHMENT

Picture D2 1: Al-Malaqi Bridge

Picture D2 2: Slope of Faria Catchment

Picture D2 3: Up Stream of Al-Badan Sub-catchment

Picture D2 4: Agriculture in Faria Catchment

Picture D2 5: Crop Fields in Faria Catchment

Picture D2 6: Bare Land in Faria Catchment

جامعة النجاح الوطنية
كلية الدراسات العليا

النمذجة الهيدرولوجية لأحواض المناطق شبه الجافة مدعوما بأنظمة المعلومات الجغرافية حالة حوض وادي الفارعه

إعداد
سمير "محمد خيري" شحاده عبد الكريم

إشراف
د. حافظ شاهين
د.عنان جيوسي

قدمت هذه الأطروحة استكمالا لمتطلبات درجة الماجستير في هندسة المياه والبيئة بكلية الدراسات العليا في جامعة النجاح الوطنية في نابلس، فلسطين.

2005

النمذجة الهيدرولوجية لأحواض المناطق شبه الجافة

مدعومة بأنظمة المعلومات الجغرافية

حالة حوض وادي الفارعه

إعداد

سمير "محمد خيري" شحاده عبد الكريم

إشراف

د. حافظ شاهين

د.عنان جيوسي

الملخص

تعتبر العواصف الشديدة، الفيضانات والجفاف من ابرز الخصائص التي تميز النظام الهيدرولوجي لأي منطقة. في الضفة الغربية والتي تعتبر من المناطق شبه الجافة، هناك عدد قليل من الدراسات المتوفرة في مجال النمذجة الهيدرولوجية (Hydrological Modeling). رسالة الماجستير هذه هي عبارة عن محاولة لدراسة ونمذجة العلاقة ما بين المطر والجريان في الحوض السطحي لوادي الفارعة. يقع حوض وادي الفارعة في شمال شرق السفوح الشرقية للضفة الغربية، حيث تبلغ مساحته حوالي 334كم^2 ويصنف على انه منطقة شبه جافة. يوجد في حوض الفارعه ست محطات لقياس الأمطار بالإضافة لمحطتين لقياس الجريان السطحي للجزء العلوي من الحوض.

في هذه الدراسة تم عمل تحليل إحصائي لأمطار جميع محطات حوض وادي الفارعة وهذا يتضمن المعدل السنوي، الانحراف المعياري والقيم العظمى والصغرى. كذلك تم اختبار التوافق لقياسات الأمطار (Internal Consistency) باستخدام طريقة المنحنى الكتلي (Double Mass Curve) حيث وجد أن قياسات المحطات متوافقة بعد ذلك تم عمل تحليل للتوزيع الإحصائي للأمطار السنوية لجميع المحطات في حوض الفارعة حيث تبين أن توزيع (Gumbel) يناسب البيانات المطرية السنوية ويمكن الاعتماد على هذا التوزيع في الحسابات المستقبلية للمنطقة بما يمكن من فهم وتقييم خصائص التوزيع الاحتمالي للأمطار في حوض الفارعه.

من ناحية أخرى تم دراسة وتحليل التوجه للأمطار السنوية حيث كانت النتيجة أن هناك توجه نحو الزيادة (Increasing Trend) في المناطق المرتفعة حيث كان هذا التوجه واضحا

لمحطتي نابلس وبيت دجن بينما كان هناك توجه نجو النقصان (Decreasing Trend) في المناطق المنخفضة. كذلك تم دراسة العلاقة بين محطات الأمطار لحوض الفارعه باستخدام طريقة الانحسار المتعدد (Multiple Regression) ووجد أن هناك علاقة قوية تربط تلك المحطات.

في هذه الرسالة تم دراسة وتفحص العلاقة ما بين المطر والجريان السطحي لحوض وادي الفارعه باستخدام النموذج الهيدرولوجي الذي يعرف باسم (KW-GIUH Model) وهو منحنى التدفق الأحادي المعتمد على الخصائص الجيومورفولوجية ومعادلة الحركة وذلك بالاستعانة ببرنامج نظم المعلومات الجغرافية (GIS) وباستخدام هذا النموذج تم اشتقاق منحنى التدفق الأحادي (IUH) للأحواض الثلاثة التي يتشكل منها وادي الفارعه. منحنيات التدفق المشتقة تدل على أن هذا النموذج الهيدرولوجي قابل للتطبيق لنمذجة الجريان السطحي في المناطق شبه الجافة وهذا يدل على إمكانية استخدام وتوظيف هذا النموذج لاشتقاق منحنيات التدفق للأحواض السطحية في فلسطين.